CRREL

REPORT 88-13

AD-A200 172

Profile properties of undeformed first-year sea ice

US Army Corps of Engineers

Cold Regions Research & Engineering Laboratory

88 11 08 005

Cover: Computer simulation of temperature and salinity profiles of sea ice.

CRREL Report 88-13

September 1988

Profile properties of undeformed first-year sea ice

Gordon F.N. Cox and Wilford F. Weeks

AD A200 172

REPORT DOCUMENTATION PAGE

1a. REPORT SECURITY CLASSIFICATION Unclassified	1b. RESTRICTIVE MARKINGS

2a. SECURITY CLASSIFICATION AUTHORITY	3. DISTRIBUTION / AVAILABILITY OF REPORT Approved for public release; distribution is unlimited.
2b. DECLASSIFICATION / DOWNGRADING SCHEDULE	

4. PERFORMING ORGANIZATION REPORT NUMBER(S) CRREL Report 88-13	5. MONITORING ORGANIZATION REPORT NUMBER(S)

6a. NAME OF PERFORMING ORGANIZATION U.S. Army Cold Regions Research and Engineering Laboratory	6b. OFFICE SYMBOL (If applicable) CECRL	7a. NAME OF MONITORING ORGANIZATION David Taylor Naval Ship Research and Development Center

6c. ADDRESS (City, State, and ZIP Code) Hanover, New Hampshire 03755-1290	7b. ADDRESS (City, State, and ZIP Code) Code 1720.4 Bethesda, Maryland 20084

8a. NAME OF FUNDING / SPONSORING ORGANIZATION Naval Sea Systems Command	8b. OFFICE SYMBOL (If applicable)	9. PROCUREMENT INSTRUMENT IDENTIFICATION NUMBER 06R26

8c. ADDRESS (City, State, and ZIP Code) Department of the Navy Washington, D.C. 20362-5101	10. SOURCE OF FUNDING NUMBERS			
	PROGRAM ELEMENT NO.	PROJECT NO.	TASK NO	WORK UNIT ACCESSION NO

11. TITLE (Include Security Classification) Profile Properties of Undeformed First-year Sea Ice

12. PERSONAL AUTHOR(S) Cox, Gordon F.N. and Weeks, Wilford F.

13a. TYPE OF REPORT	13b. TIME COVERED FROM _____ TO _____	14. DATE OF REPORT (Year, Month, Day) September 1988	15. PAGE COUNT 63

16. SUPPLEMENTARY NOTATION

17.	COSATI CODES		18. SUBJECT TERMS (Continue on reverse if necessary and identify by block number)
FIELD	GROUP	SUB-GROUP	Ice
			Ice properties
			Sea ice

19. ABSTRACT (Continue on reverse if necessary and identify by block number)

In many sea ice engineering problems the ice sheet has been assumed to be a homogeneous plate whose mechanical properties are estimated from the bulk salinity and average temperature of the ice sheet. Typically no regard has been given to the vertical variation of ice properties in the ice sheet or to the time of ice formation. This paper first reviews some of the mechanical properties of sea ice, including the ice tensile, flexural and shear strengths, as well as the ice modulus. Equations for these properties are given as functions of the ice brine volume, which can be determined from the ice salinity and temperature. Next a numerical, finite difference model is developed to predict the salinity and temperature profiles of a growing ice sheet. In this model ice temperatures are calculated by performing an energy balance of the heat fluxes at the ice surface. The conductive heat flux obtained from the energy balance is then used to calculate the rate of ice growth and ice thickness by applying the Stefan ice growth equation. Ice salinities are determined by considering the amount of initial salt entrapment at the ice/water interface and the subsequent brine drainage due to brine expulsion and gravity drainage. Ice salinity and temperature profiles are then generated using climatological data for the Central Arctic Basin. The

20. DISTRIBUTION / AVAILABILITY OF ABSTRACT ☒ UNCLASSIFIED/UNLIMITED ☐ SAME AS RPT. ☐ DTIC USERS	21 ABSTRACT SECURITY CLASSIFICATION Unclassified
22a. NAME OF RESPONSIBLE INDIVIDUAL Dr. Gordon F.N. Cox	22b TELEPHONE (Include Area Code) 603-646-4362	22c OFFICE SYMBOL CECRL-RS

19. Abstract (cont'd)

profiles appear to be realistic and agree reasonably well with field data. Finally the predicted salinity and temperature profiles are combined with the mechanical property data to provide mechanical property profiles for first-year sea ice of different thicknesses, grown at different times of the winter. The predicted profiles give composite plate properties that are significantly different from bulk properties obtained by assuming homogeneous plates. In addition the failure strength profiles give maximum strengths in the interior of the sheet as contrasted with the usual assumption of maximum strength at the cold, upper ice surface. Surprisingly, the mechanical property profiles are only a function of the ice thickness, independent of the time of ice formation.

PREFACE

DTIC
COPY
INSPECTED
6

Accession For	
NTIS GRA&I	☑
DTIC TAB	☐
Unannounced	☐
Justification	

By
Distribution/
Availability Codes

Dist	Avail and/or Special
A-1	

iii

CONTENTS

ILLUSTRATIONS

Profile Properties of Undeformed First-Year Sea Ice

GORDON F.N. COX AND WILFORD F. WEEKS

INTRODUCTION

Based on a wide variety of studies performed at sites scattered throughout the polar regions, it is clear that the physical properties of sea ice are highly variable. A significant factor affecting these variations is the state of the ice at the time it is studied, including its macroscale and microscale structure, its temperature and its composition. Also important are the details of the test itself. For instance, in mechanical property testing the results obtained vary with the type of failure, the volume and geometry of the sample, and the deformation rate. When faced with problems requiring a knowledge of sea ice properties, it is, of course, always desirable to have in situ measurements of the properties of interest done on a specific ice type under critical environmental conditions. In the real world such measurements are rarely possible. This is particularly true in pack ice areas where the ice drifts in complex patterns under the stresses exerted by the wind, by the currents and by the ice itself. To make matters worse, every ice sheet contains a variety of ice thicknesses, and each ice thickness will show different temperature and composition profiles.

At first glance the situation would appear to be hopelessly complex, making effective forecasts of ice profile properties a near impossibility. However, there are systematic relations between ice growth conditions, as controlled by the environment, and the temperature and salinity profiles. These, combined with the ice structure, can be used to specify the state of the ice. Once the state of the ice is known, it is possible to predict the composite properties of undeformed ice sheets by using appropriate experimental observations that specify the properties of interest in terms of the state variables. In the following we apply such procedures to the variations in the mechanical properties of undeformed first-year sea ice that is assumed to have grown under environmental conditions that are climatologically representative of the Arctic Basin. It should be stressed, however, that this approach is perfectly general and can be applied to the variations of any physical property, providing that there is an experimental or theoretical basis for estimating the property from a knowledge of the ice state.

In developing this subject we first review the applicable knowledge of the variations in ice structure and then discuss existing data relating the various mechanical properties of sea ice to the state of the ice. Next this information is combined with a model that calculates sea ice growth rates, ice thicknesses, temperatures and salinities based on climatological data. Finally, examples are given of the profile properties of first-year sea ice of various thicknesses in the Arctic Ocean, assuming different dates for the initial formation of the ice.

STRUCTURE

The principal first-year ice type is called congelation ice, ice that has formed through the unidirectional solidification of sea water. The ice is composed of columnar crystals with their long axes parallel to the direction of heat flow (i.e. vertical). Their grain diameters vary between a fraction of a centimeter and a few centimeters, with a general increase in grain size with depth in the ice sheet (Weeks and Assur 1967). The salt found within the ice occurs as a series of entrapped liquid inclusions (brine pockets) located in planar defect arrays within the individual ice crystals. Because these inclusions are not randomly oriented, the strength of the ice is usually considered to vary proportionally to $(1 - \sqrt{v_b})$, where v_b is the brine volume, which for first-year ice is a good representation of the total void volume (i.e. the amount of entrapped gas is relatively small). The microstructural considerations leading to the $(1 - \sqrt{v_b})$ representation of strength variations were reviewed by

Weeks and Assur (1967, 1972) and Weeks and Ackley (1982). Changes in mechanical properties are also believed to be associated with the variations in grain size and with changes in the spacing between the arrays of brine inclusions within the ice. However, both of these effects are believed to be smaller than those associated with brine volume variations and are usually neglected.

There are two structurally different varieties of congelation ice. The first of these shows a random c-axis alignment in the horizontal plane. This results in an ice sheet that is transversely isotropic; it shows property variations in the vertical direction associated with changes in brine volume, ice temperature, grain size and crystal substructure, but at any given level all properties in the horizontal plane are identical.

The second ice type is orthotropic in that there is a strong preferred c-axis alignment in the horizontal plane. This results in property differences along three orthogonal axes. Figure 1 is a schematic drawing of the structure of such ice. The c-axis alignment direction is believed to be parallel to the direction of the current (Weeks and Gow

1978, 1980) at the ice/water interface when that specific layer of ice formed (a random c-axis orientation in the horizontal plane is presumed to represent either no current or short-term changes in current direction).

The relative amounts of these two types of congelation ice in the Arctic Seas are unknown. However, orthotropic ice dominates (90–95%) in the few fast ice areas that have been sampled (Cherepanov 1971, Weeks and Gow 1980), and strong crystal alignments are also observed in pack ice (Tucker et al. 1985). As will be seen, data on the effect of these orientation changes on the mechanical properties of ice are limited, and the available data are badly in need of verification. Nevertheless, available results (Peyton 1966) suggest that the differences are large, with the ratio of hard fail to easy fail being 3.6 in tension and 4.3 in compression. The effect of these differences on composite plate problems has not been investigated. Clearly it will make realistic analyses more difficult. Also there are no experimental results available on the effect of crystal orientation on the elastic modulus.
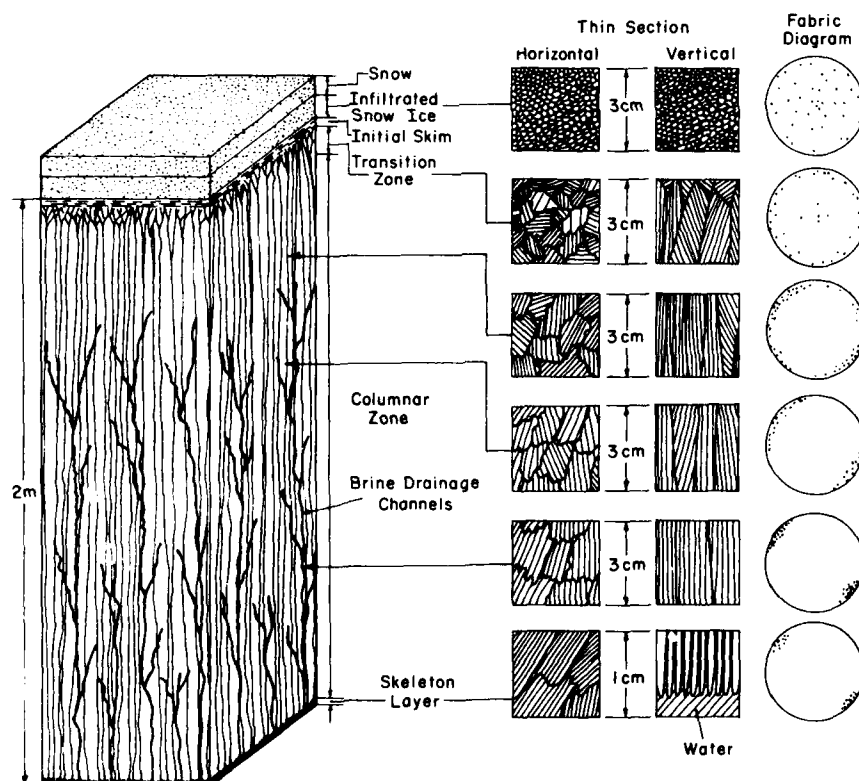

Figure 1. Schematic drawing of the structure of first-year sea ice. (After Schwarz and Weeks 1977.)

2

The other general structural type of sea ice is frazil. This is a fine-grained ice with a random c-axis orientation. The included brine occurs along the ice crystal boundaries at randomly located sites. One can think of frazil simply as frozen slush. It is presumably isotropic, and the strength of the ice would be expected to decrease as the volume of brine in the ice increases. Also, fine-grained frazil would be expected to be stronger than coarse-grained frazil, with the variation in strength inversely proportional to the square root of the grain diameter.

The present indications are that the amount of frazil in the central Arctic Basin is fairly limited, being largely restricted to the surface layers of ice formed in leads during windy periods. One would expect frazil to be more common in the marginal seas such as the Bering and Greenland, and ice conditions there are more dynamic and wave action has a significant effect in "working" the ice. However, in one of the few studies of this subject to date (Tucker et al. 1985), the ice in the Fram Strait area of East Greenland was found to contain only limited amounts of frazil, with the largest concentrations being associated with pressure ridges. This is in pronounced contrast to the ice in the Weddell Sea off the Antarctic continent, where frazil makes up a major portion of the ice cover (Weeks and Ackley 1982). Unfortunately the mechanical properties of frazil ice have not been well studied.

COMPOSITION

In relating the properties of sea ice to the state of the ice, the most important single parameter is the void volume, which is composed of the sum of the brine volume and the gas volume. As mentioned, in studies of first-year ice, it is usually assumed that the gas volume is insignificant relative to the brine volume ($v_b >> v_g$). That this assumption is reasonable is fortunate in that to date there is no method for calculating the amount of gas entrapped in the ice from a knowledge of the growth conditions. Even the amount of data on gas volumes in first-year ice is limited, although a less time-consuming method of making such determinations is now available (Cox and Weeks 1983).

The brine volume within the ice is determined precisely via the phase relations from the ice temperature and salinity (Assur 1958, Cox and Weeks 1983). Although a detailed specification of the time-dependent temperature profile of first-year ice sheets is a rather involved problem, calculations assuming a linear temperature profile are tractable and are adequate for engineering and most scientific purposes (Maykut 1978). The difficulty is in specifying the salinity profile from a knowledge of the growth conditions. These interrelations are complex, involve several different processes, and have been studied on both artificial (Weeks and Lofgren 1967, Cox and Weeks 1975) and natural sea ice (Cox and Weeks 1974, Nakawo and Sinha 1981).

Fortunately the observed trends are quite systematic and are similar to related occurrences in metals and ceramics. The initial ice salinity is a function of both the salinity of the seawater and the ice growth rate, with very fast growing ice incorporating the majority of the salt and very slow growth resulting in nearly total rejection of impurities. Once brine has been entrapped in the ice, it starts to drain down and out of the ice, resulting in a systematic change in salinity profiles with increasing ice thickness. The processes involved here are brine expulsion and drainage. Brine expulsion is caused by differences in the volumetric changes in the ice and the brine. Gravity drainage occurs in the ice growth season because the brine in the cold upper portion of the ice is denser than the brine in the warmer lower portion of the ice, which is in turn denser than the warmer (and less saline) underlying seawater. In addition, as the brine drains down and out of the ice, structural features caused by this drainage develop within the ice: the so-called brine drainage channels (Lake and Lewis 1970, Niedrauer and Martin 1979). These can be thought of as tubular river systems in which the tributaries are arranged with cylindrical symmetry around the main drainage channels. Near the bottom of thick annual ice, drainage channels appear to occur on a horizontal spacing of 15–20 cm and have a diameter of approximately 1 cm. Such features obviously affect both the observed brine drainage rates, as they serve as major brine pathways, and the mechanical properties of the ice, as they are gross macroscopic flaws. Observed salinity profiles are the result of the simultaneous operation of all these processes plus other processes as yet undiscovered.

There are a variety of solid salts that form within in cold sea ice. The crystallization temperatures of the two most common of these are $-8.2°C$ ($Na_2SO_4 \cdot 10H_2O$) and $-22.9°C$ ($NaCl \cdot 2H_2O$). The effects of these solid salts on bulk ice properties have not

3

been studied, even though the effects of dispersed solid second phases on the mechanical properties of other composite materials are well known.

We hope it is now clear what must be attempted in this paper. First, a method must be selected for calculating ice growth rates and ice temperatures in terms of realistic meteorological conditions. This program must then be used to drive a subsidiary set of equations that specify the nature of the ever-changing salinity profile. The salinity and temperature profiles must next be combined to generate a brine volume profile, which in turn specifies the appropriate physical property profiles. Finally, these physical property profiles must be used to calculate the composite properties of the ice sheet.

MECHANICAL PROPERTIES

We will now review the current state of knowledge of the more important mechanical properties of the ice and, where possible, select equations useful in specifying these properties in terms of ice state parameters.

Strength

Unconfined compressive strength

The earliest simple compression tests on cylinders of sea ice were made by Butkovich (1956, 1959), who obtained median σ_c values from vertical cores ranging from 7.6 MPa at -5°C to roughly 12.0 MPa at -16°C. The average values on horizontal cores in the same temperature range varied from 2.1 to 4.2 MPa. These pronounced differences with changes in sample orientation are reasonable; when a load is applied in the plane of the ice sheet, both the grain boundaries and the planes of inclusions within the ice crystals are oriented so that the sample will fail readily. It is not known whether or not the ice Butkovich tested showed strong c-axis alignments.

A similar strong orientation dependence was found by Peyton (1966), who ran tests on many samples of sea ice at various orientations and stress rates (Fig. 2). Much of the ice used by Peyton showed strong c-axis alignments. Therefore, his samples were essentially single crystals with their c-axes parallel to the plane of the ice sheet. The ratio of the strength values obtained from vertical cores to those obtained from horizontal cores is 3:1, in agreement with the results of Butkovich (1959).
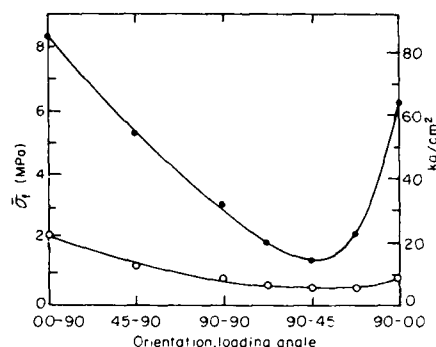
Figure 2. Average failure strength in compression (solid circles) and in direct tension (open circles) versus sample orientation for bottom ice at -10°C. The orientation notation is as follows: the first number gives the angle between the axis of the test cylinder and the vertical, and the second number gives the angle between the sample and the mean c-axis orientation of the ice being tested. (After Peyton 1966.)

Peyton's results show that the compressive strength depends strongly on the square root of the brine volume. Unfortunately his observations were not plotted directly, but instead a series of "corrections" were made, making his results difficult to use.

The test strain rate, or loading rate, also influences the compressive strength of the ice. Such effects are well known in freshwater ice. The strong dependence of σ_c on strain rate is clearly shown in the recent sea ice tests of Wang (1979, 1980) and Timco and Frederking (1986). Wang also determined the major effects of changes in grain size (a factor not usually considered) and crystal alignment (Fig. 3 and 4).

Another factor, which has been ignored in many studies because it was difficult to measure, is the amount of gas in the sea ice. At many locations, and particularly in older or deteriorated ice, the gas volume can be very important. This is well illustrated in Figure 5, which shows the effects of both ice density and ice temperature on σ_c values determined on sea ice from saline Lake Saroma in northern Hokkaido (Saeki et al. 1979). Because Cox and Weeks (1983) have recently developed a simple method for rapidly estimating the gas volume in sea ice, it is hoped that determinations of the amount of gas will soon become commonplace.

4
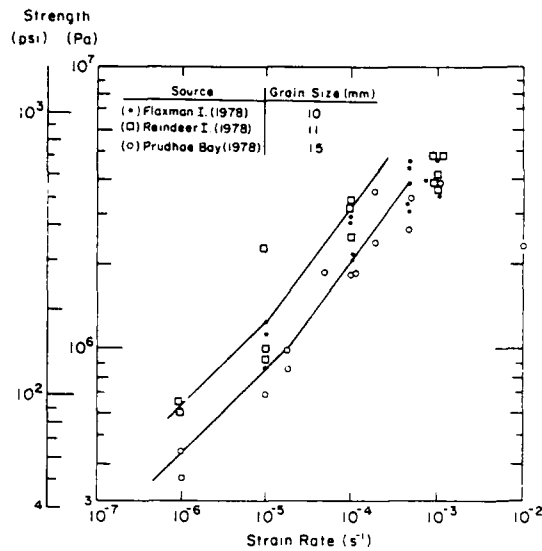
Figure 3. Compressive strength of unoriented columnar sea ice at -10°C, showing the effects of changes in grain size and strain rate. (After Wang 1979, 1980.)
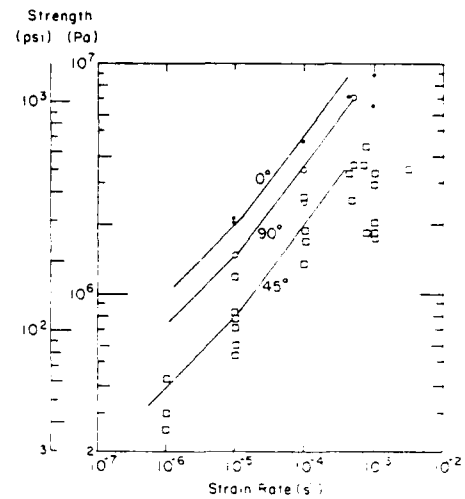
Figure 4. Compressive strength of oriented columnar sea ice at -10°C, showing the effects of changes in crystal orientation. (After Wang 1980.)
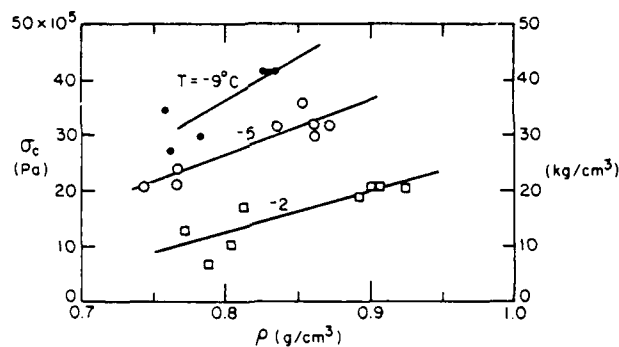
Figure 5. Interrelations between compressive strength σ_c, ice density ϱ, and ice temperature T. Samples are from saline Lake Saroma. (After Saeki et al. 1979.)

An illuminating recent study that deals with many of the above relations (Timco and Frederking 1986) described the results of both Type C and Type E tests (Fig. 6) performed on warm (-2°C), deteriorated first-year ice. Strong correlations were found between strength and the square root of void volume, supporting the earlier work of Peyton, and also between strength and strain rate. Combining their results with tests at different temperatures by earlier workers, they proposed

$$\sigma = 47(\dot{\varepsilon})^{0.26} (1 - \sqrt{v_b/320}) \qquad (1)$$

for unconfined compressive strength when the load is applied in the plane of the ice sheet (Type C) and

$$\sigma = 168(\dot{\varepsilon})^{0.22} (1 - \sqrt{v_b/280}) \qquad (2)$$

when the load is applied normal to the plane of the

5
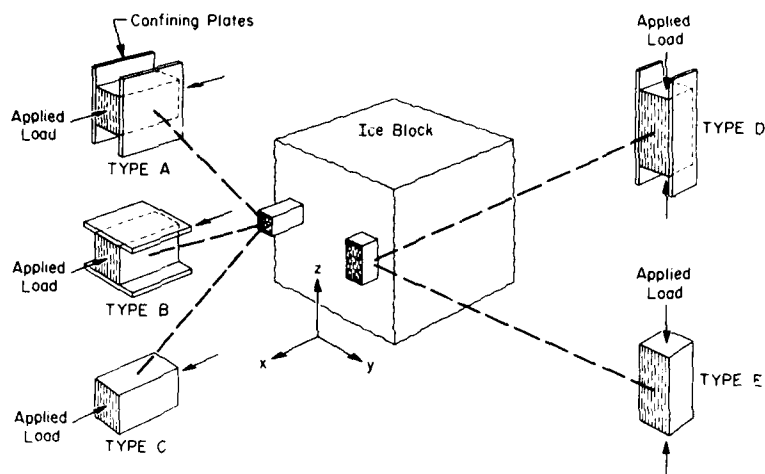
Figure 6. Compressive test types showing different confinement arrangements. (From Timco and Frederking 1986.)

sheet (Type E). Here strength σ is in MPa, strain rate $\dot{\varepsilon}$ is in s^{-1} ($5 \times 10^{-6} \leq \dot{\varepsilon} \leq 5 \times 10^{-4}$) and brine volume v_b is in parts per thousand. They also presented equations that express σ in terms of stress rate.

In summary, we now have some idea of the more important factors that influence the compressive strength of sea ice: ice structure, load orientation, brine and gas volume, temperature, strain or stress rate, and grain size. However, tests have still not been performed over the full ranges of temperature, salinity, ice structure and strain rates that occur in nature. The effects of solid salts are also far from clear. Particularly surprising is the absence of any thorough study of the σ_c values for undeformed multi-year ice.

Confined compressive strength

There are relatively few data on the confined compressive strength of ice, let alone sea ice. The most noteworthy studies on freshwater and saline ice are by Frederking (1977), Hausler (1981), Jones (1982) and Timco and Frederking (1983, 1984, 1986). Studies that are more difficult to interpret include those by Panov and Fokeev (1977), Blanchet and Hamza (1983) and Nawwar et al. (1983).

Frederking (1977) conducted plane-strain compression tests on freshwater polycrystalline snow and columnar ice. The prismatic specimens were rigidly confined in one direction and stress-free in the other. The confinement had little effect on the

confined compressive strength of the isotropic snow ice, which was at most only increased by 25%. On the other hand, the confined compressive strength of the columnar ice was substantially increased, depending on the direction of confinement relative to the long axes of the columnar crystals. When the columnar crystals were constrained from moving in the plane of the ice sheet, the Type A loading condition in Figure 6, the ice strength was increased by a factor of four at a strain rate of 10^{-7} s^{-1} (to about 2.4 MPa) and by a factor of two at 10^{-4} s^{-1} (to about 20 MPa). When the crystals were confined in a direction normal to the axis of elongation, the Type B loading condition, there was little or no change in the ice strength. The results of this study serve as the basis for Ralston's (1977) anisotropic ice yield criteria.

Recently Timco and Frederking (1983, 1984, 1986) performed a series of plane-strain compression tests on similarly shaped sea ice specimens showing both columnar and granular (frazil) structures. The tests used all of the loading conditions shown in Figure 6. Strain rates varied from 10^{-6} to 10^{-4} s^{-1} at temperatures between $-11°$ and $-13°C$ and from 10^{-5} to 10^{-3} s^{-1} at $-2°C$. As in the earlier freshwater tests, confinement had only a slight effect on the strength of granular sea ice samples, but it significantly increased the strength of Type A columnar ice. The confined compressive strength of both the Type A and Type B granular samples was about 20% higher than the unconfined uniaxial specimens. In contrast, the con-

6

fined compressive strength of Type A columnar samples was up to five times higher than the unconfined uniaxial strength. As expected, confinement had little effect on the Type B columnar specimens. There was a regular power law increase in strength with increasing strain rate in all the test types in granular ice but only for the Type B and C tests in the -2°C columnar ice. Even though the freshwater ice and the sea ice samples behaved similarly, the Type A confined compressive strength of sea ice is much lower than that of freshwater ice.

Hausler (1981) performed both biaxial and triaxial tests on cubic sea ice samples using an electrohydraulic, closed-loop triaxial testing machine equipped with brush platens. Columnar sea ice samples that had a salinity of about 10‰ were grown in the laboratory and then tested at a strain rate of 2×10^{-4} s^{-1} and a temperature of -10°C. Unfortunately Hausler's results are awkwardly presented and, as a result of the limited number of tests, difficult to interpret. The maximum confined compressive strength was about 18.6 MPa under "conventional" triaxial loading conditions where the lateral confinement was 67% of the applied stress. The uniaxial compressive strength for this orientation was about 10.3 MPa, or half the confined strength.

Jones (1982) performed conventional triaxial tests on freshwater random polycrystalline ice. At strain rates below 10^{-5} s^{-1}, the confining pressure ($\sigma_2 = \sigma_3$) had little effect on the ice yield strength ($\sigma_1 - \sigma_3$); at high strain rates, the yield strength increased nonlinearly to about twice the uniaxial compressive strength. At 1.4×10^{-2} s^{-1} and -11.5°C, the yield strength peaked at about 26 MPa at a confining pressure of 24.8 MPa. The confined compressive strength of the ice was therefore about 51 MPa.

Tensile strength

There are few data on the uniaxial tensile strength of sea ice σ_t, as direct tension tests are difficult to do. Tension specimens must be prepared to very high tolerances to minimize bending of the sample, and it is difficult to apply uniform tensile stresses to the specimen end planes.

The most detailed set of direct tension tests on first-year sea ice have been performed by Dykins (1967, 1970) and summarized by Katona and Vaudrey (1973). Samples were prepared in the laboratory from saline ice sheets grown from natural seawater and brackish (diluted) seawater. The natural seawater ice samples had salinities of 7-9‰,

densities around 0.920-0.925 Mg/m³, and grain sizes varying from about 0.25 to 8 grains/cm². The brackish ice samples had salinities of 1-2‰, densities of about 0.900-0.915 Mg/m³, and grain sizes varying from 0.25 to 1.25 grains/cm². All ice sheets had a well-defined columnar structure with a horizontal c-axis orientation. The c-axes showed no preferred orientation in the horizontal plane. In general, the grain size increased with depth in each ice sheet.

Test specimens were machined on a lathe from 7.6-cm-diameter cores using a form tool to produce dumbell-shaped specimens with neck diameters of 5.1 cm and neck lengths of 1-2.5 diameters. (The strength did not vary significantly over this range of length:diameter ratios.) Photoelastic studies of this sample geometry showed that there were no large stress concentrations near the sample end planes and that the stress was uniform in the neck of the sample.

A neck diameter of 5.1 cm was chosen to ensure fracture in the neck of the specimen. Because of the large grains in most of the specimens, a larger diameter sample would have been preferable. Recent studies have shown that diameter:grain size ratios of 10-20 are needed to characterize the bulk properties of a material (Schwarz et al. 1981). However, as a large number of tests were done at each test condition, we feel that the mean strength values are representative of the bulk material properties for unaligned sea ice.

Tests were carried out on both vertical and horizontal test specimens to evaluate the effect of sea ice anisotropy on the tensile strength. The tests were conducted on a 10,000-lb-capacity machine at a constant cross-head velocity of 1.27 cm/s, or a nominal strain rate of about 10^{-3} s^{-1}. Test temperatures were -4°, -10°, -20° and -27°C.

Tensile strength data from vertical samples are plotted against the ice brine volume in Figure 7. The strength ratios between the horizontal and vertical specimens ranged from ½ to ⅓, with the σ_t values always highest from samples oriented vertically. A least-squares analysis of the test results gives

$$\sigma_t = 1.54 - 0.0872 \sqrt{v_b} \qquad (3)$$

for the vertical samples ($r^2 = 0.8674$) and

$$\sigma_t = 0.816 - 0.0689 \sqrt{v_b} \qquad (4)$$

for the horizontal samples ($r^2 = 0.9493$), with σ_t in MPa and v_b in ‰. Dykins (1970) also gave density
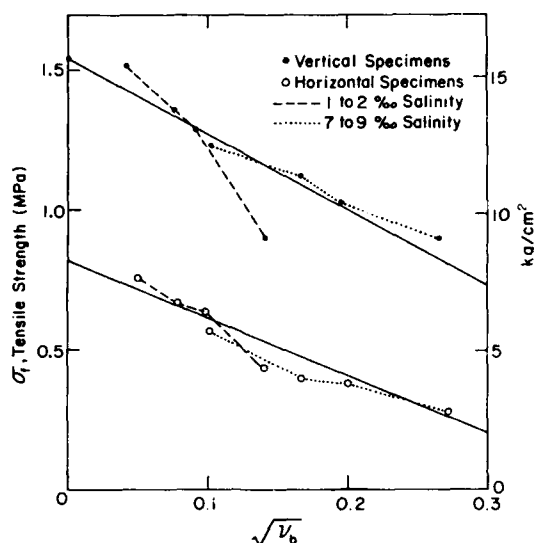
7

Figure 7. Tensile strength vs the square root of the brine volume for samples oriented vertically and horizontally relative to a horizontal ice sheet. (After Dykins 1971.)

data for each specimen, so it is possible to analyze the variation in ice strength with total porosity (air plus brine volume) although this has not been done.

The only other direct tension data on first-year sea ice are those of Peyton (1966). Unfortunately his results are presented in a manner that makes them difficult to use or compare with the results of other investigators. However, his results on oriented horizontal specimens do show a slight variation in strength with respect to the loading direction and crystal c-axis orientation (Fig. 2).

Direct tension tests have also been done on vertical ice samples from multi-year sea ice pressure ridges using state-of-the-art techniques (Cox et al. 1985, Cox and Richter-Menge 1985). Tests were conducted at nominal strain rates of 10^{-3} and 10^{-5} s^{-1} at $-20°$ and $-5°C$. The specimens had an average tensile strength of 0.72 ± 0.17 MPa and showed little variation with either strain rate or temperature. The strength decreased slightly with increasing ice porosity.

The combined results of Peyton (1966) and Dykins (1970) indicate that σ_t does not vary with stress rate $\dot{\sigma}$ in the range between 1×10^3 and 1.8×10^3 Pa s^{-1}. This agrees with the results of carefully performed tensile tests on fine-grained, bubbly freshwater ice (Hawkes and Mellor 1972), which indicated little change ($\simeq 25\%$) in σ_t over

five orders of magnitude in strain rate $\dot{\varepsilon}$. However, at $\dot{\sigma}$ values greater than 0.18 MPa s^{-1}, Dykins observed a decrease in σ_t, with the strength dropping to 52% of the initial value. This decrease probably results from imperfections in the sample preparation and testing techniques, which are more critical at higher loading rates.

We would expect that many of the factors affecting the tensile strength of sea ice also affect its compressive strength. For instance σ_c and σ_t both strongly depend on the brine volume of the ice. Yet Dykins's results (1970) indicate that σ_t does not depend on $\dot{\sigma}$ in the limited range studied, while σ_c shows a strong dependency. Also σ_t values for sea ice do not appear to be sensitive to changes in grain size while similar measurements on fine-grained, polycrystalline freshwater ice show a pronounced dependence (Currier and Schulson 1982). Clearly more tests are needed.

Because direct tension tests are difficult to perform, there has been a tendency to substitute simpler indirect tests, such as the ring-tensile test and the Brazil test. Unfortunately these substitutions have not been successful, and the use of such indirect tests should be avoided. The basic problem is that the theory behind these tests usually assumes rather idealized material behavior, an assumption that is not met by sea ice.

Flexural strength

The flexural strength is not a basic material property but only an index strength. Nevertheless it is useful in many applied problems, and considerable data are available for sea ice, so it will be discussed. In sea ice the flexural strength is usually measured with cantilever beam tests or simply supported beam tests. In lake ice (Gow et al. 1978) and low-salinity sea ice (Määttänen 1975), cantilever beams give results up to 50% less than simply supported beams, a difference believed to be the result of stress concentrations at the butt end of the cantilevers. These differences do not occur in sea ice, presumably because its more plastic nature relieves the stress concentrations.

The most extensive work on a variety of sizes of fixed-end and simply supported beams, including some beams 2.4 m thick, is by Dykins (1971). Cantilever tests were conducted first, causing the beam to fail near the cantilever root. The freed beam was then simply supported at each end and hydraulically loaded by applying a 30.5-cm line load to the middle of the beam at a rate of 0.20 to 0.24 MPa s^{-1}, causing the beam to fail in 2–4 s. Small beams were also tested in the laboratory using a

8

four-point, simply supported loading scheme. His results and other tests by the Naval Civil Engineering Laboratory (NCEL) have been summarized by Vaudrey (1977) and are presented in Figure 8. The flexural strength values are plotted against the square root of the ice brine volume, with the brine volumes determined from the average temperature and salinity of the beams. Even though many of the large in situ beams had strong temperature gradients through the beam, these results agree well with the isothermal laboratory beam tests. Furthermore the results from the in situ cantilever tests, where the top portion of the beam was in tension, agree closely with the in situ simply supported beams, where the bottom portion of the beam was in tension. Since the ice is warmer near the bottom of the sheet, we would expect the simply supported beams to give lower values. Similar results from both tests certainly facilitate using the data.

A least-squares line through the NCEL data gives

$$\sigma_f = 0.959 - 0.0608 \sqrt{v_b} \tag{5}$$

with σ_f in MPa and v_b in ‰. For brine volumes greater than 100‰, tests by Tabata et al. (1975) and Weeks and Anderson (1958) suggest that σ_f remains constant at about 0.2 MPa up to brine volumes of 250‰.

Flexural tests on small beams show that the flexural strength depends slightly on loading rate (Tabata 1960, Tabata et al. 1975, Saeki et al. 1979,

Lainey and Tinawi 1981). Unfortunately the trends obtained by different investigators are inconsistent, and it is not clear whether the differences are caused by real physical changes in the ice or by variations and imperfections in testing techniques (Mellor 1983, Weeks and Mellor 1983). On large in situ beams, the flexural strength dramatically increases with loading rate (Tabata 1960, Tabata et al. 1967). However, the results of Enkvist (1972) and Määttänen (1975) indicate that if corrections are made to eliminate the inertial forces associated with the beam mass and hydrodynamic water forces, the increases disappear and σ_f becomes independent of $\dot{\sigma}$. This result is certainly appealing, as σ_t has been found to be essentially independent of $\dot{\epsilon}$ at moderate to high strain rates.

In recent unpublished work on the effect of c-axis alignment on the flexural strength of cantilever beams, when the axis of a beam was normal to the c-axes in the ice sheet, the flexural strength values were about 50% greater than for beams parallel to the c-axes.[*] In the hard-fail orientation it is necessary to fail the ice across the platelets in individual crystals.

Shear strength

Only a limited number of shear strength tests have been reported. In fact, many tests described as "shear" are actually the result of mixed mode failures, as in punch tests. Indeed it is very difficult to obtain pure shear tests. The best sets of

---

[*] Personal communication with R. Frederking.
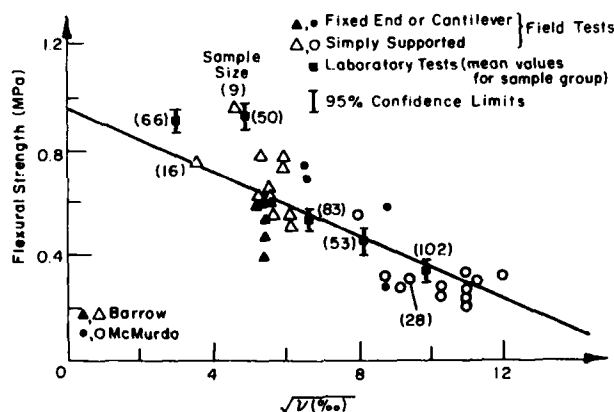
Figure 8. Flexural strength of sea ice for in situ and laboratory beam tests vs the square root of the brine volume. (After Vaudrey 1977.)

9
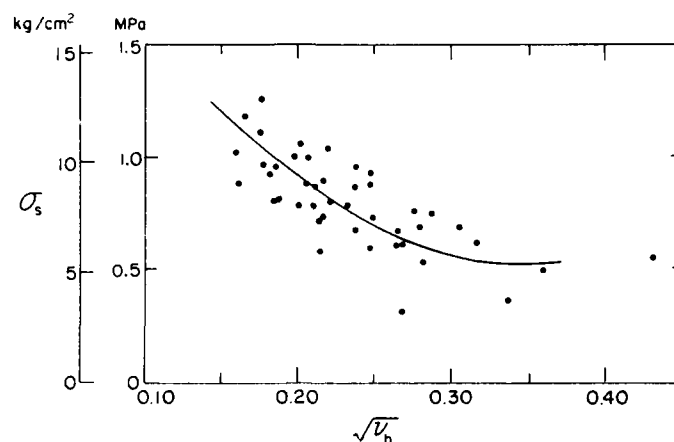
Figure 9. Shear strength of Antarctic sea ice as a function of the square root of the brine volume. (After Paige and Lee 1967.)

shear tests available are those of Paige and Lee (1967) and Dykins (1971). Paige and Lee's results for vertical samples (shear plane parallel to the growth direction) are plotted against the square root of the brine volume in Figure 9. A least-squares analysis of the shear strength data gives

$$\sigma_s = 1.68 - 0.118\sqrt{v_b} \qquad (6)$$

with σ_s in MPa and v_b in %.

The data obtained by Paige and Lee are the best available for columnar sea ice, but unfortunately the apparatus holding their samples produced an unknown normal stress on the shear plane, and the strength values are probably conservative. The tests need to be repeated using better testing techniques. Recently Frederking and Timco (1984) proposed a four-point bending test device to determine the shear strength of sea ice. Their tests on granular ice show much lower strength values. Their data for columnar samples have not yet been published.

Results indicate that there is a strong dependence on loading rate, although the data are very limited. Dykins's results suggest that shear strength is not appreciably affected by changes in crystal orientation. If further experimentation supports this finding, it will have a considerable effect on current thinking about how ice strength is influenced by ice structure.

Shear strengths reported for lake ice are lower than those reported for sea ice. Whether this is the result of structural differences or of differences in testing procedures is unknown.

Yield criteria

It is beyond the scope of this review to provide a lengthy discussion of pure ice or sea ice yield criteria. However, a few general comments can be made based on a recent discussion by Mellor (1983).

At very low strain rates ($< 10^{-6}$ s^{-1}) the tensile strength σ_t of ice is approximately equal to the compressive strength σ_c, and confinement has little or no effect on the ice yield strength. Such ice can be well described by a Von Mises or Tresca failure criterion. At higher strain rates the compressive strength becomes greater than the tensile strength, and a Mohr-Coulomb failure criterion may be more appropriate. At low confining pressures a straight-line extrapolation from σ_t to σ_c into the compression–compression quadrant is probably a good approximation. For higher confining pressures Mellor (1983) suggested using a nonlinear Mohr-Coulomb criterion that takes pressure-melting effects into consideration.

Unfortunately, because of the paucity of multi-axial test data, we can only guess at the nature of the ice yield surface at high confining pressures. Such an attempt was made by Ralston (1977), who used Frederking's (1977) freshwater ice plane-strain confined data to formulate an anisotropic yield criterion for columnar ice (Fig. 10). Uniaxial and plane-strain confined test data were used to define a parabolic Mohr-Coulomb yield criterion (a Pariseau [1972] yield surface) for planar isotropic columnar ice (c-axis horizontal with no preferred alignment). Timco and Frederking (1983) have also used their plane-strain compressive

10
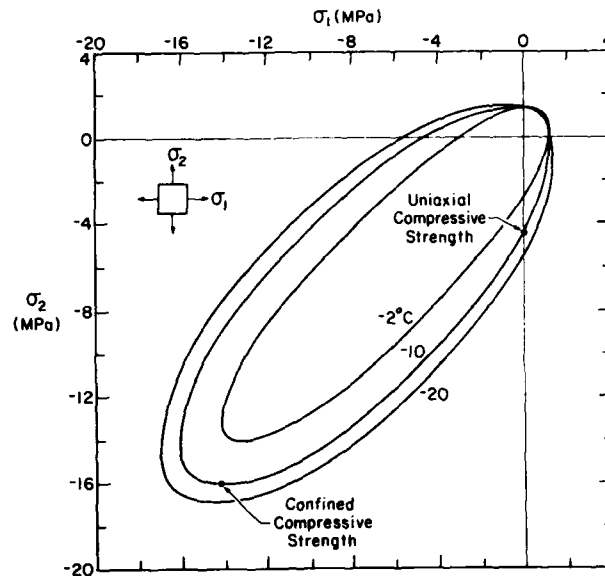
Figure 10. Parabolic Mohr–Coulomb yield criterion for un-oriented columnar ice. (After Ralston 1979.)

strength data for sea ice to calculate Pariseau yield surfaces for both granular and columnar sea ice under plane-strain and plane-stress loading conditions. The results are compared to Ralston's (1979) freshwater ice yield surfaces in Figure 11. At comparable temperatures and strain rates, the
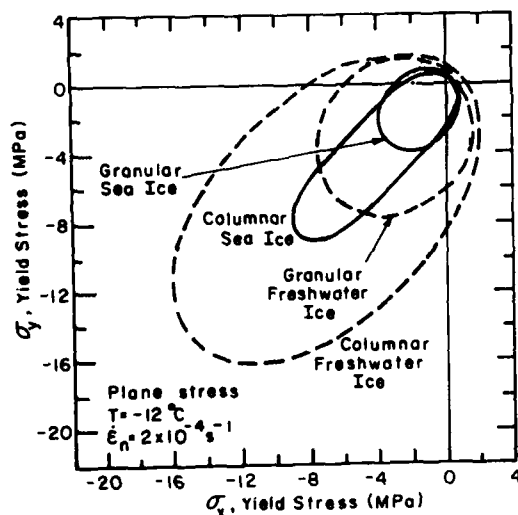
Figure 11. Yield surfaces for both columnar and granular sea ice and freshwater ice. (After Timco and Frederking 1984.)

sea ice yield surface is much smaller. The three-dimensional yield surface for columnar ice changes in both size and shape with changes in loading rate. With a decrease in ice temperature, the failure envelope becomes appreciably larger but remains similar in shape (Timco and Frederking 1986). Timco and Frederking also presented equations for the failure envelope of columar sea ice at both $-2°C$ and $-10°C$. Analytical models that have used Ralston's freshwater ice yield surface for sea ice loading problems should therefore be reevaluated.

Recently Hausler (1983) reanalyzed his multi-axial loading test results for saline ice and suggested that a Smith yield criterion may be more appropriate for sea ice. Smith's (1974) yield criterion is similar to that developed by Pariseau with the addition of an extra term that more realistically describes the compaction of ice under hydrostatic pressure.

Elastic constants

Dynamic measurements

Dynamic measurements of the elastic modulus E are determined by either measuring the rate of wave propagation in the ice or by exciting the natural resonant frequencies of different vibration modes. The induced displacements are very small, and anelastic effects are also commonly small.

11

Therefore, dynamic measurements of E tend to be more reproducible than typical static values.

In situ seismic determinations of E were reviewed by Weeks and Assur (1967). They vary from 1.7 to 5.7 GPa when measured by flexural waves and from 1.7 to 9.1 GPa when determined by in situ body wave velocities. This is reasonable because the flexural wave velocity is controlled by the overall properties of the ice sheet, while the body wave velocity is controlled by the high-velocity channel in the commonly colder and stronger upper section of the ice. As the sheet ice salinity and temperature vary, E changes markedly throughout the year. The results of Anderson (1958), plotted as a function of brine volume in Figure 12, show a large decrease in E with increasing brine volume.

Most dynamic determinations of E are not from in situ measurements but are determined on small, reasonably homogeneous samples that have been removed from the ice sheet. Figure 13 shows a typical series of such tests. E values at zero brine volume are characteristically found to be 9–10 GPa, in good agreement with the seismic determinations. Within the range of brine volumes studied, E decreases linearly with increasing v_b, where

$$E = 10.00 - 0.0351 v_b \qquad (7)$$

with E in GPa and v_b in ‰. At v_b values greater than 0.15 there is some evidence that E becomes a very weak function of v_b (Slesarenko and Frolov
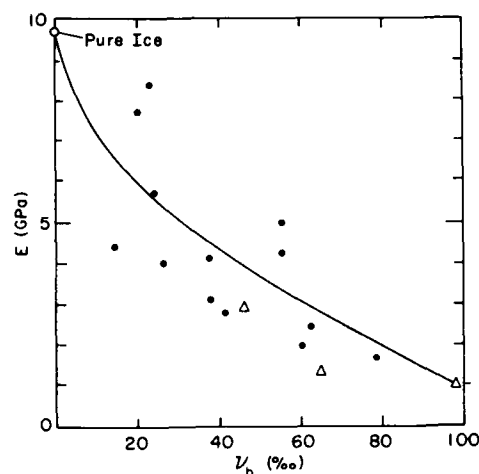
Figure 12. Elastic modulus of sea ice as determined by seismic measurements vs brine volume (Anderson 1958). The three triangular points are from the static tests performed by Dykins (1971).

1974). Tests on small samples give much larger values of E at moderate brine volumes. Since there is considerable uncertainty in determining the depth of the high-velocity layer in in situ tests, we recommend using the small-sample data to estimate Young's modulus for sea ice.

As yet, dynamic determinations of E are almost completely from first-year columnar sea ice. It is
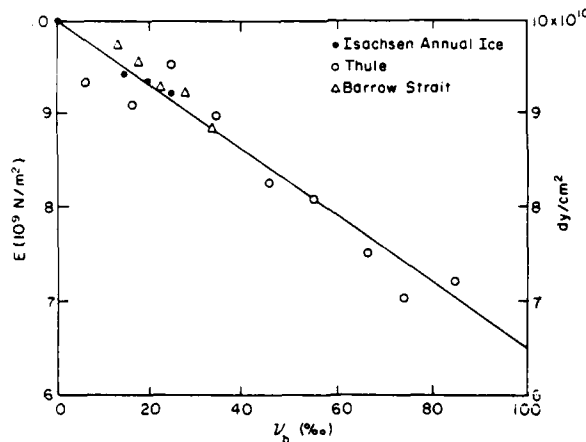
Figure 13. Elastic modulus vs brine volume for small specimens of cold arctic sea ice. (After Langleben and Pounder 1963.)

12

important that measurements be obtained from other ice types. Also, in spite of the relative ease of dynamic tests, the number of available measurements is very small. It would also be useful to try to develop an adequate theory for the observed variation in E with changes in void volume and crystal orientation based on a realistic model of the arrangement of inclusions in sea ice.

Static measurements

Static measurements of E are more variable and difficult to interpret than dynamic measurements because of the viscoelastic behavior of ice when subjected to significant stresses for finite periods of time. Nevertheless, it is these effective E values that are applicable to most engineering problems. The most extensive work on the static modulus of sea ice is by Dykins (1971), who tested small beams in bending. His stress–strain curves, obtained at stress rates of 0.25 MPa s⁻¹, are nearly linear. The plots of E vs temperature suggest discontinuities at temperatures where $Na_2SO_4 \cdot 10H_2O$ and $NaCl \cdot 2H_2O$ precipitate (–8.2°C and –22.9°C, respectively). However, the testing was not sufficiently detailed to clearly establish this effect. When E_{eff} was plotted against v_b, the values indicated by the triangles in Figure 12 were obtained. The values obtained by static measurements generally agree with the "seismic" values obtained by Anderson. Finally, Vaudrey (1977) used strain data from both large-beam field tests and small-beam laboratory tests to determine E_{eff} as a func-

tion of brine volume. The E values were linear when plotted vs $v_b^{1/2}$ (Fig. 14). A least-squares analysis of the data gives

$$E_{eff} = 5.31 - 0.436 \sqrt{v_b} \qquad (8)$$

with E_{eff} in GPa and v_b in ‰.

Information on the time dependence of E in sea ice is inadequate. The best studies of this problem are by Tabata and his group (see references in Weeks and Assur 1967). Their results from small beams and from in situ cantilevers suggest that $\log E$ increases as a linear function of $\log \dot{\sigma}$, approaching the dynamic value at large values of $\dot{\sigma}$.
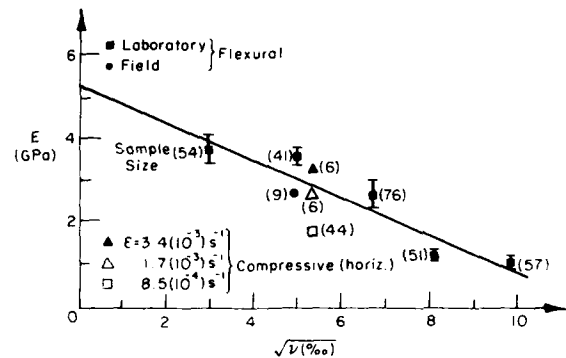
Figure 14. Effective elastic modulus of sea ice vs the square root of the brine volume. (After Vaudrey 1977.)
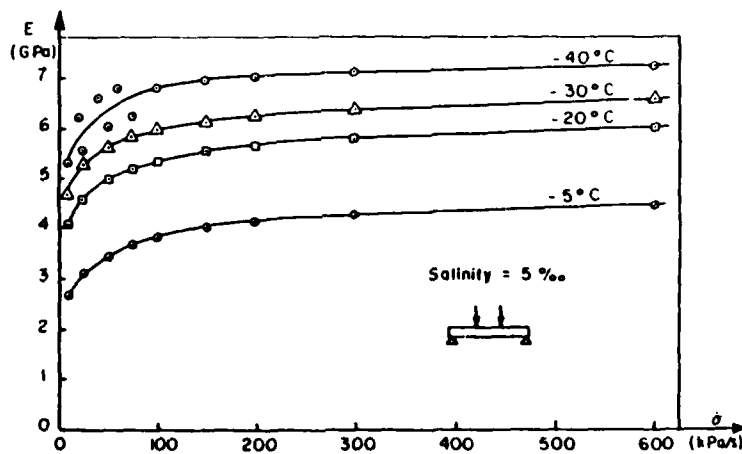
Figure 15. Effective elastic modulus of saline ice with a salinity of 5‰ at different loading rates and temperatures. (From Lainey and Tinawi 1981.)

13

Even Tabata's highest value for E (2 MPa) is much lower than Dykins's or Peyton's lowest value (0.6 GPa). This large difference may be explained by differences in the test conditions. Tabata's tests were performed at very high temperatures. Subsequent work by Lainey and Tinawi (1981) demonstrated how the effective modulus of laboratory saline ice varies with temperature and loading rate. They conducted flexural tests on saline ice beams having a salinity of 5‰ (Fig. 15). The effective modulus increased with increasing loading rate and decreasing temperature. The high-rate loading tests are in general agreement with the values reported by Vaudrey (1977). Compression tests by Tratteberg et al. (1975) for freshwater ice also support the trends noted above. They also found that the effective modulus of columnar ice is greater than that of granular ice.

As was the case for dynamic determinations of E, available observations have largely been made using first-year sea ice. Only recently have static measurements of E been made on multi-year sea ice. Cox et al. (1984a,b, 1985) gave modulus values in compression and tension for ice samples from multi-year pressure ridges (Fig. 16) that are comparable in magnitude to those reported by Tratteberg et al. (1975) for freshwater ice. The effective modulus increased with increasing strain rate and decreasing temperature. When the compression and tension effective modulus values are compared at low strain rates (10^{-5} s^{-1}), the modulus values in tension are greater. This is because at 10^{-5} s^{-1}, ice loaded in compression macroscopical-

ly behaves in a ductile manner, whereas ice loaded in tension is still largely brittle. At 10^{-3} s^{-1} the ice is brittle in both tension and compression, and modulus values are similar. The data did not exhibit considerable scatter, which was attributed to large variations in the structure of the ridge samples (Richter and Cox 1984). The 10^{-3} s^{-1} values are very close to dynamic E values for first-year sea ice. It is important that observations also include the other varieties of ice that occur in the sea.

Poisson's ratio

As with the effective Young's modulus, it is the effective Poisson's ratio that is of interest in most ice engineering problems. The only available published data on the effective Poisson's ratio for sea ice are by Murat and Lainey (1982), who measured the longitudinal and transverse strains on simply supported sea ice beams loaded in flexure. Tests were conducted at different temperatures and loading rates. The sea ice beams consisted of columnar ice with horizontal c-axes and a salinity of 5‰. The effective Poisson's ratio decreased with increasing stress rate and decreasing temperature. At very low stress rates the ratio approached the expected limit of 0.5, and at high stress rates the ratio approached 0.33, the dynamic or seismic value of Poisson's ratio for sea ice.

A general expression was obtained expressing the effective Poisson's ratio μ' in terms of the stress rate and the dynamic Poisson's ratio at the temperature of interest:
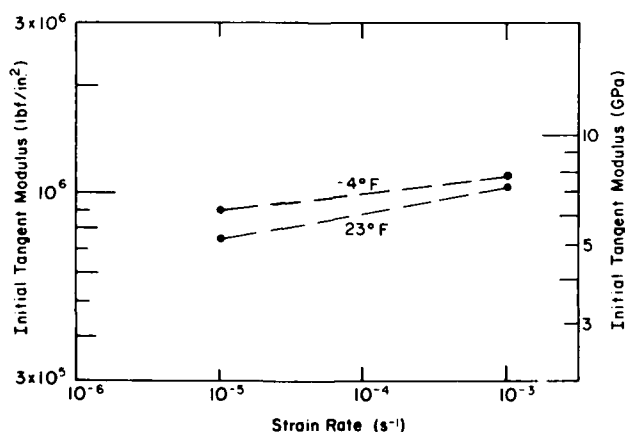
Figure 16. Average initial tangent modulus of multi-year pressure ridge ice samples vs strain rate for tests at -5°C (23°F) and -20°C (-4°F).

14

$$\mu' = (2.4 \times 10^{-1})(\dot{\sigma}/\dot{\sigma}_1)^{-0.29} + \mu_D \qquad (9)$$

where $\dot{\sigma}$ is the stress rate, $\dot{\sigma}_1$ is a unit stress rate (1 kPa s^{-1}), and μ_D is the dynamic Poisson's ratio determined from

$$\mu_D = 0.333 + (6.105 \times 10^{-2}) \exp(T/5.48) \qquad (10)$$

where T is the ice temperature in °C (Weeks and Assur 1967). Murat and Lainey also assumed that the strain rate could be approximated by

$$\dot{\epsilon} = \dot{\sigma}/E' \qquad (11)$$

where $\dot{\epsilon}$ is the strain rate and E' is the effective Young's modulus and obtained

$$\mu' = (2.4 \times 10^{-3})(\dot{\epsilon}/\dot{\epsilon}_1)^{-0.30} + \mu_D \qquad (12)$$

where $\dot{\epsilon}_1$ is a unit strain rate (1 s^{-1}).

These expressions are for unoriented columnar sea ice. In compression tests on horizontal, oriented columnar sea ice samples having aligned c-axes, Wang (1981) reported that μ' ranged from 0.8 to 1.2 in the horizontal direction (normal to the columnar crystals) and from 0 to 0.2 in the vertical direction (parallel to the columns). Insufficient data are given to use these results properly.

Fortunately a detailed examination of the theoretical effects of the vertical variation of μ through a floating ice sheet on the mechanical response of the sheet (Hutter 1975) has indicated that for many real problems it is not necessary to consider such variations.

THE TEMPERATURE-SALINITY MODEL

To obtain a brine volume profile that can be used to estimate ice property profiles, one must first develop a model for predicting temperature and salinity profiles. Fortunately the ice sheet temperature and growth problem has received considerable attention because of its importance in heat and mass balance studies. Therefore, a suitable temperature and growth model can be developed by combining and slightly modifying existing studies (Maykut 1978, Miller 1979). The problem of calculating the salinity profiles from the ice growth conditions has been less thoroughly studied. The model developed here serves as a preliminary, but encouraging, probe into this complex problem.

Temperature profiles

Because first-year ice temperature profiles are essentially linear (Maykut 1978), the ice surface temperature, the freezing temperature of the underlying sea water and the thickness are sufficient to describe the temperature distribution in the ice sheet. In the following the ice surface temperature for a representative location in the Arctic Ocean is determined by doing an energy balance of the heat fluxes at the ice surface. The conductive heat flux obtained from the surface energy balance is then used to calculate the rate of growth and the thickness of the ice via the Stefan equation.

Ice surface energy balance

The detailed equations for calculating the ice surface temperature and the conductive heat flux can be found in Maykut (1978) and are summarized in Appendix A of this report. As environmental input we have used his recommended values for incoming short-wave and long-wave radiation, ambient temperature and relative humidity for different times during the ice growth period of September–June over the Arctic Basin.

Our analysis deviates slightly from Maykut's in that we have used Ono's (1975) formulation for the thermal conductivity of sea ice. We also used the salinity of the ice surface layer that is given by our salinity model in the calculations of the conductive heat flux. In addition, the half-interval method, rather than the Newton-Raphson method, was used to solve for the ice surface temperature in the energy balance equation. This simplifies the calculation of the ice surface temperature if changes are made in the input to the energy balance equation (Miller 1979).

We did not consider what effect the presence of varying amounts of snow on the sea ice surface would have on our simulations. This important omission will be considered in subsequent work. Maykut (1978) provided additional details on the energy balance method and the significance of snow in ice growth problems.

Ice growth

A finite difference scheme was used to describe the ice growth and to calculate the changes in ice temperature. In our model, 0.5-cm layers of ice were incrementally added to the bottom of the ice sheet. The time required to grow each layer was then calculated from Stefan's equation:

15

$$\Delta t = \frac{\varrho L}{\bar{F}_c} \Delta H \qquad (15)$$

where Δt = time required to grow the ice layer of thickness ΔH (0.5 cm)

ϱ = ice layer density

L = latent heat of freezing

$\bar{F}_c$ = average conductive heat flux.

The ice density was calculated using the equations given by Cox and Weeks (1983) with the ice air volume set equal to zero. The latent heat of freezing was assumed to be constant at 70 cal/g, and the average conductive heat flux was taken as the arithmetic mean of the conductive heat flux at the top and bottom of each layer obtained from the surface energy balance. We attempted to use a more rigorous description of the latent heat of freezing (Ono 1967, 1975), but the growth rates and initial ice salinities were unrealistically high. The choice of the latent heat of freezing greatly affects the computed thickness and salinity of the ice, so it will require further consideration.

The average ice growth rate for a given layer is obtained from equation 15:

$$\frac{\Delta H}{\Delta t} \approx \frac{\bar{F}_c}{\varrho L} \cdot \qquad (16)$$

Salinity profiles

Initial salt entrapment

The initial ice salinity at the base of the ice sheet (the bridging layer) is determined by the growth velocity of the ice and the concentration of the underlying seawater. The initial salinity of the ice S_i is usually expressed as

$$S_i = k_{eff} S_w \qquad (17)$$

where k_{eff} is the effective distribution coefficient and S_w is the salinity of the seawater away from the growing ice interface. The best available data on the distribution coefficient are given by Cox and Weeks (1975), who gave equations for k_{eff} at high and low velocities. When these equations were used with the ice growth model, there was a salinity discontinuity at the transition growth velocity of 2.0×10^{-5} cm/s. The original data given by Cox and Weeks were therefore reanalyzed to produce high- and low-velocity k_{eff} equations that were continuous at the transition velocity. The following equations were used in the model. At velocities greater than 3.6×10^{-5} cm/s

$$k_{eff} = \frac{0.26}{0.26 + 0.74 \exp(-7243\,V)} \qquad (18)$$

where V is the ice growth velocity in cm/s. Between 3.6×10^{-5} and 2.0×10^{-6} cm/s

$$k_{eff} = 0.8925 + 0.0568 \ln V \qquad (19)$$

and below 2.0×10^{-6} cm/s k_{eff} was assumed to be constant at 0.12. No data are available at growth velocities less than 2.0×10^{-6} cm/s.

Brine expulsion

Immediately after brine is trapped in a growing ice sheet it begins to drain out into the underlying seawater by both brine expulsion and gravity drainage (Cox and Weeks 1975).

Brine expulsion occurs because the temperature in the ice sheet decreases during growth. As the ice sheet cools, water freezes on the interior of the brine cavities to concentrate on the brine and maintain phase equilibrium with the surrounding ice. Since the ice formed on the cavity walls occupies about a 10% greater volume than the original water in the brine, some brine is expelled out of the cavities into the underlying seawater.

Recently Cox and Weeks (1986) derived an equation to predict the amount of brine expelled from sea ice samples during sampling and storage. For air-free sea ice

$$\frac{S_i(T_2)}{S_i(T_1)} = \frac{S_b(T_2)}{S_b(T_1)} \frac{\varrho_b(T_2)}{\varrho_b(T_1)} \frac{v_b(T_2)}{v_b(T_1)} \qquad (20)$$

where S_i = ice salinity

S_b = brine salinity

ϱ_b = brine density

v_b = brine volume at temperatures T_2 and T_1.

If the ice is cooled ($T_2 < T_1$), the ratio of the brine volumes at T_2 and T_1 can be expressed as

$$\frac{v_b(T_2)}{v_b(T_1)} = \frac{S_b(T_1)}{S_b(T_2)}^{(1/\varrho_i)} e^{c/\varrho_i[S_b(T_1)-S_b(T_2)]} \qquad (21)$$

and equation 20 becomes

$$\frac{S_i(T_2)}{S_i(T_1)} = \frac{S_b(T_2)}{S_b(T_1)}^{(1-1/\varrho_i)} \frac{\varrho_b(T_2)}{\varrho_b(T_1)} e^{c/\varrho_i[S_b(T_1)-S_b(T_2)]} \qquad (22)$$

where ϱ_i is the density of pure ice (assumed to be constant at 0.918 g/cm³) and c is a constant equal

16

to $d\varrho_b/dT$ (0.0008 g/cm^3 °C). If the ice is warmed ($T_2 \geq T_1$), then

$$\frac{v_b(T_2)}{v_b(T_1)} = \frac{S_b(T_1)}{S_b(T_2)} \frac{\varrho_b(T_1)}{\varrho_b(T_2)} \qquad (23)$$

and

$$\frac{S_i(T_2)}{S_i(T_1)} = 1. \qquad (24)$$

Equations for calculating S_b and ϱ_b are also given by Cox and Weeks (1986).

These equations were used in our model to calculate the change in salinity in a given layer of ice due to brine expulsion. In applying this equation, we assumed that all the expelled salt from a given level was rejected directly out of the ice sheet. In reality the expelled brine and salt move downward, and the amount of expelled brine in the model was over-predicted (Cox and Weeks 1975). However, as the amount of brine drainage due to brine expulsion is considerably less than the brine lost by gravity drainage, this assumption resulted in only a small error.

Gravity drainage

In addition to brine expulsion, salt is lost from a growing ice sheet by gravity drainage. In sea ice the salinity and density of the brine are determined by the ice temperature. The colder the ice, the greater the brine salinity and density. In a growing ice sheet we have a positive temperature gradient (top colder than bottom) and an unstable brine density profile (denser brine on top). This results in convective overturn of brine within the ice, as well as the exchange of denser brine in the ice with the underlying less-saline seawater. The amount of gravity drainage depends not only on the ice temperature gradient but also on the ice permeability.

While we do not yet have a rigorous theoretical model of gravity drainage in sea ice, Cox and Weeks (1975) provided quantitative estimates of the amount of gravity drainage in growing sodium chloride ice. Their results show that as either the temperature gradient or the brine volume of the ice increases, the amount of desalination by gravity drainage increases. Also, at ice brine volumes less than 50%, gravity drainage stops. From their plots of the gravity drainage vs the temperature gradient and brine volume, we obtained for brine volumes greater than 50%:

$$\frac{\Delta S_i}{\Delta t} = 1.68 \times 10^{-5} \frac{\Delta T_i}{\Delta z} - 3.37 \times 10^{-7} v_b \frac{\Delta T}{\Delta z} \qquad (25)$$

where $\Delta S_i/\Delta t$ = rate of change in salinity due to gravity drainage (‰ per s)

$\Delta T/\Delta z$ = temperature gradient (°C/cm)

v_b = ice brine volume (‰) of a given layer.

This equation was used in our model to calculate the amount of salt lost by gravity drainage. If the brine volume of a given layer was less than 50‰, $\Delta S_i/\Delta t$ was set to zero. Furthermore, if there was an impermeable layer at depth ($v_b < 50$‰), $\Delta S_i/\Delta t$ was again set to zero for all layers above the impermeable boundary. The brine volume used in eq 25 was the average brine volume determined from eq 21, and the temperature gradient was the average temperature gradient during the given growth increment. The time ΔT was obtained from eq 15. The results from eq 22 and 25 were then used to calculate the new ice salinity, and given the new salinity and temperature of each layer, new ice brine volumes were calculated.

No attempt was made to calculate the volume of gas entrapped in the ice. This term is important, as the thermal properties of sea ice depend on the gas volume in the ice (Ono 1975). We hope to consider this term in more detail in subsequent publications. We have also ignored the skeleton layer at the base of the ice sheet, as the salinity of this 2.5-cm layer is poorly understood (sampling the salinity of the skeleton layer is extremely difficult because of rapid brine drainage). We believe that this omission is not critical, as this layer has little or no strength, and for thicker ice sheets that are important in ice load calculations, it is thin compared to the full thickness of the sheet.

COMPOSITE PLATE PROPERTIES

Several authors have stressed that the vertical variation in the properties of sea ice sheets must be considered in treating problems that deal with the sheet as a plate (Assur 1967, Weeks and Assur 1967, Kerr and Palmer 1972). For instance, to calculate the bending stresses in such composite sheets, both the position of the neutral axis and the flexural rigidity must be known. To investigate conditions requisite for failure, the stress distribu-

17

tion must be specified and coupled with the appropriate strength profile.

The position of the neutral axis from the top of the sheet z_N is calculated from

$$z_N = H - \frac{\int_0^H E_{eff}(z)(H-z)dz}{\int_0^H E_{eff}(z)dz} \qquad (26)$$

where H is the ice thickness, and $E_{eff}(z)$ is the effective modulus at depth z from the ice surface. For a homogeneous ice sheet, eq 26 reduces to

$$z_N = \frac{H}{2}. \qquad (27)$$

Once the position of the neutral axis is known, the flexural rigidity of ice sheet D can be obtained from

$$D = \int_0^H \frac{E_{eff}(z)(z-z_N)^2}{1-\mu^2} \, dz \qquad (28)$$

where μ is Poisson's ratio. For a homogeneous ice sheet, eq 28 reduces to

$$D = \frac{E_{eff} H^3}{12(1-\mu^2)}. \qquad (29)$$

Given the position of the neutral axis and the flexural rigidity, the fiber stress at depth z can be calculated for a bending moment M:

$$\sigma = \frac{M}{(1-\mu^2)D} (z-z_N) E_{eff}(z). \qquad (30)$$

RESULTS

Two types of simulations are presented here and in Appendices B and C. In the first set an ice sheet is assumed to form during the first part of the winter (1 October), and its subsequent properties are presented at growth increments of 15 cm (0.5 ft). The growth of the sheet is followed until the ice thickness reaches 213 cm (7.0 ft). In the second set of simulations the properties of 30-cm (1-ft) and 91-cm (3-ft) ice sheets are compared, assuming initial freezing dates of 1 October, 1 November and 1 February. These include, at 1-cm intervals, the estimated salinity (‰) and temperature (°C), which

Figure 17. Calculated salinity profiles for different thicknesses of a sea ice sheet that formed on 1 October. The assumed weather conditions are based on the climatological averages for the Arctic Basin given by Maykut (1978).

from the phase relations determine the brine volume v_b (‰), which in turn is then used to estimate the tensile σ_t and flexural σ_f strengths (MPa) and the effective elastic modulus E_{eff} (GPa). Based on the profile properties, values for the location of the neutral axis, the flexural rigidity and the characteristic length are calculated. For comparative purposes the bulk strengths and the effective elastic modulus are also presented based on the bulk brine volume calculated from the average ice salinity and temperature. These bulk values have typically been used in most ice mechanics studies.

Figure 17 shows the calculated salinity profiles for different thicknesses of an ice sheet that started to grow on 1 October. The general shapes of the profiles are reasonable when compared with idealizations of observational data (see Weeks and Assur 1967, Fig. 51). Since the calculations used meteorological conditions that varied smoothly with time, the salinity profiles lack the high-frequency variations observed in most field salinity profiles; if hourly meteorological data had been used in the model, we would have produced the
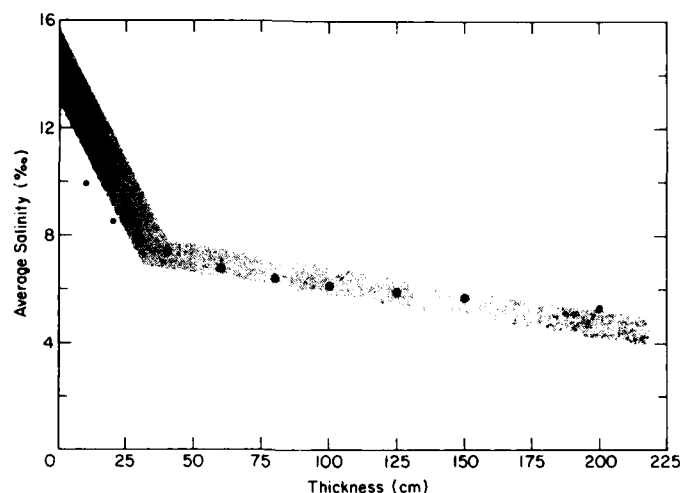
Figure 18. Calculated average ice sheet salinity vs ice thickness. The stippled band indicates the distribution of mean first-year ice salinities. (From Cox and Weeks 1974.)

high-frequency salinity variations. Figure 18 shows the average ice sheet salinity vs the thickness of the calculated profiles and the profiles of real sea ice sheets. The agreement is quite good, except that the calculated salinity of thin ice is slightly low while that of thick ice is slightly high. Both of these deviations are reasonable in terms of the model inputs: ice growth is assumed to start on 1 October when air temperatures are still relatively high, and the effect of a snow cover is not included. As most of the thin real ice composing the stippled band in Figure 18 grew when air temperatures were lower (most sampling was done during February–April), the growth rates of the thin ice were higher, and more salt was entrapped. The model simulations give an average salinity of $11.0\%_o$ for 30-cm ice that started to grow on 1 February, compared to $7.9\%_o$ for ice that started to grow on 1 October, values more in line with the observational data. If the presence of a snow cover had been included in the calculations, the result, because snow's insulating characteristics would slow the growth of the thicker ice, would be a lower average salinity.

Figure 19 shows the calculated temperature profiles for the different thicknesses of ice assuming a 1 October date for initial ice growth. For the period considered, the thicker the ice, the lower the ice temperature at any given level in the sheet and the
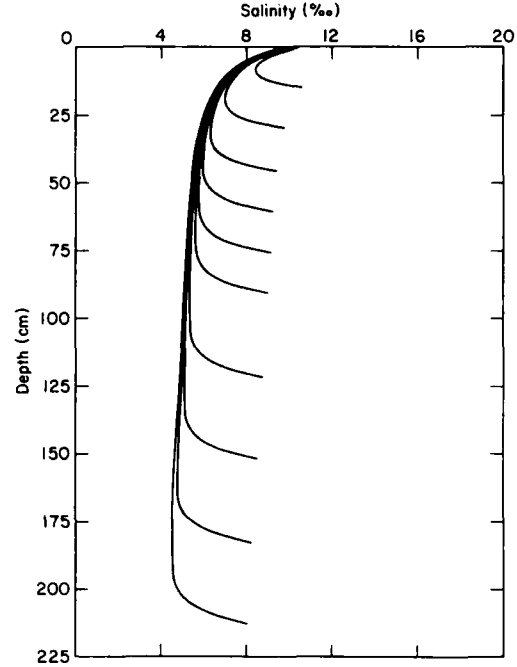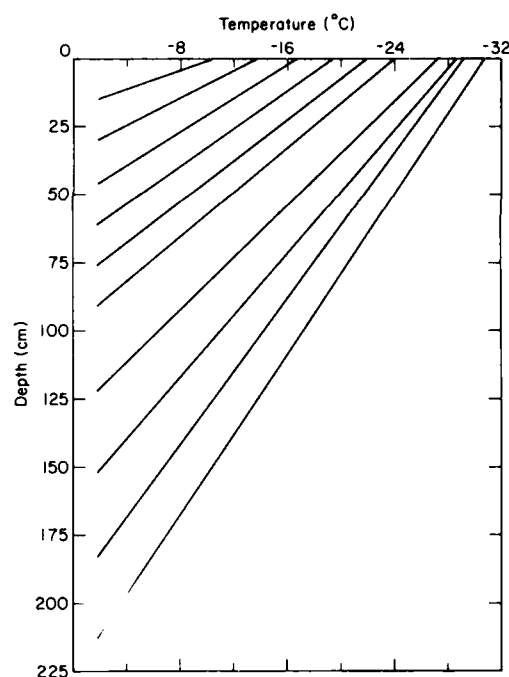

Figure 19. Calculated ice temperature profiles for different ice thicknesses for a sea ice sheet that formed on 1 October. The assumed weather conditions are based on the climatological averages for the Arctic Basin given by Maykut (1978).

19
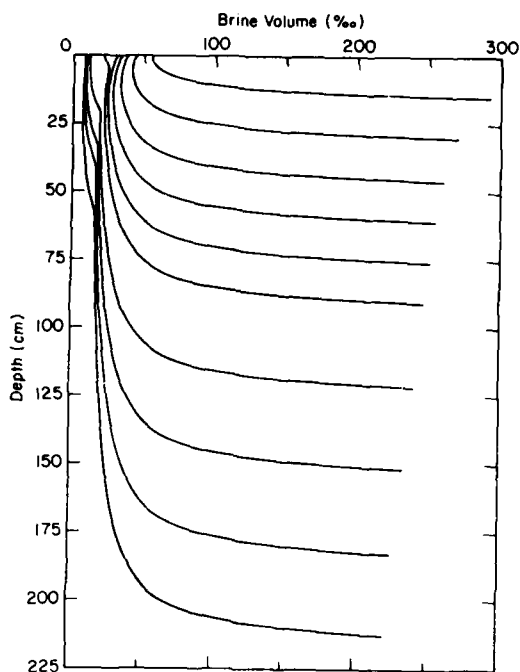
Figure 20. Brine volume profiles resulting from the calculated salinity and temperature profiles given in Figures 17 and 19.
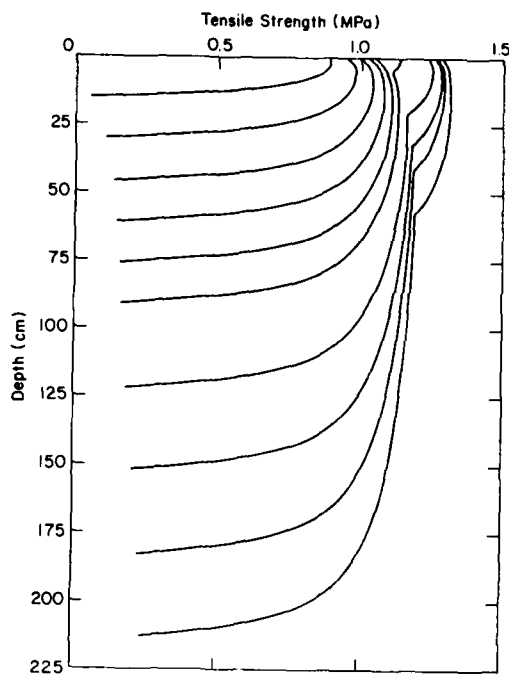
Figure 21. Tensile strength profiles calculated using eq 4 and the brine volume profiles given in Figure 20.
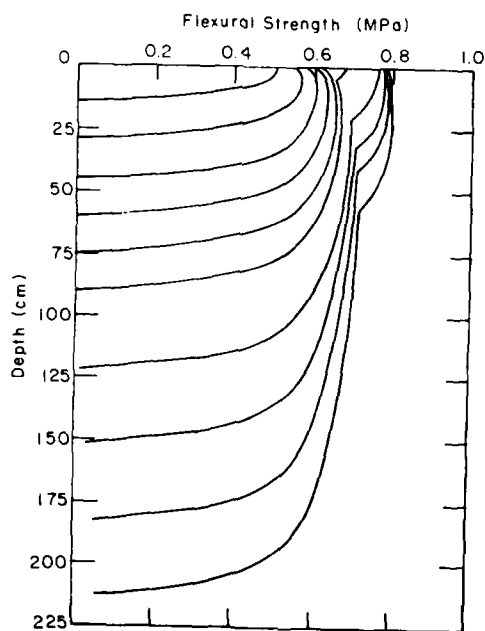
Figure 22. Flexural strength profiles calculated using eq 5 and the brine volume profiles given in Figure 20.
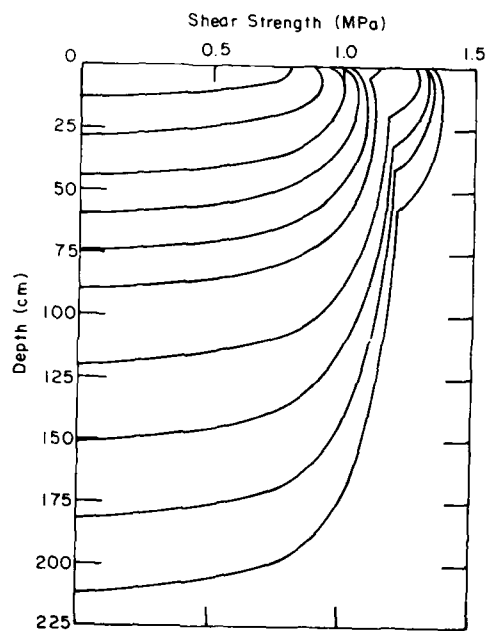
Figure 23. Shear strength profiles calculated using eq 6 and the brine volume profiles given in Figure 20.

20
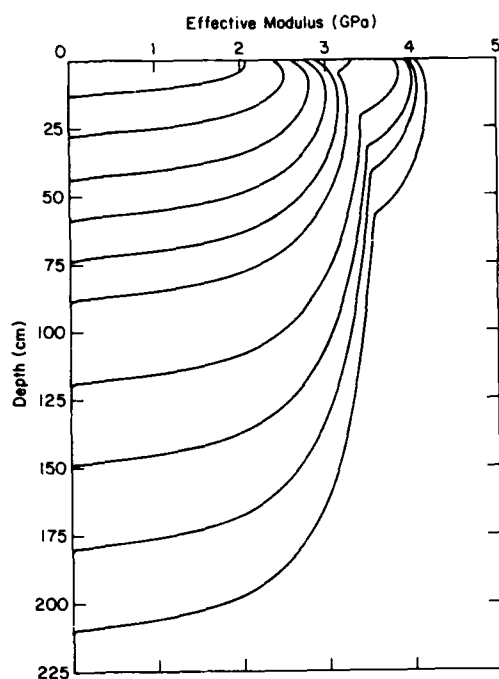
Figure 24. Effective elastic modulus profiles calculated using eq 8 and the brine volume profiles given in Figure 20.

Figure 25. Salinity profiles for 30- and 91-cm-thick ice assuming that ice growth starts on 1 October, 1 November and 1 February.

nearer the ice surface temperature to the ambient air temperature. Combining the temperature and salinity profiles gives the brine volume profiles shown in Figure 20. The ice brine volumes were calculated using the equations given by Cox and Weeks (1983). The kinks in the brine volume profiles for the five thicker ice sheets result from the ice in the upper parts of these sheets being colder than -22.9°C, with the subsequent crystallization of $NaCl \cdot 2H_2O$ and decrease in brine volume. Figures 21-24 show the vertical variations in tensile, flexural and shear strengths and effective elastic moduli calculated from the v_b profiles using eq 4, 5, 6 and 8. Again, the breaks in the curves are caused by the precipitation of $NaCl \cdot 2H_2O$. In all the profiles the strongest ice and the ice with the largest elastic modulus is not at the upper ice surface where the ice is coldest but at an intermediate depth that varies with ice thickness.

Figures 25 and 26 give the salinity and temperature profiles for 30- and 91-cm-thick ice (1 and 3 ft) that started to form on 1 October, 1 November and 1 February. In the calculated air temperature input for the model, the ambient temperature for the first day of each month from 1 October through 1 March was, respectively, -16.0, -25.3, -29.5, -29.8, -31.5 and -33.8°C (Maykut 1978). It is not

Figure 26. Temperature profiles for 30- and 91-cm-thick ice assuming that ice growth starts on 1 October, 1 November and 1 February.

21
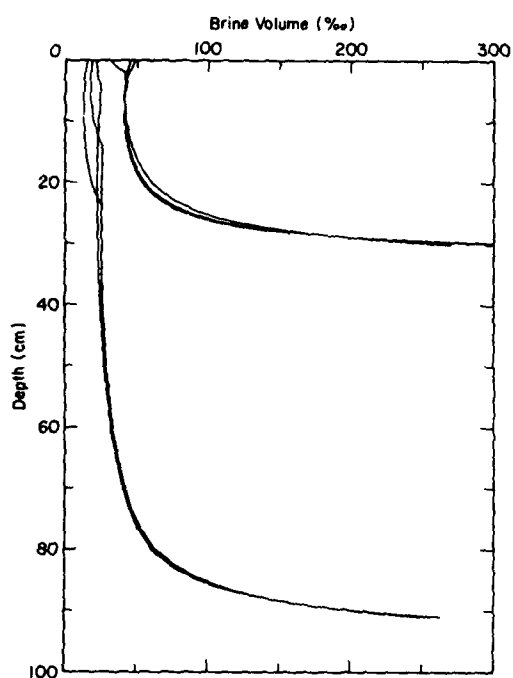
Figure 27. Brine volume profiles for 30- and 91-cm-thick ice assuming that ice growth starts on 1 October, 1 November and 1 February based on the salinity and temperature profiles shown in Figures 25 and 26.
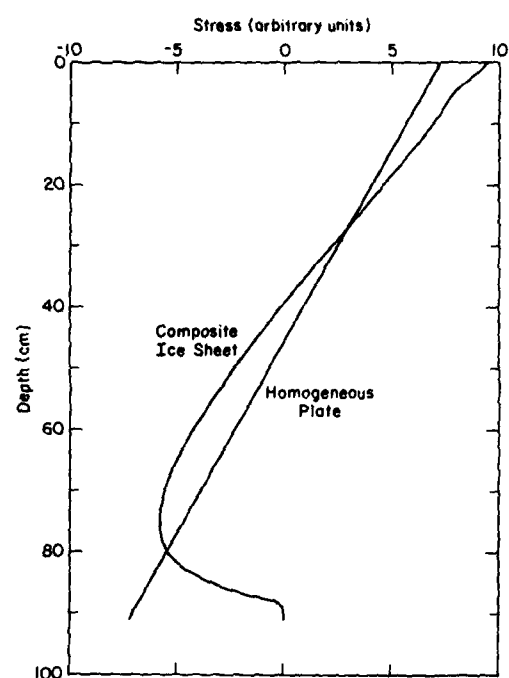
Figure 28. Calculated stress distribution at the butt end of a cantilever under loading such that the end of the cantilever is deflected downward (positive stress = tension).
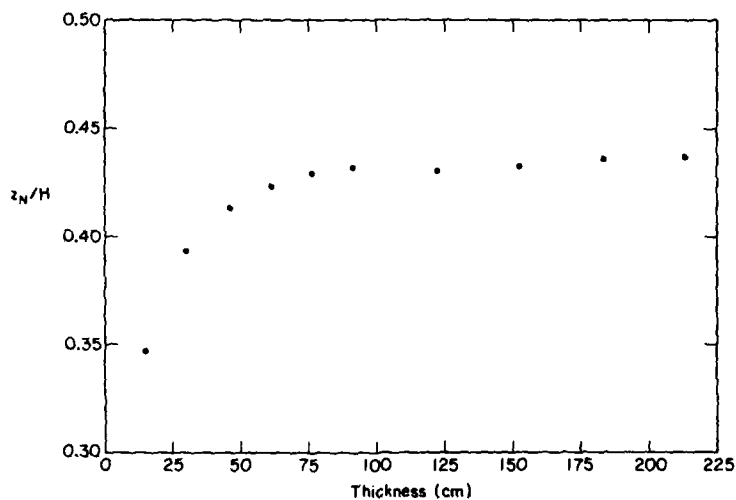
Figure 29. The dimensionless ratio z_N/H (distance to the neutral axis below the upper ice surface/total ice thickness) vs ice thickness. For a homogeneous plate, $z_N/H \approx \frac{1}{2}$.
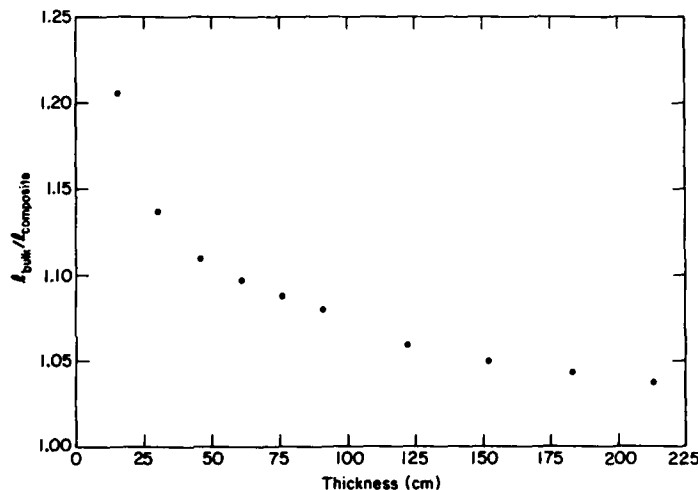
Figure 30. The ratio of the action radius ℓ based on bulk ice properties to ℓ based on composite ice properties plotted vs ice thickness for ice that formed on 1 October.

surprising that ice that starts to grow in February is both colder and more saline. What is surprising is that the temperature and salinity changes effectively offset each other and that the brine volume profiles are effectively independent of when the ice sheet started to grow (Fig. 27). This suggests that ice properties for the Arctic Basin can generally be considered to be a simple function of ice thickness during the ice growth season. Although it is easy to conceive of exceptions, such simple, albeit oversimplified, idealizations can be very useful in many types of studies dealing with long-term trends in ice behavior.

Figure 28 shows the calculated stress distribution in the butt end of a 91-cm-thick cantilever for an arbitrary bending moment under loading conditions such that the end of the cantilever is forced downward. The maximum stress for the composite ice sheet is 30% larger than the maximum stress for a homogeneous plate of the same thickness. Also the location of the neutral axis is 39.3 cm below the upper ice surface for the composite beam as compared with 45.5 cm for a homogeneous plate.

The trend in the location of the neutral axis expressed in a normalized form as the ratio of the distance to the axis below the upper ice surface z_N to total ice thickness H is shown in Figure 29. For a homogeneous plate, z_N is, of course, always equal to $H/2$ so $z_N/H = \frac{1}{2}$. Figure 29 clearly shows that the deviation of the neutral axis from

the midpoint of the plate is largest for thin ice sheets. Even for thick ice sheets the ratio z_N/H is only 0.44, compared to 0.50 for a homogeneous plate.

Figure 30 shows a plot of another plate parameter, the characteristic length or action radius ℓ, plotted as the ratio of the bulk ℓ to the composite ℓ vs ice thickness for the ice that formed on 1 October. For 15-cm-thick ice the bulk value is over 20% larger than the correct composite value, dropping to 4% larger for thick ice.

CONCLUSIONS

Data on the mechanical properties of sea ice are coupled with the results of a combined temperature–salinity model and are used to generate mechanical property profiles for undeformed, snow-free, first-year sea ice in the Arctic Basin. The results from the ice temperature–salinity model appear to be quite reasonable in that they show characteristic C-shaped profiles similar to natural profiles. The average ice sheet salinities are also in reasonable agreement with field data. The predicted profiles give composite plate properties that are significantly different from bulk properties obtained by assuming homogeneous plates. In addition, the failure strength profiles give maximum strengths in the interior of the sheet, unlike the usual assumption of maximum strength at the

23

cold, upper ice surface. Surprisingly, property profiles do not appear to be particularly sensitive to the date on which a given ice sheet started to form, suggesting that for some purposes ice properties can be taken as a simple function of ice thickness.

The mechanical property profile data presented in this report are only as good as the mechanical property test data used to generate the profiles from the predicted ice brine volumes. Furthermore, the ice salinity–temperature model is rather idealized, because we have not yet considered the ice air volume or snow on the ice surface. The model also needs to be verified with field and laboratory data. Should it be desired to predict the salinity and temperature from other than mean meteorological data, it will be necessary to improve the ice growth equations in the model to allow for nonlinear temperature gradients.

LITERATURE CITED

Anderson, D.L. (1958) Preliminary results and review of sea ice elasticity and related studies. *Transactions of the Engineering Institute of Canada,* 2: 116–122.

Assur, A. (1958) Composition of sea ice and its tensile strength. In *Arctic Sea Ice.* Washington, D.C.: U.S. National Academy of Sciences–National Research Council Publication 598, p. 106–138.

Assur, A. (1967) Flexural and other properties of sea ice sheets. In *Physics of Snow and Ice. Proceedings of International Conference on Low Temperature Science, 1966* (H. Oura, Ed.). Institute of Low Temperature Science, Hokkaido University, vol. 1, part 1, p. 557–567.

Blanchet, D. and H. Hamza (1983) Plane-strain compressive strength of first-year Beaufort Sea ice. In *Proceedings, International Conference on Port and Ocean Engineering under Arctic Conditions, POAC '83, (VTT Symposium 37).* Technical Research Centre of Finland, vol. 3, p. 84–96. Technical Research Centre of Finland.

Butkovich, T.R. (1956) Strength studies of sea ice. USA Snow, Ice and Permafrost Research Establishment, Research Report 20.

Butkovich, T.R. (1959) On the mechanical properties of sea ice, Thule, Greenland, 1957. USA Snow, Ice and Permafrost Research Establishment, Research Report 54.

Cherepanov, N.V. (1971) Spatial arrangement of sea ice crystal structure. *Problemy Arktiki i Antarktiki,* 38: 176–181 (in Russian).

Cox, G.F.N. and W.F. Weeks (1974) Salinity variations in sea ice. *Journal of Glaciology,* 13(67): 109–120.

Cox, G.F.N. and W.F. Weeks (1975) Brine drainage and initial salt entrapment in sodium chloride ice. USA Cold Regions Research and Engineering Laboratory, Research Report 345.

Cox, G.F.N. and W.F. Weeks (1983) Equations for determining the gas and brine volumes in sea ice samples. *Journal of Glaciology,* 29(102): 306–316.

Cox, G.F.N., J.A. Richter, W.F. Weeks and M. Mellor (1984a) A summary of the strength and modulus of ice samples from multi-year pressure ridges. In *Proceedings of the 3rd International Offshore Mechanics and Arctic Engineering Symposium.* New York: American Society of Mechanical Engineers, vol. 3, p. 126–133.

Cox, G.F.N., J.A. Richter-Menge, W.F. Weeks and M. Mellor (1984b) The mechanical properties of multi-year sea ice. Phase I: Test results. USA Cold Regions Research and Engineering Laboratory, CRREL Report 84-9.

Cox, G.F.N., J.A. Richter-Menge, W.F. Weeks, M. Mellor, H.W. Bosworth, G. Durell and N. Perron (1985) Mechanical properties of multi-year sea ice. Phase II: Test results. USA Cold Regions Research and Engineering Laboratory, CRREL Report 85-16.

Cox, G.F.N. and J.A. Richter-Menge (1985) Tensile strength of multi-year pressure ridge sea ice samples. *Journal of Energy Resources Technology,* 107(3): 375–380.

Cox, G.F.N. and W.F. Weeks (1986) Changes in salinity and porosity of sea ice samples during sampling and storage. *Journal of Glaciology,* 32: 371–375.

Currier, J.H. and E.M. Schulson (1982) The tensile strength of ice as a function of grain size. *Acta Metallurgica,* 30: 1511–1514.

Dykins, J.E. (1967) Tensile properties of sea ice grown in a confined system. In *Physics of Snow and Ice. Proceedings of International Conference on Low Temperature Science, 1966* (H. Oura, Ed.). Institute of Low Temperature Science, Hokkaido University, vol. 1, part 1, p. 523–537.

Dykins, J.E. (1970) Ice engineering: Tensile properties of sea ice grown in a confined system. Naval Civil Engineering Laboratory, Port Hueneme, California, Technical Report R689.

Dykins, J.E. (1971) Ice engineering: Material properties of saline ice for a limited range of conditions. Naval Civil Engineering Laboratory, Port Hueneme, California, Technical Report R720.

Enkvist, E. (1972) On the ice resistance encountered by ships operating in the continuous mode of icebreaking. Swedish Academy of Engineering Sciences in Finland, Helsinki, Report 24.

Frederking, R. (1977) Plane-strain compressive strength of columnar-grained and granular snow ice. *Journal of Glaciology*, 18(80): 505–516.

Frederking, R. and G. Timco (1984) Measurement of shear strength of granular/discontinuous-columnar sea ice. *Cold Regions Science and Technology*, 9: 215–220.

Gow, A.J., H.T. Ueda and J.A. Richard (1978) Flexural strength of ice on temperate lakes. Comparative tests of large cantilever and simply supported beams. USA Cold Regions Research and Engineering Laboratory, CRREL Report 78-9.

Hausler, F.U. (1981) Multi-axial compressive strength tests on saline ice with brush type loading patterns. In *Proceedings, IAHR International Symposium on Ice, Quebec City*, vol. 2, p. 526–539.

Hausler, F.U. (1983) Comparison between different yield functions for saline ice. *Annals of Glaciology*, 4: 105–109.

Hawkes, I. and M. Mellor (1972) Deformation and fracture of ice under uniaxial stress. *Journal of Glaciology*, 11(61): 103–131.

Hutter, K. (1975) Floating sea ice plates and the significance of the dependence of the Poisson ratio on brine volume. *Proceedings of the Royal Society of London, A*, 343(1962): 85–108.

Jones, S.J. (1982) The confined compressive strength of polycrystalline ice. *Journal of Glaciology*, 28(98): 171–178.

Katona, M.G. and K.D. Vaudrey (1973) Ice engineering: Summary of elastic properties research and introduction of viscoelastic and nonlinear analysis of saline ice. Naval Civil Engineering Laboratory, Port Hueneme, California, Technical Report R797.

Kerr, A.D. and W.T. Palmer (1972) The deformations and stresses in floating ice plates. *Acta Mechanica*, 15(1-2): 57–72.

Lainey, L. and R. Tinawi (1981) Parametric studies of sea ice beams under short- and long-term loadings. In *Proceedings, IAHR International Symposium on Ice, Quebec City*, vol. 2, p. 607–623.

Lake, R.A. and E.L. Lewis (1970) Salt rejection by sea ice during growth. *Journal of Geophysical Research*, 75(3): 583–597.

Langleben, M.P. and E.R. Pounder (1963) Elastic parameters of sea ice. In *Ice and Snow: Processes,*

Properties and Applications (W.D. Kingery, Ed.). Cambridge, Massachusetts: MIT Press, p. 67–78.

Määttänen, M. (1975) On the flexural strength and elasticity of saline ice. In *Proceedings, Third International Symposium on Ice Problems* (G.E. Frankenstein, Ed.). International Association of Hydraulic Research, p. 373–386.

Maykut, G.A. (1978) Energy exchange over young sea ice in the central Arctic. *Journal of Geophysical Research*, 83(C7): 3646–3658.

Mellor, M. (1983) Mechanical behavior of sea ice. USA Cold Regions Research and Engineering Laboratory, Monograph 83-1.

Miller, J.D. (1979) An equilibrium surface temperature climate model applied to first-year sea ice growth. M.S. thesis, Department of Geography, Carleton University.

Murat, J.R. and L.M. Lainey (1982) Some experimental observations on the Poisson's ratio of sea ice. *Cold Regions Science and Technology*, 6: 105–113.

Nakawo, M. and N.K. Sinha (1981) Growth rate and salinity profile of first-year sea ice in the high Arctic. *Journal of Glaciology*, 27(96): 315–330.

Nawwar, A.M., J.P. Nadreau and Y.W. Wang (1983) Triaxial compressive strength of saline ice. In *Proceedings, 6th International Conference on Port and Ocean Engineering under Arctic Conditions, POAC '83, Quebec, Canada, 27-31 July*, vol. 3, p. 193–202. Technical Research Centre of Finland.

Neidrauer, T.M. and S. Martin (1979) An experimental study of brine drainage and convection in young sea ice. *Journal of Geophysical Research*, 84(C3): 1176–1186.

Ono, N. (1967) Specific heat and heat of fusion of sea ice. In *Physics of Snow and Ice: Proceedings of International Conference on Low Temperature Science, 1966* (H. Oura, Ed.). Institute of Low Temperature Science, Hokkaido University, vol. 1, part 1, p. 599–610.

Ono, N. (1975) Thermal properties of sea ice. IV. Thermal constants of sea ice. USA Cold Regions Research and Engineering Laboratory, Draft Translation 467.

Paige, R.A. and C.W. Lee (1967) Preliminary studies on sea ice in McMurdo Sound, Antarctica, during "Deep Freeze 65." *Journal of Glaciology*, 6(46): 515–528.

Panov, V.V. and N.V. Fokeev (1977) Compression strength of sea ice specimens under complex loading. *Problems of the Arctic and Antarctic*, 49: 81–86.

Pariseau, W.G. (1972) Plasticity theory for anisotropic rocks and soils. In *Proceedings, Tenth Annual Symposium on Rock Mechanics*. Baltimore: Port City Press.

Peyton, H.R. (1966) Sea ice strength. Geophysical Institute, University of Alaska, Report UAG-182.

Ralston, T.D. (1977) Yield and plastic deformation in ice crushing failure. In *Sea Ice Processes and Models, Proceedings of AIDJEX Symposium*. Seattle: University of Washington Press, p. 234-245.

Ralston, T.D. (1979) Sea ice loads. Presented at Technical Seminar on Alaska Beaufort Sea Gravel Inland Design. Exxon Company U.S.A., Houston.

Richter, J.A. and G.F.N. Cox (1984) A preliminary examination of the effect of structure on the compressive strength of ice samples from multiyear pressure ridges. In *Proceedings of the 3rd International Offshore Mechanics and Arctic Engineering Symposium*. New York: American Society of Mechanical Engineers, vol. 3, p. 140-144.

Saeki, H., T. Nomura and A. Ozaki (1979) Experimental study on the testing methods of strength and mechanical properties of sea ice. In *Proceedings, IAHR Symposium on Ice Problems, Lulea, Sweden*, vol. 1, p. 135-149.

Schwarz, J., R. Frederking, V. Gavrillo, I.G. Petrov, K.I. Hirayama, M. Mellor, P. Tryde and K.D. Vaudrey (1981) Standardized testing methods for measuring mechanical properties of ice. *Cold Regions Science and Technology*, 4: 245-253.

Slesarenko, Yu.Ye. and A.D. Frolov (1974) Comparison of elasticity and strength characteristics of salt-water ice. In *Proceedings, IAHR Symposium on Ice and Its Action on Hydraulic Structures, Leningrad*, vol. 2, p. 85-87.

Smith, M.B. (1974) A parabolic yield condition for anisotropic rocks and soils. Ph.D. thesis, Rice University, Houston.

Tabata, T. (1960) Studies on mechanical properties of sea ice. V. Measurement of flexural strength. *Low Temperature Science*, ser. A, no. 19, p. 187-201.

Tabata, T., K. Fujino and A. Aota (1967) Studies of the mechanical properties of sea ice: The flexural strength of sea ice in situ. In *Physics of Snow and Ice. Proceedings of International Conference on Low Temperature Science, 1966* (H. Oura, Ed.). Institute of Low Temperature Science, Hokkaido University, vol. 1, part 1, p. 539-550.

Tabata, T., Y. Suzuki and M. Aota (1975) Ice study in the Gulf of Bothnia II. Measurements of flexural strength. *Low Temperature Science*, ser. A, no. 33, p. 199- 06.

Timco, G.W. and R. Frederking (1983) Confined compressive strength of sea ice. In *Proceedings, 6th International Conference on Port and Ocean Engineering under Arctic Conditions, POAC '83, Quebec, Canada, 27-31 July*, vol. 1, p. 243-253. Technical Research Centre of Finland.

Timco, G.W. and R.M.W. Frederking (1984) An investigation of the failure envelope of granular/ discontinuous-columnar ice. *Cold Regions Science and Technology*, 9: 17-27.

Timco, G.W. and R.M.W. Frederking (1986) Confined compression tests: Outlining the failure envelope of columnar sea ice. *Cold Regions Science and Technology*, 12(1): 13-28.

Tratteberg, A., L.W. Gold and R. Frederking (1975) The strain rate and temperature dependence of Young's modulus of ice. In *Proceedings, IAHR Symposium on Ice Problems, Hanover, N.H.*, p. 479-486.

Tucker, W.B., A.J. Gow and W.F. Weeks (1985) Physical properties of sea ice in the Greenland Sea. In In *Proceedings, International Conference on Port and Ocean Engineering under Arctic Conditions, POAC '85, Narssarssuaq, Greenland*, vol. 1, p. 177-188.

Vaudrey, K.D. (1977) Ice engineering: Study of related properties of floating sea-ice sheets and summary of elastic and viscoelastic analysis. Naval Civil Engineering Laboratory, Port Hueneme, California, Report TR-860.

Wang, Y.S. (1979) Sea ice properties. Presented at Technical Seminar on Alaskan Beaufort Sea Gravel Island Design. Exxon Company U.S.A., Houston.

Wang, Y.S. (1980) Crystallographic studies and strength tests of field ice in the Alaskan Beaufort Sea. In *Proceedings, International Conference on Port and Ocean Engineering under Arctic Conditions, POAC '79, Trondheim, Norway*, vol. 1, p. 651-665.

Wang, Y.S. (1981) Uniaxial compression testing of arctic sea ice. In *Proceedings, International Conference on Port and Ocean Engineering under Arctic Conditions, POAC '81, Quebec City*, vol. 1, p. 346-355.

Weeks, W.F. and D.L. Anderson (1958) An experimental study of strength of young sea ice. *Transactions, American Geophysical Union*, 39(4): 641-647.

Weeks, W.F. and A. Assur (1967) The mechanical properties of sea ice. USA Cold Regions Research and Engineering Laboratory, Monograph II-C3.

Weeks, W.F. and G. Lofgren (1967) The effective solute distribution coefficient during the freezing

of NaCl solution. In *Physics of Snow and Ice. Proceedings of International Conference on Low Temperature Science, 1966* (H. Oura, Ed.). Institute of Low Temperature Science, Hokkaido University, vol. 1, part 1, p. 579–597.

Weeks, W.F. and Assur, A. (1972) Fracture of lake and sea ice. In *Fracture, An Advanced Treatise,* Vol. 7. *Fracture of Nonmetals and Composites.* (H. Liebowitz, Ed.). New York: Academic Press, p. 879–978.

Weeks, W.F. and A.J. Gow (1978) Preferred crystal orientations in the fast ice along the margins of the Arctic Ocean. *Journal of Geophysical Research,* **83**(C10): 5105–5125.

Weeks, W.F. and A.J. Gow (1980) Crystal alignments in the fast ice of Arctic Alaska. *Journal of Geophysical Research,* **85**(C2): 1137–1146.

Weeks, W.F. and S.F. Ackley (1982) The growth, structure and properties of sea ice. USA Cold Regions Research and Engineering Laboratory, Monograph 82-1.

Weeks, W.F. and M. Mellor (1983) Mechanical properties of ice in the arctic seas. In *Arctic Technology and Policy* (I. Dyer and C. Chryssostomidis, Ed.). Hemisphere Publishing Company, p. 235–259.

Weller, G. (1972) Radiation flux investigation. *AIDJEX Bulletin,* **14**: 28–30.

27

APPENDIX A: DETAILS OF THE EQUATIONS FOR ICE SURFACE TEMPERATURE
AND CONDUCTIVE HEAT FLUX

The energy fluxes at the ice surface considered in Maykut's (1978) and our analyses include

F_r = incoming short-wave radiation
αF_r = reflected short-wave radiation, where α is the ice albedo
I_0 = net flux of radiative energy that passes into the interior of the ice
F_L = incoming long-wave radiation
F_E = emitted long-wave radiation
F_s = sensible heat flux
F_e = latent heat flux
F_c = conductive heat flux.

Except where noted, all equations and variable values are from Maykut (1978).
I_0 is taken as a percentage i_0 (17%) of the net short-wave radiation, where

$$I_0 = i_0(1 - \alpha)F_r. \tag{A1}$$

The albedo α for snow-free sea ice depends on the ice thickness H and is given by

$$\alpha = \beta_1 + \beta_2 H + \beta_3 H^2 + \beta_4 H^3 \tag{A2}$$

where H is in centimeters and $\beta_1 = 0.2386$, $\beta_2 = 6.015 \times 10^{-3}$, $\beta_3 = -4.882 \times 10^{-5}$, and $\beta_4 = 1.267 \times 10^{-7}$.

The curve is based on measurements by Weller (1972) and is compared to his data points in Figure A1. For ice thicknesses greater than 100 cm, α is assumed to be constant at 0.47.
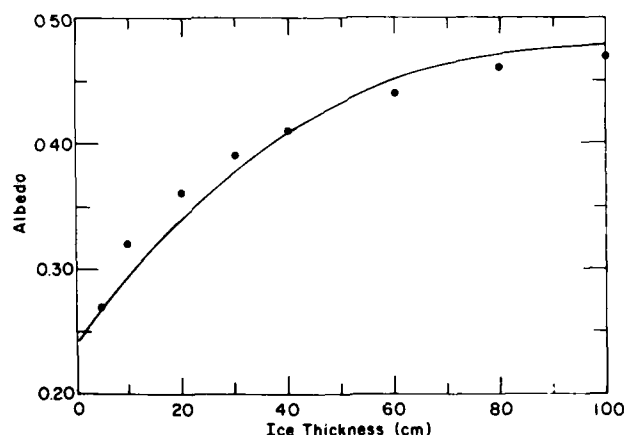
Figure A1. Albedo for snow-free sea ice vs ice thickness (Weller 1972). The approximate curve was determined by least-squares polynomial curve fit.

29

The emitted long-wave radiation is given by

$$F_E = \epsilon \sigma T_o^4 \tag{A3}$$

where ϵ = long-wave emissivity (1)
σ = Stefan-Boltzman constant (5.67×10^{-8} W/m^2 K^4)
T_o = ice surface temperature (K).

The sensible heat flux is expressed as

$$F_s = \varrho c_p C_s u (T_a - T_o) \tag{A4}$$

where ϱ = average air density (1.3 kg/m^3)
c_p = specific heat at constant pressure (1006 J/kg K)
C_s = sensible heat transfer coefficient (0.003)
u = wind speed (5 m/s)
T_a and T_o = ambient and ice surface temperatures, respectively (K).

The latent heat flux is calculated from

$$F_e = \varrho L C_e u (q_a - q_o) \tag{A5}$$

where L = latent heat of vaporization (J/kg)
C_e = evaporation coefficient (0.00175)
q_a and q_o = specific humidities 10 m above the ice and at the ice surface, respectively.

The latent heat of vaporization is equal to

$$L = [2.5 \times 10^6 - 2.274 \times 10^3 (T_a - 273.15)] \tag{A6}$$

where L is in J/kg and T_a is in kelvins. The difference in specific humidity is obtained from

$$(q_a - q_o) = \frac{0.622}{\varrho_o} [a(fT_a^4 - T_o^4) + b(fT_a^3 - T_o^3) + c(fT_a^2 - T_o^2) + d(fT_a - T_o) + e(f - 1)] \tag{A7}$$

where ϱ_o = surface atmospheric pressure (1013 mb)
f = relative humidity
a = 2.7798202×10^{-6}/K^4
b = $-2.6913393 \times 10^{-3}$/K^3
c = 0.97920849/K^2
d = -158.63779/K
e = 9653.1925.

The conductive heat flux is derived from

$$F_c = (k/H)(T_b - T_o) \tag{A8}$$

where k = thermal conductivity of the surface ice layer (W/m K)
H = ice thickness (m)
T_b = ice bottom temperature (K).

The thermal conductivity is obtained from (Ono 1975)

$$k = k_i(1 - v_b) + k_b v_b$$

where k_i (W/m K) is the conductivity of pure ice, equal to

$$k_i = 4.186 \times 10^4 [5.35 \times 10^{-3} - 2.568 \times 10^{-5}(T_0 - 273.15)]$$

and k_b (W/m K) is the conductivity of pure brine, equal to

$$k_b = 4.186 \times 10^4 [1.25 \times 10^{-3} + 3.0 \times 10^{-5}(T_0 - 273.15) + 1.4 \times 10^{-7}(T_0 - 273.15)^2]$$

and v_b is the brine volume of the surface layer calculated from the equations given in Cox and Weeks (1983). In calculating the brine volume, solid salts are neglected and the surface layer salinity from the previous growth increment is used.

The remaining input variables include the ambient temperature T_a, the incoming short-wave radiation F_r, the incoming long-wave radiation F_L and the relative humidity f. Maykut (1978) gave average values of these variables for the first day of each month during the winter. Step-wise polynomial curve fits were obtained for each data set to provide mean daily values for each input variable during the ice growth season. The results are shown in Figures A2-A5. Equations and coefficients for each of the curves are given in Tables A1-A4.

In the surface energy balance equation

$$(1 - \alpha)F_r - I_0 + F_L - F_E + F_s + F_e + F_c = 0 \tag{A9}$$

the ice surface temperature T_0 is the only unknown for a given ice thickness. Maykut (1978) used the Newton-Raphson method to solve for T_0. We adopted Miller's (1979) suggestion and used the half-interval method to solve the equation. This method is more straightforward, and it simplifies the calculation of the ice surface temperature if changes are made to the energy balance equation.
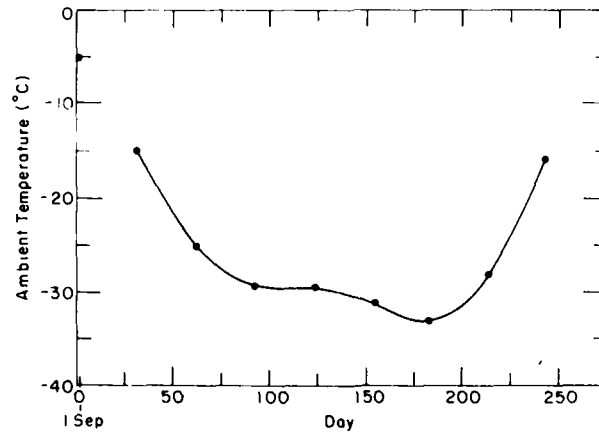
Figure A2. Ambient temperature of the Central Arctic Basin during the ice growth season. The data are from Maykut (1978). The curve was determined by step-wise polynomial least-squares curve fit.

31
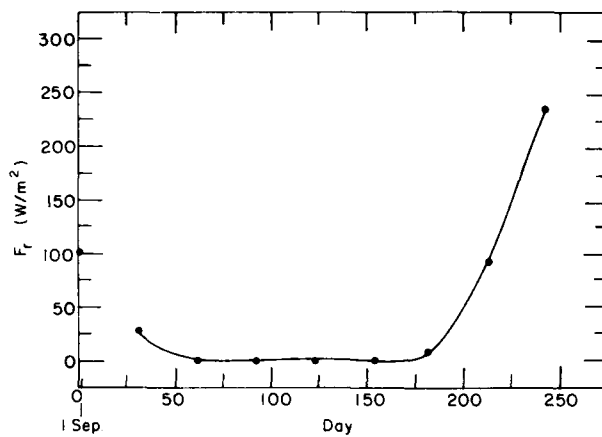
Figure A3. Incoming short-wave radiation for the Central Arctic Basin during the ice growth season. The data are from Maykut (1978). The curve was determined by stepwise polynomial least-squares curve fit.
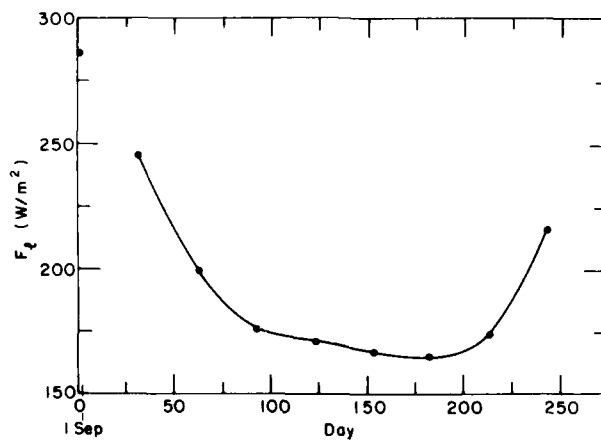
Figure A4. Incoming long-wave radiation for the Central Arctic Basin during the ice growth season. The data are from Maykut (1978). The curve was determined by stepwise polynomial least-squares curve fit.
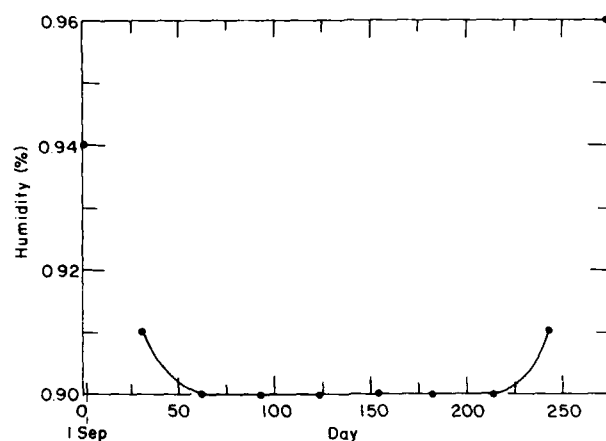
Figure A5. Relative humidity for the Central Arctic Basin during the growth season. The data are from Maykut (1978). The curve was determined by step-wise polynomial least-squares curve fit.

Table A1. Coefficients for temperature step-wise polynomial curve.*

Day	A	B	C	D
31-61	-5.0481	-0.24845	-3.4474×10^{-3}	3.5681×10^{-5}
62-91	3.2193	-0.73835	5.2023×10^{-3}	-1.1075×10^{-5}
92-122	17.680	-1.2463	1.0912×10^{-2}	-3.1686×10^{-5}
123-153	-47.205	0.40778	-2.8274×10^{-3}	5.5475×10^{-6}
154-181	-187.85	3.2372	-2.1553×10^{-2}	4.6343×10^{-5}
182-212	69.031	-1.0482	2.0699×10^{-3}	3.3148×10^{-6}
213-242	572.784	-8.2542	3.6188×10^{-2}	-5.0161×10^{-5}

* $T = A + (B \times \text{Day}) + (C \times \text{Day}^2) + (D \times \text{Day}^3)$

where T is in °C and Day is in days where Day 1 = 1 September.

Table A2. Coefficients for short-wave incoming radiation step-wise polynomial least-squares curve.*

Day	A	B	C	D
31-61	211.58	-7.1567	7.6088×10^{-2}	-2.5321×10^{-4}
62-91	0	0	0	0
92-122	0	0	0	0
123-153	0	0	0	0
154-181	-2706.5	55.489	-0.37555	8.4000×10^{-4}
182-212	3659.8	-50.718	0.20989	-2.2643×10^{-4}
213-242	15516.0	-220.32	1.0129	-1.4851×10^{-3}

* $F_r = [A + (B \times \text{Day}) + (C \times \text{Day}^2) + (D \times \text{Day}^3)] \times 0.485$

where F_r is in W/m² and Day is in days where Day 1 = 1 September.

Table A3. Coefficients for long-wave incoming radiation step-wise polynomial least-squares curve.*

Day	A	B	C	D
31-61	591.48	-2.0507	-3.2818×10^{-2}	3.0635×10^{-4}
62-91	651.17	-5.5875	2.9628×10^{-2}	-3.1193×10^{-5}
92-122	792.11	-10.539	8.5273×10^{-2}	-2.3208×10^{-4}
123-153	313.66	1.5587	-1.6036×10^{-2}	4.2471×10^{-5}
154-181	126.03	5.4334	-4.1017×10^{-2}	9.6896×10^{-5}
182-212	-970.86	23.733	-0.14189	2.8063×10^{-4}
213-242	4078.0	-48.488	0.20005	-2.5533×10^{-4}

* $F_c = [A + (B \times \text{Day}) + (C \times \text{Day}^2) + (D \times \text{Day}^3)] \times 0.485$

where F_c is in W/m^2 and Day is in days where day 1 = 1 September.

Table A4. Coefficients for humidity step-wise polynomial least-squares curve.*

Day	A	B	C	D
31-61	0.94147	-1.4842×10^{-3}	1.7111×10^{-5}	-6.3923×10^{-8}
62-91	0	0	0	0
92-122	0	0	0	0
123-153	0	0	0	0
154-181	0	0	0	0
182-212	0	0	0	0
213-242	-0.47649	2.0562×10^{-3}	-1.0211×10^{-4}	1.6861×10^{-7}

* $f = A + (B \times \text{Day}) + (C \times \text{Day}^2) + (D \times \text{Day}^3)$

where f is dimensionless and D is in days where Day 1 = 1 September.

34

APPENDIX B: CALCULATED PROFILE AND BULK PROPERTIES OF
AN ICE SHEET OF VARYING THICKNESS

The ice sheet formed on 1 October and grew under climatological conditions representative of the Arctic Basin. Ice thicknesses are 15, 30, 46, 61, 76, 91, 122, 152, 183 and 213 cm.

PROFILE: SG5E-31   DEPTH: 15 CM (.5 FT)

Depth (cm)	Salinity (o/oo)	Temp (C)	VB (o/oo)	Sigma T (MPa)	Sigma F (MPa)	Sigma S (MPa)	Eeff (GPa)
.3	10.4	-10.5	55.4	.89	.51	.80	2.06
1.0	10.0	-10.1	55.5	.89	.51	.80	2.06
2.0	9.6	-9.5	55.5	.89	.51	.80	2.06
3.0	9.2	-8.9	56.2	.89	.50	.80	2.04
4.0	8.9	-8.3	57.6	.88	.50	.78	2.00
5.0	8.7	-7.7	59.8	.87	.49	.77	1.94
6.0	8.6	-7.1	62.8	.85	.48	.74	1.85
7.0	8.5	-6.5	66.7	.83	.46	.72	1.75
8.0	8.4	-5.9	72.0	.80	.44	.68	1.61
9.0	8.4	-5.3	79.1	.76	.42	.63	1.43
10.0	8.5	-4.7	88.6	.72	.39	.57	1.21
11.0	8.6	-4.2	102.0	.66	.34	.49	.91
12.0	8.9	-3.6	121.5	.58	.29	.38	.50
13.0	9.3	-3.0	151.6	.47	.21	.23	0.00
14.0	9.9	-2.4	202.3	.30	.09	.00	0.00
15.0	10.6	-1.8	292.4	.05	0.00	0.00	0.00
MEAN	9.2	-6.2	98.7	.71	.38	.57	1.34
SDEV	.7	2.8	66.2	.25	.16	.28	.80
MIN	8.4	-10.5	55.4	.05	0.00	0.00	0.00
MAX	10.6	-1.8	292.4	.89	.51	.80	2.06

NEUTRAL AXIS (CM)	5.3
FLEXURAL RIGIDITY (N-M)	2.44E+05
CHARACTERISTIC LENGTH (M)	2.22
AVERAGE ICE SALINITY (o/oo)	9.16
AVERAGE ICE TEMPERATURE (C)	-6.2
BULK BRINE VOLUME (o/oo)	75.3
BULK TENSILE STRENGTH (MPA)	.78
BULK FLEXURAL STRENGTH (MPA)	.43
BULK SHEAR STRENGTH (MPA)	.66
BULK EFFECTIVE MODULUS (GPA)	1.53
BULK FLEXURAL RIGIDITY (N-M)	4.83E+05
BULK CHARACTERISTIC LENGTH (M)	2.64

PROFILE: SG5E-31   DEPTH: 30 CM (1 FT)

Depth (cm)	Salinity (o/oo)	Temp (C)	VB (o/oo)	Sigma T (MPa)	Sigma F (MPa)	Sigma S (MPa)	Eeff (GPa)
.3	10.1	-13.7	44.5	.96	.55	.89	2.40
1.0	9.8	-13.4	43.8	.96	.56	.90	2.43
2.0	9.3	-13.0	42.6	.97	.56	.91	2.47
3.0	9.0	-12.6	41.8	.98	.57	.92	2.49
4.0	8.6	-12.2	41.3	.98	.57	.92	2.51
5.0	8.4	-11.8	41.1	.98	.57	.92	2.51
6.0	8.2	-11.4	41.1	.98	.57	.92	2.52
7.0	8.0	-1..0	41.2	.98	.57	.92	2.51
8.0	7.8	-10.6	41.5	.98	.57	.92	2.50
9.0	7.7	-10.2	42.0	.98	.57	.92	2.49
10.0	7.6	-9.8	42.6	.97	.56	.91	2.46
11.0	7.4	-9.4	43.4	.97	.56	.90	2.44
12.0	7.3	-9.0	44.3	.96	.55	.89	2.41

35

Depth (cm)	Salinity (o/oo)	Temp (C)	VB (o/oo)	Sigma T (MPa)	Sigma F (MPa)	Sigma S (MPa)	Eeff (GPa)
13.0	7.3	-8.6	45.4	.95	.55	.88	2.37
14.0	7.2	-8.2	46.7	.94	.54	.87	2.33
15.0	7.1	-7.8	48.2	.93	.54	.86	2.28
16.0	7.1	-7.4	50.0	.92	.53	.85	2.23
17.0	7.0	-7.0	52.0	.91	.52	.83	2.17
18.0	7.0	-6.6	54.4	.90	.51	.81	2.09
19.0	7.0	-6.2	57.4	.88	.50	.79	2.01
20.0	7.0	-5.8	60.9	.86	.48	.76	1.91
21.0	7.0	-5.4	65.2	.84	.47	.73	1.79
22.0	7.1	-5.0	70.4	.81	.45	.69	1.65
23.0	7.2	-4.6	77.1	.77	.43	.64	1.48
24.0	7.3	-4.2	85.4	.73	.40	.59	1.28
25.0	7.5	-3.8	96.4	.68	.36	.52	1.03
26.0	7.7	-3.4	110.3	.62	.32	.44	.73
27.0	8.0	-3.0	130.2	.55	.27	.33	.34
28.0	8.5	-2.6	159.1	.44	.19	.19	0.00
29.0	9.2	-2.2	203.5	.30	.09	0.00	0.00
30.0	9.8	-1.8	270.1	.11	0.00	0.00	0.00
MEAN	7.9	-7.8	72.1	.83	.47	.73	1.87
SDEV	1.0	3.6	53.1	.22	.15	.27	.84
MIN	7.0	-13.7	41.1	.11	0.00	0.00	0.00
MAX	10.1	-1.8	270.1	.98	.57	.92	2.52

NEUTRAL AXIS (CM)	11.8
FLEXURAL RIGIDITY (N-M)	3.26E+06
CHARACTERISTIC LENGTH (M)	4.25
AVERAGE ICE SALINITY (o/oo)	7.90
AVERAGE ICE TEMPERATURE (C)	-7.8
BULK BRINE VOLUME (o/oo)	53.6
BULK TENSILE STRENGTH (MPA)	.90
BULK FLEXURAL STRENGTH (MPA)	.51
BULK SHEAR STRENGTH (MPA)	.82
BULK EFFECTIVE MODULUS (GPA)	2.12
BULK FLEXURAL RIGIDITY (N-M)	5.36E+06
BULK CHARACTERISTIC LENGTH (M)	4.81

PROFILE: SG5E-31   DEPTH: 46 CM (1.5 FT)

Depth (cm)	Salinity (o/oo)	Temp (C)	VB (o/oo)	Sigma T (MPa)	Sigma F (MPa)	Sigma S (MPa)	Eeff (GPa)
.3	10.0	-16.7	38.3	1.00	.58	.95	2.61
1.0	9.7	-16.4	37.5	1.01	.59	.96	2.64
2.0	9.2	-16.1	36.1	1.02	.59	.97	2.69
3.0	8.8	-15.8	35.2	1.02	.60	.98	2.72
4.0	8.5	-15.4	34.4	1.03	.60	.99	2.75
5.0	8.3	-15.1	33.9	1.03	.61	.99	2.77
6.0	8.0	-14.8	33.5	1.04	.61	1.00	2.79
7.0	7.8	-14.5	33.2	1.04	.61	1.00	2.80
8.0	7.7	-14.1	33.0	1.04	.61	1.00	2.81
9.0	7.5	-13.8	32.9	1.04	.61	1.00	2.81
10.0	7.4	-13.5	32.9	1.04	.61	1.00	2.81
11.0	7.3	-13.2	33.0	1.04	.61	1.00	2.81
12.0	7.2	-12.8	33.0	1.04	.61	1.00	2.80
13.0	7.1	-12.5	33.2	1.04	.61	1.00	2.80
14.0	7.0	-12.2	33.5	1.04	.61	1.00	2.79
15.0	6.9	-11.9	33.7	1.03	.61	.99	2.78
16.0	6.8	-11.5	34.1	1.03	.60	.99	2.76
17.0	6.8	-11.2	34.5	1.03	.60	.99	2.75
18.0	6.7	-10.9	35.0	1.02	.60	.98	2.73
19.0	6.7	-10.6	35.5	1.02	.60	.98	2.71
20.0	6.6	-10.2	36.1	1.02	.59	.97	2.69
21.0	6.6	-9.9	36.7	1.01	.59	.96	2.67
22.0	6.5	-9.6	37.5	1.01	.59	.96	2.64
23.0	6.5	-9.3	38.3	1.00	.58	.95	2.61
24.0	6.5	-8.9	39.3	.99	.58	.94	2.58
25.0	6.4	-8.6	40.2	.99	.57	.93	2.54
26.0	6.4	-8.3	41.2	.98	.57	.92	2.51
27.0	6.4	-8.0	42.4	.97	.56	.91	2.47
28.0	6.4	-7.6	43.8	.96	.56	.90	2.43

36

Depth (cm)	Salinity (o/oo)	Temp (C)	VB (o/oo)	Sigma T (MPa)	Sigma F (MPa)	Sigma S (MPa)	Eeff (GPa)
29.0	6.3	-7.3	45.2	.95	.55	.89	2.38
30.0	6.3	-7.0	46.9	.94	.54	.87	2.32
31.0	6.3	-6.7	48.7	.93	.53	.86	2.27
32.0	6.3	-6.3	50.8	.92	.53	.84	2.20
33.0	6.3	-6.0	53.2	.90	.52	.82	2.13
34.0	6.3	-5.7	56.0	.89	.50	.80	2.05
35.0	6.4	-5.4	59.3	.87	.49	.77	1.95
36.0	6.4	-5.0	63.2	.85	.48	.74	1.84
37.0	6.5	-4.7	67.9	.82	.46	.71	1.72
38.0	6.6	-4.4	73.6	.79	.44	.67	1.57
39.0	6.7	-4.1	80.6	.76	.41	.62	1.40
40.0	6.9	-3.7	89.4	.72	.38	.56	1.19
41.0	7.1	-3.4	100.7	.66	.35	.50	.93
42.0	7.4	-3.1	115.5	.60	.31	.41	.63
43.0	7.7	-2.8	135.2	.53	.25	.31	.24
44.0	8.2	-2.4	163.0	.43	.18	.17	0.00
45.0	8.8	-2.1	203.7	.30	.09	0.00	0.00
46.0	9.5	-1.8	260.5	.13	0.00	0.00	0.00
MEAN	7.2	-9.3	58.6	.90	.52	.82	2.19
SDEV	1.0	4.5	46.9	.21	.14	.26	.84
MIN	6.3	-16.7	32.9	.13	0.00	0.00	0.00
MAX	10.0	-1.8	260.5	1.04	.61	1.00	2.81

NEUTRAL AXIS (CM)	19.0
FLEXURAL RIGIDITY (N-M)	1.49E+07
CHARACTERISTIC LENGTH (M)	6.21
AVERAGE ICE SALINITY (o/oo)	7.22
AVERAGE ICE TEMPERATURE (C)	-9.3
BULK BRINE VOLUME (o/oo)	42.6
BULK TENSILE STRENGTH (MPA)	.97
BULK FLEXURAL STRENGTH (MPA)	.56
BULK SHEAR STRENGTH (MPA)	.91
BULK EFFECTIVE MODULUS (GPA)	2.46
BULK FLEXURAL RIGIDITY (N-M)	2.25E+07
BULK CHARACTERISTIC LENGTH (M)	6.88

PROFILE: SG5E-31   DEPTH: 61 CM (2 FT)

Depth (cm)	Salinity (o/oo)	Temp (C)	VB (o/oo)	Sigma T (MPa)	Sigma F (MPa)	Sigma S (MPa)	Eeff (GPa)
.3	9.9	-19.3	34.3	1.03	.60	.99	2.76
1.0	9.6	-19.1	33.4	1.04	.61	1.00	2.79
2.0	9.1	-18.8	32.1	1.05	.61	1.01	2.84
3.0	8.7	-18.5	31.1	1.05	.62	1.02	2.88
4.0	8.4	-18.2	30.4	1.06	.62	1.03	2.91
5.0	8.2	-17.9	29.8	1.06	.63	1.04	2.93
6.0	8.0	-17.7	29.3	1.07	.63	1.04	2.95
7.0	7.8	-17.4	28.9	1.07	.63	1.05	2.97
8.0	7.6	-17.1	28.6	1.07	.63	1.05	2.98
9.0	7.4	-16.8	28.4	1.08	.64	1.05	2.99
10.0	7.3	-16.5	28.2	1.08	.64	1.05	3.00
11.0	7.2	-16.2	28.1	1.08	.64	1.05	3.00
12.0	7.1	-15.9	28.0	1.08	.64	1.06	3.00
13.0	7.0	-15.6	28.0	1.08	.64	1.06	3.00
14.0	6.9	-15.3	28.0	1.08	.64	1.06	3.00
15.0	6.8	-15.1	28.0	1.08	.64	1.06	3.00
16.0	6.7	-14.8	28.1	1.08	.64	1.05	3.00
17.0	6.7	-14.5	28.2	1.08	.64	1.05	2.99
18.0	6.6	-14.2	28.4	1.08	.64	1.05	2.99
19.0	6.6	-13.9	28.5	1.07	.63	1.05	2.98
20.0	6.5	-13.6	28.7	1.07	.63	1.05	2.97
21.0	6.5	-13.3	29.0	1.07	.63	1.05	2.96
22.0	6.4	-13.0	29.2	1.07	.63	1.04	2.95
23.0	6.4	-12.8	29.5	1.07	.63	1.04	2.94
24.0	6.3	-12.5	29.8	1.06	.63	1.04	2.93
25.0	6.3	-12.2	30.1	1.06	.63	1.03	2.92
26.0	6.2	-11.9	30.4	1.06	.62	1.03	2.90
27.0	6.2	-11.6	30.9	1.06	.62	1.02	2.89
28.0	6.2	-11.3	31.3	1.05	.62	1.02	2.87

37

Depth (cm)	Salinity	Temp	VB				
29.0	6.2	-11.0	31.7	1.05	.62	1.02	2.85
30.0	6.1	-10.7	32.3	1.04	.61	1.01	2.83
31.0	6.1	-10.4	32.8	1.04	.61	1.00	2.81
32.0	6.1	-10.2	33.4	1.04	.61	1.00	2.79
33.0	6.1	-9.9	34.1	1.03	.60	.99	2.76
34.0	6.1	-9.6	34.8	1.03	.60	.98	2.74
35.0	6.0	-9.3	35.6	1.02	.60	.98	2.71
36.0	6.0	-9.0	36.3	1.01	.59	.97	2.68
37.0	6.0	-8.7	37.2	1.01	.59	.96	2.65
38.0	6.0	-8.4	38.2	1.00	.58	.95	2.62
39.0	6.0	-8.1	39.2	.99	.58	.94	2.58
40.0	6.0	-7.9	40.3	.99	.57	.93	2.54
41.0	6.0	-7.6	41.6	.98	.57	.92	2.50
42.0	6.0	-7.3	42.9	.97	.56	.91	2.45
43.0	6.0	-7.0	44.4	.96	.55	.89	2.41
44.0	6.0	-6.7	46.0	.95	.55	.88	2.35
45.0	6.0	-6.4	47.8	.94	.54	.86	2.30
46.0	6.0	-6.1	49.8	.92	.53	.85	2.23
47.0	6.0	-5.8	51.9	.91	.52	.83	2.17
48.0	6.0	-5.5	54.5	.90	.51	.81	2.09
49.0	6.0	-5.3	57.4	.88	.50	.79	2.01
50.0	6.1	-5.0	60.9	.86	.48	.76	1.91
51.0	6.2	-4.7	65.1	.84	.47	.73	1.79
52.0	6.2	-4.4	69.9	.81	.45	.69	1.66
53.0	6.3	-4.1	75.8	.78	.43	.65	1.51
54.0	6.5	-3.8	83.2	.74	.40	.60	1.33
55.0	6.7	-3.5	92.2	.70	.38	.55	1.12
56.0	6.9	-3.2	103.6	.65	.34	.48	.87
57.0	7.2	-3.0	118.3	.59	.30	.40	.57
58.0	7.6	-2.7	137.9	.52	.24	.29	.19
59.0	8.0	-2.4	164.9	.42	.18	.16	0.00
60.0	8.7	-2.1	203.5	.30	.09	0.00	0.00
61.0	9.3	-1.8	255.2	.15	0.00	0.00	0.00
MEAN	6.8	-10.6	50.8	.95	.55	.89	2.41
SDEV	1.0	5.2	43.1	.20	.14	.26	.84
MIN	6.0	-19.3	28.0	.15	0.00	0.00	0.00
MAX	9.9	-1.8	255.2	1.08	.64	1.06	3.00

```
NEUTRAL AXIS (CM)                    25.8
FLEXURAL RIGIDITY (N-M)              3.95E+07
CHARACTERISTIC LENGTH (M)            7.93

AVERAGE ICE SALINITY (o/oo)          6.81
AVERAGE ICE TEMPERATURE (C)          -10.6
BULK BRINE VOLUME (o/oo)             36.3
BULK TENSILE STRENGTH (MPA)          1.01
BULK FLEXURAL STRENGTH (MPA)         .59
BULK SHEAR STRENGTH (MPA)            .97
BULK EFFECTIVE MODULUS (GPA)         2.68
BULK FLEXURAL RIGIDITY (N-M)         5.71E+07
BULK CHARACTERISTIC LENGTH (M)       8.69
```

PROFILE: SG5E-31   DEPTH: 76 CM (2.5 FT)

Depth (cm)	Salinity (o/oo)	Temp (C)	VB (o/oo)	Sigma T (MPa)	Sigma F (MPa)	Sigma S (MPa)	Eeff (GPa)
.3	9.8	-21.9	31.0	1.05	.62	1.02	2.88
1.0	9.5	-21.7	30.2	1.06	.62	1.03	2.91
2.0	9.0	-21.4	29.0	1.07	.63	1.04	2.96
3.0	8.6	-21.1	28.0	1.08	.64	1.06	3.00
4.0	8.3	-20.9	27.3	1.08	.64	1.06	3.03
5.0	8.1	-20.6	26.7	1.09	.64	1.07	3.06
6.0	7.9	-20.3	26.2	1.09	.65	1.08	3.08
7.0	7.7	-20.1	25.8	1.10	.65	1.08	3.09
8.0	7.5	-19.8	25.5	1.10	.65	1.08	3.11
9.0	7.4	-19.5	25.3	1.10	.65	1.09	3.12
10.0	7.2	-19.3	25.0	1.10	.65	1.09	3.13
11.0	7.1	-19.0	24.9	1.11	.66	1.09	3.14
12.0	7.0	-18.7	24.7	1.11	.66	1.09	3.14
13.0	6.9	-18.5	24.6	1.11	.66	1.09	3.15
14.0	6.8	-18.2	24.5	1.11	.66	1.10	3.15

15.0	6.7	-18.0	24.5	1.11	.66	1.10	3.15
16.0	6.7	-17.7	24.5	1.11	.66	1.10	3.15
17.0	6.6	-17.4	24.5	1.11	.66	1.10	3.15
18.0	6.5	-17.2	24.5	1.11	.66	1.10	3.15
19.0	6.5	-16.9	24.6	1.11	.66	1.09	3.15
20.0	6.4	-16.6	24.7	1.11	.66	1.09	3.14
21.0	6.4	-16.4	24.7	1.11	.66	1.09	3.14
22.0	6.3	-16.1	24.8	1.11	.66	1.09	3.14
23.0	6.3	-15.8	25.0	1.10	.66	1.09	3.13
24.0	6.2	-15.6	25.1	1.10	.65	1.09	3.13
25.0	6.2	-15.3	25.2	1.10	.65	1.09	3.12
26.0	6.2	-15.0	25.3	1.10	.65	1.09	3.12
27.0	6.1	-14.8	25.5	1.10	.65	1.08	3.11
28.0	6.1	-14.5	25.7	1.10	.65	1.08	3.10
29.0	6.1	-14.2	25.9	1.10	.65	1.08	3.09
30.0	6.0	-14.0	26.2	1.09	.65	1.08	3.08
31.0	6.0	-13.7	26.4	1.09	.65	1.07	3.07
32.0	6.0	-13.5	26.7	1.09	.65	1.07	3.06
33.0	6.0	-13.2	26.9	1.09	.64	1.07	3.05
34.0	5.9	-12.9	27.2	1.09	.64	1.06	3.04
35.0	5.9	-12.7	27.5	1.08	.64	1.06	3.02
36.0	5.9	-12.4	27.9	1.08	.64	1.06	3.01
37.0	5.9	-12.1	28.3	1.08	.64	1.05	2.99
38.0	5.9	-11.9	28.6	1.07	.63	1.05	2.98
39.0	5.9	-11.6	29.1	1.07	.6.	1.04	2.96
40.0	5.8	-11.3	29.5	1.07	.63	1.04	2.94
41.0	5.8	-11.1	30.0	1.06	.63	1.03	2.92
42.0	5.8	-10.8	30.5	1.06	.62	1.03	2.90
43.0	5.8	-10.5	31.0	1.05	.62	1.02	2.88
44.0	5.8	-10.3	31.5	1.05	.62	1.02	2.86
45.0	5.8	-10.0	32.1	1.05	.61	1.01	2.84
46.0	5.8	-9.7	32.8	1.04	.61	1.00	2.81
47.0	5.8	-9.5	33.4	1.04	.61	1.00	2.79
48.0	5.8	-9.2	34.1	1.03	.60	.99	2.76
49.0	5.8	-8.9	34.9	1.02	.60	.98	2.73
50.0	5.8	-8.7	35.8	1.02	.60	.97	2.70
51.0	5.8	-8.4	36.6	1.01	.59	.97	2.67
52.0	5.8	-8.2	37.6	1.01	.59	.96	2.64
53.0	5.8	-7.9	38.6	1.00	.58	.95	2.60
54.0	5.8	-7.6	39.7	.99	.58	.94	2.56
55.0	5.8	-7.4	40.9	.98	.57	.93	2.52
56.0	5.8	-7.1	42.2	.97	.56	.91	2.48
57.0	5.8	-6.8	43.6	.96	.56	.90	2.43
58.0	5.8	-6.6	45.1	.95	.55	.89	2.38
59.0	5.8	-6.3	46.9	.94	.54	.87	2.33
60.0	5.8	-6.0	48.7	.93	.53	.86	2.27
61.0	5.8	-5.8	50.7	.92	.53	.84	2.21
62.0	5.8	-5.5	53.0	.91	.52	.82	2.14
63.0	5.8	-5.2	55.7	.89	.51	.80	2.06
64.0	5.9	-5.0	58.8	.87	.49	.78	1.97
65.0	5.9	-4.7	62.4	.85	.48	.75	1.87
66.0	6.0	-4.4	66.6	.83	.46	.72	1.75
67.0	6.1	-4.2	71.6	.80	.44	.68	1.62
68.0	6.2	-3.9	77.8	.77	.42	.64	1.46
69.0	6.4	-3.7	85.1	.74	.40	.59	1.29
70.0	6.6	-3.4	94.3	.69	.37	.53	1.08
71.0	6.8	-3.1	105.7	.64	.33	.47	.83
72.0	7.1	-2.9	120.5	.58	.29	.38	.52
73.0	7.5	-2.6	139.9	.51	.24	.28	.15
74.0	7.9	-2.3	166.2	.42	.18	.16	0.00
75.0	8.6	-2.1	203.3	.30	.09	0.00	0.00
76.0	9.2	-1.8	251.7	.16	0.00	0.00	0.00
MEAN	6.5	-11.9	45.3	.99	.57	.93	2.57
SDEV	1.0	5.9	40.4	.19	.13	.25	.83
MIN	5.8	-21.9	24.5	.16	0.00	0.00	0.00
MAX	9.8	-1.8	251.7	1.11	.66	1.10	3.15

NEUTRAL AXIS (CM)	32.6
FLEXURAL RIGIDITY (N-M)	8.37E+07
CHARACTERISTIC LENGTH (M)	9.56
AVERAGE ICE SALINITY (o/oo)	6.52
AVERAGE ICE TEMPERATURE (C)	-11.9
BULK BRINE VOLUME (o/oo)	31.9
BULK TENSILE STRENGTH (MPA)	1.05

39

BULK FLEXURAL STRENGTH (MPA)   .62
BULK SHEAR STRENGTH (MPA)   1.01
BULK EFFECTIVE MODULUS (GPA)   2.85
BULK FLEXURAL RIGIDITY (N-M)   1.17E+08
BULK CHARACTERISTIC LENGTH (M)   10.40

PROFILE: SG5E-31   DEPTH: 91 CM (3 FT)

Depth (cm)	Salinity (o/oo)	Temp (C)	VB (o/oo)	Sigma T (MPa)	Sigma F (MPa)	Sigma S (MPa)	Eeff (GPa)
.3	9.8	-24.0	21.3	1.14	.68	1.14	3.30
1.0	9.4	-23.8	21.6	1.13	.68	1.13	3.28
2.0	9.0	-23.6	22.1	1.13	.67	1.13	3.26
3.0	8.6	-23.3	22.9	1.12	.67	1.11	3.22
4.0	8.3	-23.1	24.1	1.11	.66	1.10	3.17
5.0	8.0	-22.8	24.5	1.11	.66	1.10	3.15
6.0	7.8	-22.6	24.0	1.11	.66	1.10	3.17
7.0	7.6	-22.4	23.7	1.12	.66	1.11	3.19
8.0	7.4	-22.1	23.3	1.12	.67	1.11	3.20
9.0	7.3	-21.9	23.0	1.12	.67	1.11	3.22
10.0	7.2	-21.6	22.8	1.12	.67	1.12	3.23
11.0	7.0	-21.4	22.7	1.12	.67	1.12	3.23
12.0	6.9	-21.1	22.5	1.13	.67	1.12	3.24
13.0	6.8	-20.9	22.4	1.13	.67	1.12	3.25
14.0	6.8	-20.6	22.3	1.13	.67	1.12	3.25
15.0	6.7	-20.4	22.2	1.13	.67	1.12	3.26
16.0	6.6	-20.2	22.2	1.13	.67	1.12	3.26
17.0	6.5	-19.9	22.1	1.13	.67	1.13	3.26
18.0	6.5	-19.7	22.1	1.13	.67	1.13	3.26
19.0	6.4	-19.4	22.1	1.13	.67	1.13	3.26
20.0	6.4	-19.2	22.1	1.13	.67	1.13	3.26
21.0	6.3	-18.9	22.1	1.13	.67	1.12	3.26
22.0	6.3	-18.7	22.2	1.13	.67	1.12	3.26
23.0	6.2	-18.4	22.2	1.13	.67	1.12	3.25
24.0	6.2	-18.2	22.3	1.13	.67	1.12	3.25
25.0	6.1	-18.0	22.4	1.13	.67	1.12	3.25
26.0	6.1	-17.7	22.4	1.13	.67	1.12	3.25
27.0	6.1	-17.5	22.5	1.13	.67	1.12	3.24
28.0	6.0	-17.2	22.6	1.13	.67	1.12	3.24
29.0	6.0	-17.0	22.7	1.12	.67	1.12	3.23
30.0	6.0	-16.7	22.8	1.12	.67	1.12	3.23
31.0	5.9	-16.5	22.9	1.12	.67	1.12	3.22
32.0	5.9	-16.2	23.1	1.12	.67	1.11	3.22
33.0	5.9	-16.0	23.2	1.12	.67	1.11	3.21
34.0	5.9	-15.8	23.4	1.12	.67	1.11	3.20
35.0	5.8	-15.5	23.6	1.12	.66	1.11	3.19
36.0	5.8	-15.3	23.7	1.12	.66	1.11	3.19
37.0	5.8	-15.0	23.9	1.11	.66	1.10	3.18
38.0	5.8	-14.8	24.1	1.11	.66	1.10	3.17
39.0	5.8	-14.5	24.4	1.11	.66	1.10	3.16
40.0	5.8	-14.3	24.6	1.11	.66	1.10	3.15
41.0	5.7	-14.0	24.8	1.11	.66	1.09	3.14
42.0	5.7	-13.8	25.1	1.10	.65	1.09	3.13
43.0	5.7	-13.5	25.3	1.10	.65	1.09	3.12
44.0	5.7	-13.3	25.6	1.10	.65	1.08	3.10
45.0	5.7	-13.1	25.9	1.10	.65	1.08	3.09
46.0	5.7	-12.8	26.2	1.09	.65	1.08	3.08
47.0	5.7	-12.6	26.5	1.09	.65	1.07	3.07
48.0	5.7	-12.3	26.8	1.09	.64	1.07	3.05
49.0	5.7	-12.1	27.2	1.08	.64	1.06	3.03
50.0	5.6	-11.8	27.6	1.08	.64	1.06	3.02
51.0	5.6	-11.6	28.0	1.08	.64	1.06	3.00
52.0	5.6	-11.3	28.4	1.08	.64	1.05	2.99
53.0	5.6	-11.1	28.9	1.07	.63	1.05	2.97
54.0	5.6	-10.9	29.3	1.07	.63	1.04	2.95
55.0	5.6	-10.6	29.8	1.06	.63	1.04	2.93
56.0	5.6	-10.4	30.3	1.06	.62	1.03	2.91
57.0	5.6	-10.1	30.8	1.06	.62	1.02	2.89
58.0	5.6	-9.9	31.4	1.05	.62	1.02	2.87
59.0	5.6	-9.6	32.0	1.05	.62	1.01	2.84
60.0	5.6	-9.4	32.7	1.04	.61	1.01	2.82
61.0	5.6	-9.1	33.3	1.04	.61	1.00	2.79

40

62.0	5.6	-8.9	34.1	1.03	.60	.99	2.77
63.0	5.6	-8.7	34.8	1.03	.60	.98	2.74
64.0	5.6	-8.4	35.7	1.02	.60	.98	2.71
65.0	5.6	-8.2	36.5	1.01	.59	.97	2.68
66.0	5.6	-7.9	37.4	1.01	.59	.96	2.64
67.0	5.6	-7.7	38.4	1.00	.58	.95	2.61
68.0	5.6	-7.4	39.5	.99	.58	.94	2.57
69.0	5.6	-7.2	40.7	.98	.57	.93	2.53
70.0	5.6	-6.9	41.9	.98	.57	.92	2.49
71.0	5.6	-6.7	43.2	.97	.56	.90	2.44
72.0	5.6	-6.5	44.7	.96	.55	.89	2.39
73.0	5.6	-6.2	46.3	.95	.55	.88	2.34
74.0	5.6	-6.0	48.0	.94	.54	.86	2.29
75.0	5.6	-5.7	49.9	.92	.53	.85	2.23
76.0	5.7	-5.5	52.0	.91	.52	.83	2.17
77.0	5.7	-5.2	54.4	.90	.51	.81	2.09
78.0	5.7	-5.0	57.1	.88	.50	.79	2.01
79.0	5.8	-4.7	60.3	.86	.49	.76	1.92
80.0	5.8	-4.5	64.0	.84	.47	.74	1.82
81.0	5.9	-4.2	68.4	.82	.46	.70	1.70
82.0	6.0	-4.0	73.5	.79	.44	.67	1.57
83.0	6.1	-3.8	79.8	.76	.42	.63	1.42
84.0	6.3	-3.5	87.3	.73	.39	.58	1.24
85.0	6.5	-3.3	96.5	.68	.36	.52	1.03
86.0	6.7	-3.0	108.0	.63	.33	.45	.78
87.0	7.0	-2.8	122.8	.57	.29	.37	.48
88.0	7.4	-2.5	141.9	.50	.23	.27	.12
89.0	7.9	-2.3	167.5	.41	.17	.15	0.00
90.0	8.5	-2.0	203.2	.30	.09	0.00	0.00
91.0	9.0	-1.8	248.6	.17	.00	0.00	0.00
MEAN	6.3	-12.9	41.2	1.01	.59	.97	2.70
SDEV	1.0	6.5	38.4	.19	.13	.25	.83
MIN	5.6	-24.0	21.3	.17	.00	0.00	0.00
MAX	9.8	-1.8	248.6	1.14	.68	1.14	3.30

NEUTRAL AXIS (CM)	39.3
FLEXURAL RIGIDITY (N-M)	1.54E+08
CHARACTERISTIC LENGTH (M)	11.15
AVERAGE ICE SALINITY (o/oo)	6.30
AVERAGE ICE TEMPERATURE (C)	-12.9
BULK BRINE VOLUME (o/oo)	28.9
BULK TENSILE STRENGTH (MPA)	1.07
BULK FLEXURAL STRENGTH (MPA)	.63
BULK SHEAR STRENGTH (MPA)	1.05
BULK EFFECTIVE MODULUS (GPA)	2.97
BULK FLEXURAL RIGIDITY (N-M)	2.10E+08
BULK CHARACTERISTIC LENGTH (M)	12.03

PROFILE: SG5E-31   DEPTH: 122 CM (4 FT)

Depth	Salinity	Temp	VB	Sigma T	Sigma F	Sigma S	Eeff
(cm)	(o/oo)	(C)	(o/oo)	(MPa)	(MPa)	(MPa)	(GPa)
.3	9.7	-27.2	11.8	1.24	.75	1.27	3.81
1.0	9.4	-27.0	11.6	1.24	.75	1.28	3.82
2.0	8.9	-26.8	11.4	1.25	.75	1.28	3.84
3.0	8.6	-26.6	11.2	1.25	.76	1.28	3.85
4.0	8.3	-26.4	11.2	1.25	.76	1.29	3.85
5.0	8.0	-26.2	11.2	1.25	.76	1.29	3.85
6.0	7.8	-26.0	11.2	1.25	.76	1.28	3.85
7.0	7.6	-25.8	11.3	1.25	.75	1.28	3.84
8.0	7.4	-25.6	11.5	1.24	.75	1.28	3.83
9.0	7.2	-25.3	11.7	1.24	.75	1.28	3.82
10.0	7.1	-25.1	12.0	1.24	.75	1.27	3.80
11.0	7.0	-24.9	12.3	1.23	.75	1.27	3.78
12.0	6.9	-24.7	12.6	1.23	.74	1.26	3.76
13.0	6.8	-24.5	13.0	1.23	.74	1.25	3.74
14.0	6.7	-24.3	13.5	1.22	.74	1.25	3.71
15.0	6.6	-24.1	14.1	1.21	.73	1.24	3.68
16.0	6.5	-23.9	14.7	1.21	.73	1.23	3.64
17.0	6.5	-23.7	15.5	1.20	.72	1.22	3.60

18.0	6.4	-23.5	16.3	1.19	.71	1.20	3.55
19.0	6.3	-23.3	17.3	1.18	.71	1.19	3.49
20.0	6.3	-23.1	18.5	1.16	.70	1.17	3.43
21.0	6.2	-22.8	19.0	1.16	.69	1.17	3.41
22.0	6.2	-22.6	19.0	1.16	.69	1.17	3.41
23.0	6.1	-22.4	19.0	1.16	.69	1.17	3.41
24.0	6.1	-22.2	19.0	1.16	.69	1.17	3.41
25.0	6.0	-22.0	19.0	1.16	.69	1.17	3.41
26.0	6.0	-21.8	19.0	1.16	.69	1.17	3.41
27.0	6.0	-21.6	19.0	1.16	.69	1.17	3.41
28.0	5.9	-21.4	19.0	1.16	.69	1.17	3.41
29.0	5.9	-21.2	19.1	1.16	.69	1.16	3.41
30.0	5.9	-21.0	19.1	1.16	.69	1.16	3.40
31.0	5.8	-20.8	19.2	1.16	.69	1.16	3.40
32.0	5.8	-20.6	19.2	1.16	.69	1.16	3.40
33.0	5.8	-20.3	19.3	1.16	.69	1.16	3.39
34.0	5.8	-20.1	19.4	1.16	.69	1.16	3.39
35.0	5.7	-19.9	19.4	1.16	.69	1.16	3.39
36.0	5.7	-19.7	19.5	1.15	.69	1.16	3.38
37.0	5.7	-19.5	19.6	1.15	.69	1.16	3.38
38.0	5.7	-19.3	19.7	1.15	.69	1.16	3.38
39.0	5.7	-19.1	19.7	1.15	.69	1.16	3.37
40.0	5.7	-18.9	19.9	1.15	.69	1.15	3.37
41.0	5.6	-18.7	19.9	1.15	.69	1.15	3.36
42.0	5.6	-18.5	20.1	1.15	.69	1.15	3.36
43.0	5.6	-18.3	20.2	1.15	.69	1.15	3.35
44.0	5.6	-18.1	20.3	1.15	.69	1.15	3.35
45.0	5.6	-17.8	20.4	1.15	.68	1.15	3.34
46.0	5.6	-17.6	20.5	1.15	.68	1.15	3.34
47.0	5.6	-17.4	20.6	1.14	.68	1.14	3.33
48.0	5.5	-17.2	20.8	1.14	.68	1.14	3.32
49.0	5.5	-17.0	20.9	1.14	.68	1.14	3.32
50.0	5.5	-16.8	21.0	1.14	.68	1.14	3.31
51.0	5.5	-16.6	21.2	1.14	.68	1.14	3.30
52.0	5.5	-16.4	21.3	1.14	.68	1.13	3.30
53.0	5.5	-16.2	21.5	1.14	.68	1.13	3.29
54.0	5.5	-16.0	21.7	1.13	.68	1.13	3.28
55.0	5.5	-15.8	21.8	1.13	.68	1.13	3.27
56.0	5.5	-15.6	22.0	1.13	.67	1.13	3.27
57.0	5.5	-15.3	22.1	1.13	.67	1.12	3.26
58.0	5.4	-15.1	22.3	1.13	.67	1.12	3.25
59.0	5.4	-14.9	22.5	1.13	.67	1.12	3.24
60.0	5.4	-14.7	22.7	1.12	.67	1.12	3.23
61.0	5.4	-14.5	22.9	1.12	.67	1.12	3.22
62.0	5.4	-14.3	23.1	1.12	.67	1.11	3.21
63.0	5.4	-14.1	23.3	1.12	.67	1.11	3.20
64.0	5.4	-13.9	23.6	1.12	.66	1.11	3.19
65.0	5.4	-13.7	23.8	1.11	.66	1.10	3.18
66.0	5.4	-13.5	24.1	1.11	.66	1.10	3.17
67.0	5.4	-13.3	24.3	1.11	.66	1.10	3.16
68.0	5.4	-13.1	24.6	1.11	.66	1.10	3.15
69.0	5.4	-12.8	24.8	1.11	.66	1.09	3.14
70.0	5.4	-12.6	25.1	1.10	.65	1.09	3.13
71.0	5.4	-12.4	25.4	1.10	.65	1.09	3.11
72.0	5.4	-12.2	25.7	1.10	.65	1.08	3.10
73.0	5.4	-12.0	26.0	1.10	.65	1.08	3.09
74.0	5.4	-11.8	26.3	1.09	.65	1.07	3.07
75.0	5.4	-11.6	26.6	1.09	.65	1.07	3.06
76.0	5.4	-11.4	27.0	1.09	.64	1.07	3.04
77.0	5.4	-11.2	27.3	1.08	.64	1.06	3.03
78.0	5.4	-11.0	27.7	1.08	.64	1.06	3.01
79.0	5.4	-10.8	28.1	1.08	.64	1.05	3.00
80.0	5.4	-10.6	28.5	1.07	.63	1.05	2.98
81.0	5.3	-10.3	28.9	1.07	.63	1.05	2.96
82.0	5.3	-10.1	29.4	1.07	.63	1.04	2.95
83.0	5.3	-9.9	29.9	1.06	.63	1.04	2.93
84.0	5.3	-9.7	30.4	1.06	.62	1.03	2.91
85.0	5.3	-9.5	30.9	1.06	.62	1.02	2.89
86.0	5.3	-9.3	31.4	1.05	.62	1.02	2.87
87.0	5.3	-9.1	32.0	1.05	.62	1.01	2.84
88.0	5.3	-8.9	32.6	1.04	.61	1.01	2.82
89.0	5.3	-8.7	33.2	1.04	.61	1.00	2.80
90.0	5.3	-8.5	33.8	1.03	.61	.99	2.78
91.0	5.3	-8.3	34.5	1.03	.60	.99	2.75
92.0	5.3	-8.1	35.2	1.02	.60	.98	2.72
93.0	5.3	-7.8	36.0	1.02	.59	.97	2.69
94.0	5.3	-7.6	36.9	1.01	.59	.96	2.66

42

95.0	5.3	−7.4	37.7	1.00	.59	.96	2.63
96.0	5.3	−7.2	38.6	1.00	.58	.95	2.60
97.0	5.3	−7.0	39.6	.99	.58	.94	2.57
98.0	5.3	−6.8	40.6	.98	.57	.93	2.53
99.0	5.3	−6.6	41.7	.98	.57	.92	2.49
100.0	5.4	−6.4	43.0	.97	.56	.91	2.45
101.0	5.4	−6.2	44.2	.96	.55	.90	2.41
102.0	5.4	−6.0	45.6	.95	.55	.88	2.36
103.0	5.4	−5.8	47.1	.94	.54	.87	2.32
104.0	5.4	−5.6	48.7	.93	.53	.86	2.27
105.0	5.4	−5.3	50.4	.92	.53	.84	2.21
106.0	5.4	−5.1	52.4	.91	.52	.83	2.15
107.0	5.4	−4.9	54.6	.90	.51	.81	2.09
108.0	5.4	−4.7	57.1	.88	.50	.79	2.02
109.0	5.5	−4.5	60.1	.86	.49	.77	1.93
110.0	5.5	−4.3	63.3	.85	.48	.74	1.84
111.0	5.6	−4.1	67.2	.83	.46	.71	1.74
112.0	5.7	−3.9	71.7	.80	.44	.68	1.62
113.0	5.8	−3.7	77.1	.77	.43	.64	1.48
114.0	5.9	−3.5	83.4	.74	.40	.60	1.33
115.0	6.1	−3.3	91.0	.71	.38	.55	1.15
116.0	6.3	−3.1	100.3	.67	.35	.50	.94
117.0	6.5	−2.8	111.8	.62	.32	.43	.70
118.0	6.8	−2.6	126.3	.56	.28	.35	.41
119.0	7.2	−2.4	144.8	.49	.23	.26	.06
120.0	7.7	−2.2	169.1	.41	.17	.15	0.00
121.0	8.3	−2.0	201.8	.30	.10	.00	0.00
122.0	8.8	−1.8	241.8	.18	.01	0.00	0.00
MEAN	6.0	−14.5	34.9	1.06	.62	1.03	2.93
SDEV	.9	7.4	35.5	.19	.13	.25	.86
MIN	5.3	−27.2	11.2	.18	.01	0.00	0.00
MAX	9.7	−1.8	241.8	1.25	.76	1.29	3.85

NEUTRAL AXIS (CM)   52.5
FLEXURAL RIGIDITY (N-M)   4.22E+08
CHARACTERISTIC LENGTH (M)   14.33

AVERAGE ICE SALINITY (o/oo)   5.96
AVERAGE ICE TEMPERATURE (C) −14.5
BULK BRINE VOLUME (o/oo)   25.2
BULK TENSILE STRENGTH (MPA)   1.10
BULK FLEXURAL STRENGTH (MPA) .65
BULK SHEAR STRENGTH (MPA)   1.09
BULK EFFECTIVE MODULUS (GPA) 3.12
BULK FLEXURAL RIGIDITY (N-M) 5.31E+08
BULK CHARACTERISTIC LENGTH (M) 15.18

PROFILE: SG5E-31   DEPTH: 152 CM (5 FT)

Depth (cm)	Salinity (o/oo)	Temp (C)	VB (o/oo)	Sigma T (MPa)	Sigma F (MPa)	Sigma S (MPa)	Eeff (GPa)
.3	9.7	−28.6	10.0	1.26	.77	1.31	3.93
1.0	9.4	−28.5	9.8	1.27	.77	1.31	3.95
2.0	8.9	−28.3	9.5	1.27	.77	1.32	3.97
3.0	8.6	−28.1	9.2	1.27	.77	1.32	3.98
4.0	8.3	−28.0	9.1	1.28	.78	1.32	3.99
5.0	8.0	−27.8	9.0	1.28	.78	1.33	4.00
6.0	7.8	−27.6	8.9	1.28	.78	1.33	4.01
7.0	7.6	−27.4	8.9	1.28	.78	1.33	4.01
8.0	7.4	−27.2	8.9	1.28	.78	1.33	4.01
9.0	7.2	−27.1	8.9	1.28	.78	1.33	4.01
10.0	7.1	−26.9	8.9	1.28	.78	1.33	4.01
11.0	7.0	−26.7	9.0	1.28	.78	1.33	4.00
12.0	6.9	−26.5	9.1	1.28	.78	1.32	4.00
13.0	6.8	−26.4	9.2	1.28	.77	1.32	3.99
14.0	6.7	−26.2	9.3	1.27	.77	1.32	3.98
15.0	6.6	−26.0	9.5	1.27	.77	1.32	3.97
16.0	6.5	−25.8	9.6	1.27	.77	1.31	3.96
17.0	6.4	−25.7	9.8	1.27	.77	1.31	3.94
18.0	6.4	−25.5	10.0	1.26	.77	1.31	3.93
19.0	6.3	−25.3	10.3	1.26	.76	1.30	3.91

20.0	6.3	-25.1	10.5	1.26	.76	1.30	3.89
21.0	6.2	-25.0	10.8	1.25	.76	1.29	3.87
22.0	6.2	-24.8	11.2	1.25	.76	1.29	3.85
23.0	6.1	-24.6	11.5	1.24	.75	1.28	3.83
24.0	6.1	-24.4	11.9	1.24	.75	1.27	3.80
25.0	6.0	-24.2	12.3	1.23	.75	1.27	3.78
26.0	6.0	-24.1	12.8	1.23	.74	1.26	3.75
27.0	5.9	-23.9	13.3	1.22	.74	1.25	3.72
28.0	5.9	-23.7	14.0	1.21	.73	1.24	3.68
29.0	5.8	-23.5	14.6	1.21	.73	1.23	3.64
30.0	5.8	-23.4	15.4	1.20	.72	1.22	3.60
31.0	5.8	-23.2	16.3	1.19	.71	1.20	3.55
32.0	5.8	-23.0	17.3	1.18	.71	1.19	3.49
33.0	5.7	-22.8	17.5	1.17	.70	1.19	3.48
34.0	5.7	-22.7	17.6	1.17	.70	1.19	3.48
35.0	5.7	-22.5	17.6	1.17	.70	1.18	3.48
36.0	5.7	-22.3	17.7	1.17	.70	1.18	3.48
37.0	5.6	-22.1	17.7	1.17	.70	1.18	3.48
38.0	5.6	-21.9	17.7	1.17	.70	1.18	3.47
39.0	5.6	-21.8	17.8	1.17	.70	1.18	3.47
40.0	5.6	-21.6	17.9	1.17	.70	1.18	3.47
41.0	5.6	-21.4	17.9	1.17	.70	1.18	3.47
42.0	5.6	-21.2	17.9	1.17	.70	1.18	3.46
43.0	5.5	-21.1	18.0	1.17	.70	1.18	3.46
44.0	5.5	-20.9	18.1	1.17	.70	1.18	3.46
45.0	5.5	-20.7	18.1	1.17	.70	1.18	3.45
46.0	5.5	-20.5	18.2	1.17	.70	1.18	3.45
47.0	5.5	-20.4	18.3	1.17	.70	1.18	3.44
48.0	5.5	-20.2	18.3	1.17	.70	1.18	3.44
49.0	5.5	-20.0	18.4	1.17	.70	1.17	3.44
50.0	5.5	-19.8	18.5	1.16	.70	1.17	3.43
51.0	5.4	-19.6	18.6	1.16	.70	1.17	3.43
52.0	5.4	-19.5	18.7	1.16	.70	1.17	3.43
53.0	5.4	-19.3	18.8	1.16	.70	1.17	3.42
54.0	5.4	-19.1	18.9	1.16	.70	1.17	3.42
55.0	5.4	-18.9	18.9	1.16	.69	1.17	3.41
56.0	5.4	-18.8	19.0	1.16	.69	1.17	3.41
57.0	5.4	-18.6	19.1	1.16	.69	1.17	3.40
58.0	5.4	-18.4	19.3	1.16	.69	1.16	3.40
59.0	5.4	-18.2	19.3	1.16	.69	1.16	3.39
60.0	5.4	-18.1	19.4	1.16	.69	1.16	3.39
61.0	5.4	-17.9	19.5	1.15	.69	1.16	3.38
62.0	5.4	-17.7	19.7	1.15	.69	1.16	3.38
63.0	5.3	-17.5	19.8	1.15	.69	1.16	3.37
64.0	5.3	-17.4	19.9	1.15	.69	1.15	3.37
65.0	5.3	-17.2	20.0	1.15	.69	1.15	3.36
66.0	5.3	-17.0	20.1	1.15	.69	1.15	3.35
67.0	5.3	-16.8	20.2	1.15	.69	1.15	3.35
68.0	5.3	-16.6	20.4	1.15	.69	1.15	3.34
69.0	5.3	-16.5	20.5	1.15	.68	1.15	3.34
70.0	5.3	-16.3	20.6	1.14	.68	1.15	3.33
71.0	5.3	-16.1	20.8	1.14	.68	1.14	3.32
72.0	5.3	-15.9	20.9	1.14	.68	1.14	3.32
73.0	5.3	-15.8	21.1	1.14	.68	1.14	3.31
74.0	5.3	-15.6	21.2	1.14	.68	1.14	3.30
75.0	5.3	-15.4	21.3	1.14	.68	1.13	3.30
76.0	5.3	-15.2	21.5	1.14	.68	1.13	3.29
77.0	5.3	-15.1	21.7	1.13	.68	1.13	3.28
78.0	5.3	-14.9	21.8	1.13	.68	1.13	3.27
79.0	5.3	-14.7	22.0	1.13	.68	1.13	3.27
80.0	5.2	-14.5	22.1	1.13	.67	1.13	3.26
81.0	5.2	-14.3	22.3	1.13	.67	1.12	3.25
82.0	5.2	-14.2	22.5	1.13	.67	1.12	3.24
83.0	5.2	-14.0	22.7	1.12	.67	1.12	3.23
84.0	5.2	-13.8	22.8	1.12	.67	1.12	3.23
85.0	5.2	-13.6	23.0	1.12	.67	1.12	3.22
86.0	5.2	-13.5	23.2	1.12	.67	1.11	3.21
87.0	5.2	-13.3	23.4	1.12	.67	1.11	3.20
88.0	5.2	-13.1	23.6	1.12	.66	1.11	3.19
89.0	5.2	-12.9	23.9	1.11	.66	1.11	3.18
90.0	5.2	-12.8	24.0	1.11	.66	1.10	3.17
91.0	5.2	-12.6	24.3	1.11	.66	1.10	3.16
92.0	5.2	-12.4	24.5	1.11	.66	1.10	3.15
93.0	5.2	-12.2	24.8	1.11	.66	1.10	3.14
94.0	5.2	-12.1	25.0	1.10	.66	1.09	3.13
95.0	5.2	-11.9	25.2	1.10	.65	1.09	3.12
96.0	5.2	-11.7	25.5	1.10	.65	1.08	3.11

97.0	5.2	-11.5	25.8	1.10	.65	1.08	3.10
98.0	5.2	-11.3	26.0	1.10	.65	1.08	3.09
99.0	5.2	-11.2	26.3	1.09	.65	1.07	3.07
100.0	5.1	-11.0	26.6	1.09	.65	1.07	3.06
101.0	5.1	-10.8	26.9	1.09	.64	1.07	3.05
102.0	5.1	-10.6	27.3	1.08	.64	1.06	3.03
103.0	5.1	-10.5	27.6	1.08	.64	1.06	3.02
104.0	5.1	-10.3	27.9	1.08	.64	1.06	3.01
105.0	5.1	-10.1	28.2	1.08	.64	1.05	2.99
106.0	5.1	-9.9	28.6	1.07	.63	1.05	2.98
107.0	5.1	-9.8	29.0	1.07	.63	1.04	2.96
108.0	5.1	-9.6	29.4	1.07	.63	1.04	2.95
109.0	5.1	-9.4	29.8	1.06	.63	1.04	2.93
110.0	5.1	-9.2	30.3	1.06	.62	1.03	2.91
111.0	5.1	-9.0	30.7	1.06	.62	1.03	2.90
112.0	5.1	-8.9	31.2	1.05	.62	1.02	2.88
113.0	5.1	-8.7	31.7	1.05	.62	1.02	2.86
114.0	5.1	-8.5	32.1	1.05	.61	1.01	2.84
115.0	5.1	-8.3	32.7	1.04	.61	1.01	2.82
116.0	5.1	-8.2	33.3	1.04	.61	1.00	2.80
117.0	5.1	-8.0	33.9	1.03	.61	.99	2.77
118.0	5.1	-7.8	34.5	1.03	.60	.99	2.75
119.0	5.1	-7.6	35.1	1.02	.60	.98	2.73
120.0	5.1	-7.5	35.8	1.02	.60	.97	2.70
121.0	5.1	-7.3	36.5	1.01	.59	.97	2.68
122.0	5.1	-7.1	37.2	1.01	.59	.96	2.65
123.0	5.1	-6.9	38.1	1.00	.58	.95	2.62
124.0	5.1	-6.7	38.9	1.00	.58	.94	2.59
125.0	5.1	-6.6	39.8	.99	.58	.94	2.56
126.0	5.1	-6.4	40.7	.98	.57	.93	2.53
127.0	5.1	-6.2	41.7	.98	.57	.92	2.49
128.0	5.1	-6.0	42.8	.97	.56	.91	2.46
129.0	5.1	-5.9	43.9	.96	.56	.90	2.42
130.0	5.1	-5.7	45.1	.95	.55	.89	2.38
131.0	5.1	-5.5	46.4	.95	.54	.88	2.34
132.0	5.1	-5.3	47.8	.94	.54	.86	2.30
133.0	5.1	-5.2	49.3	.93	.53	.85	2.25
134.0	5.1	-5.0	50.9	.92	.53	.84	2.20
135.0	5.1	-4.8	52.7	.91	.52	.82	2.14
136.0	5.1	-4.6	54.7	.90	.51	.81	2.09
137.0	5.1	-4.5	57.0	.88	.50	.79	2.02
138.0	5.2	-4.3	59.7	.87	.49	.77	1.94
139.0	5.2	-4.1	62.6	.85	.48	.75	1.86
140.0	5.3	-3.9	66.0	.83	.47	.72	1.77
141.0	5.4	-3.7	70.0	.81	.45	.69	1.66
142.0	5.5	-3.6	74.5	.79	.43	.66	1.55
143.0	5.6	-3.4	80.0	.76	.42	.62	1.41
144.0	5.7	-3.2	86.4	.73	.39	.58	1.26
145.0	5.9	-3.0	94.0	.69	.37	.54	1.08
146.0	6.1	-2.9	103.3	.65	.34	.48	.88
147.0	6.3	-2.7	114.5	.61	.31	.42	.64
148.0	6.6	-2.5	128.5	.55	.27	.34	.37
149.0	7.0	-2.3	146.3	.49	.22	.25	.04
150.0	7.4	-2.2	169.1	.41	.17	.15	0.00
151.0	8.0	-2.0	199.0	.31	.10	.02	0.00
152.0	8.5	-1.8	234.1	.21	.03	0.00	0.00

MEAN	5.7	-15.2	31.6	1.09	.64	1.07	3.05
SDEV	.9	7.8	32.9	.18	.13	.25	.86
MIN	5.1	-28.6	8.9	.21	.03	0.00	0.00
MAX	9.7	-1.8	234.1	1.28	.78	1.33	4.01

NEUTRAL AXIS (CM)	65.7
FLEXURAL RIGIDITY (N-M)	8.69E+08
CHARACTERISTIC LENGTH (M)	17.16

AVERAGE ICE SALINITY (o/oo)	5.71
AVERAGE ICE TEMPERATURE (C)	-15.2
BULK BRINE VOLUME (o/oo)	23.3
BULK TENSILE STRENGTH (MPA)	1.12
BULK FLEXURAL STRENGTH (MPA)	.67
BULK SHEAR STRENGTH (MPA)	1.11
BULK EFFECTIVE MODULUS (GPA)	3.21
BULK FLEXURAL RIGIDITY (N-M)	1.05E+09
BULK CHARACTERISTIC LENGTH (M)	18.02

PROFILE: SG5E-31   DEPTH: 183 CM (6 FT)

Depth (cm)	Salinity (o/oo)	Temp (C)	VB (o/oo)	Sigma T (MPa)	Sigma F (MPa)	Sigma S (MPa)	Eeff (GPa)
.3	9.7	-29.1	9.5	1.27	.77	1.32	3.97
1.0	9.4	-29.0	9.3	1.27	.77	1.32	3.98
2.0	8.9	-28.9	9.0	1.28	.78	1.33	4.00
3.0	8.6	-28.7	8.7	1.28	.78	1.33	4.02
4.0	8.2	-28.6	8.5	1.29	.78	1.34	4.04
5.0	8.0	-28.4	8.4	1.29	.78	1.34	4.05
6.0	7.8	-28.3	8.3	1.29	.78	1.34	4.06
7.0	7.6	-28.1	8.2	1.29	.78	1.34	4.06
8.0	7.4	-28.0	8.2	1.29	.79	1.34	4.07
9.0	7.2	-27.8	8.1	1.29	.79	1.34	4.07
10.0	7.1	-27.7	8.1	1.29	.79	1.34	4.07
11.0	7.0	-27.5	8.1	1.29	.79	1.34	4.07
12.0	6.9	-27.4	8.1	1.29	.79	1.34	4.07
13.0	6.8	-27.2	8.2	1.29	.79	1.34	4.06
14.0	6.7	-27.1	8.2	1.29	.78	1.34	4.06
15.0	6.6	-26.9	8.3	1.29	.78	1.34	4.06
16.0	6.5	-26.8	8.4	1.29	.78	1.34	4.05
17.0	6.4	-26.6	8.4	1.29	.78	1.34	4.04
18.0	6.4	-26.5	8.5	1.29	.78	1.34	4.04
19.0	6.3	-26.3	8.6	1.28	.78	1.33	4.03
20.0	6.3	-26.2	8.8	1.28	.78	1.33	4.02
21.0	6.2	-26.0	8.9	1.28	.78	1.33	4.01
22.0	6.1	-25.9	9.0	1.28	.78	1.33	4.00
23.0	6.1	-25.7	9.2	1.28	.77	1.32	3.99
24.0	6.1	-25.6	9.4	1.27	.77	1.32	3.97
25.0	6.0	-25.4	9.6	1.27	.77	1.31	3.96
26.0	6.0	-25.3	9.8	1.27	.77	1.31	3.95
27.0	5.9	-25.1	10.0	1.26	.77	1.31	3.93
28.0	5.9	-25.0	10.2	1.26	.76	1.30	3.92
29.0	5.8	-24.8	10.5	1.26	.76	1.30	3.90
30.0	5.8	-24.7	10.8	1.25	.76	1.29	3.88
31.0	5.8	-24.5	11.1	1.25	.76	1.29	3.86
32.0	5.8	-24.4	11.5	1.24	.75	1.28	3.83
33.0	5.7	-24.2	11.8	1.24	.75	1.27	3.81
34.0	5.7	-24.1	12.2	1.24	.75	1.27	3.79
35.0	5.7	-23.9	12.7	1.23	.74	1.26	3.76
36.0	5.6	-23.8	13.2	1.22	.74	1.25	3.73
37.0	5.6	-23.6	13.7	1.22	.73	1.24	3.69
38.0	5.6	-23.5	14.3	1.21	.73	1.23	3.66
39.0	5.6	-23.3	15.0	1.20	.72	1.22	3.62
40.0	5.6	-23.2	15.8	1.19	.72	1.21	3.58
41.0	5.5	-23.0	16.6	1.19	.71	1.20	3.54
42.0	5.5	-22.9	16.9	1.18	.71	1.20	3.52
43.0	5.5	-22.7	16.9	1.18	.71	1.19	3.52
44.0	5.5	-22.6	16.9	1.18	.71	1.19	3.52
45.0	5.5	-22.4	17.0	1.18	.71	1.19	3.51
46.0	5.5	-22.3	17.0	1.18	.71	1.19	3.51
47.0	5.4	-22.1	17.1	1.18	.71	1.19	3.51
48.0	5.4	-22.0	17.1	1.18	.71	1.19	3.51
49.0	5.4	-21.8	17.2	1.18	.71	1.19	3.50
50.0	5.4	-21.7	17.2	1.18	.71	1.19	3.50
51.0	5.4	-21.5	17.3	1.18	.71	1.19	3.50
52.0	5.4	-21.4	17.3	1.18	.71	1.19	3.49
53.0	5.4	-21.2	17.4	1.18	.71	1.19	3.49
54.0	5.4	-21.1	17.5	1.18	.70	1.19	3.49
55.0	5.4	-20.9	17.5	1.18	.70	1.19	3.49
56.0	5.4	-20.8	17.6	1.17	.70	1.19	3.48
57.0	5.3	-20.6	17.6	1.17	.70	1.18	3.48
58.0	5.3	-20.5	17.7	1.17	.70	1.18	3.48
59.0	5.3	-20.3	17.7	1.17	.70	1.18	3.47
60.0	5.3	-20.2	17.8	1.17	.70	1.18	3.47
61.0	5.3	-20.0	17.9	1.17	.70	1.18	3.47
62.0	5.3	-19.9	18.0	1.17	.70	1.18	3.46
63.0	5.3	-19.7	18.0	1.17	.70	1.18	3.46
64.0	5.3	-19.6	18.1	1.17	.70	1.18	3.45
65.0	5.3	-19.4	18.2	1.17	.70	1.18	3.45
66.0	5.3	-19.3	18.3	1.17	.70	1.18	3.45
67.0	5.3	-19.1	18.4	1.17	.70	1.17	3.44
68.0	5.3	-19.0	18.4	1.17	.70	1.17	3.44
69.0	5.3	-18.8	18.5	1.17	.70	1.17	3.44
70.0	5.3	-18.7	18.6	1.16	.70	1.17	3.43
71.0	5.2	-18.5	18.7	1.16	.70	1.17	3.43

72.0	5.2	-18.4	18.7	1.16	.70	1.17	3.42
73.0	5.2	-18.2	18.8	1.16	.70	1.17	3.42
74.0	5.2	-18.1	18.9	1.16	.69	1.17	3.41
75.0	5.2	-17.9	19.0	1.16	.69	1.17	3.41
76.0	5.2	-17.8	19.1	1.16	.69	1.16	3.40
77.0	5.2	-17.6	19.2	1.16	.69	1.16	3.40
78.0	5.2	-17.5	19.3	1.16	.69	1.16	3.40
79.0	5.2	-17.3	19.4	1.16	.69	1.16	3.39
80.0	5.2	-17.2	19.4	1.16	.69	1.16	3.39
81.0	5.2	-17.0	19.6	1.15	.69	1.16	3.38
82.0	5.2	-16.9	19.6	1.15	.69	1.16	3.38
83.0	5.2	-16.7	19.8	1.15	.69	1.16	3.37
84.0	5.2	-16.6	19.8	1.15	.69	1.15	3.37
85.0	5.2	-16.4	20.0	1.15	.69	1.15	3.36
86.0	5.2	-16.3	20.1	1.15	.69	1.15	3.36
87.0	5.1	-16.1	20.2	1.15	.69	1.15	3.35
88.0	5.1	-16.0	20.3	1.15	.69	1.15	3.35
89.0	5.1	-15.8	20.4	1.15	.68	1.15	3.34
90.0	5.1	-15.7	20.5	1.15	.68	1.15	3.34
91.0	5.1	-15.5	20.6	1.14	.68	1.14	3.33
92.0	5.1	-15.4	20.7	1.14	.68	1.14	3.33
93.0	5.1	-15.3	20.8	1.14	.68	1.14	3.32
94.0	5.1	-15.1	21.0	1.14	.68	1.14	3.31
95.0	5.1	-15.0	21.1	1.14	.68	1.14	3.31
96.0	5.1	-14.8	21.2	1.14	.68	1.14	3.30
97.0	5.1	-14.7	21.3	1.14	.68	1.14	3.30
98.0	5.1	-14.5	21.4	1.14	.68	1.13	3.29
99.0	5.1	-14.4	21.6	1.13	.68	1.13	3.28
100.0	5.1	-14.2	21.7	1.13	.68	1.13	3.28
101.0	5.1	-14.1	21.9	1.13	.67	1.13	3.27
102.0	5.1	-13.9	22.0	1.13	.67	1.13	3.27
103.0	5.0	-13.8	22.1	1.13	.67	1.13	3.26
104.0	5.0	-13.6	22.3	1.13	.67	1.12	3.25
105.0	5.0	-13.5	22.4	1.13	.67	1.12	3.25
106.0	5.0	-13.3	22.6	1.13	.67	1.12	3.24
107.0	5.0	-13.2	22.7	1.12	.67	1.12	3.23
108.0	5.0	-13.0	22.9	1.12	.67	1.12	3.22
109.0	5.0	-12.9	23.1	1.12	.67	1.11	3.22
110.0	5.0	-12.7	23.2	1.12	.67	1.11	3.21
111.0	5.0	-12.6	23.4	1.12	.66	1.11	3.20
112.0	5.0	-12.4	23.6	1.12	.66	1.11	3.19
113.0	5.0	-12.3	23.8	1.12	.66	1.10	3.19
114.0	5.0	-12.1	24.0	1.11	.66	1.10	3.18
115.0	5.0	-12.0	24.1	1.11	.66	1.10	3.17
116.0	5.0	-11.8	24.3	1.11	.66	1.10	3.16
117.0	5.0	-11.7	24.5	1.11	.66	1.10	3.15
118.0	5.0	-11.5	24.7	1.11	.66	1.09	3.14
119.0	5.0	-11.4	25.0	1.10	.66	1.09	3.13
120.0	4.9	-11.2	25.2	1.10	.65	1.09	3.12
121.0	4.9	-11.1	25.4	1.10	.65	1.09	3.11
122.0	4.9	-10.9	25.6	1.10	.65	1.08	3.10
123.0	4.9	-10.8	25.9	1.10	.65	1.08	3.09
124.0	4.9	-10.6	26.1	1.09	.65	1.08	3.08
125.0	4.9	-10.5	26.4	1.09	.65	1.07	3.07
126.0	4.9	-10.3	26.6	1.09	.65	1.07	3.06
127.0	4.9	-10.2	26.9	1.09	.64	1.07	3.05
128.0	4.9	-10.0	27.1	1.09	.64	1.07	3.04
129.0	4.9	-9.9	27.5	1.08	.64	1.06	3.03
130.0	4.9	-9.7	27.7	1.08	.64	1.06	3.01
131.0	4.9	-9.6	28.1	1.08	.64	1.05	3.00
132.0	4.9	-9.4	28.4	1.08	.64	1.05	2.99
133.0	4.9	-9.3	28.7	1.07	.63	1.05	2.97
134.0	4.9	-9.1	29.0	1.07	.63	1.04	2.96
135.0	4.9	-9.0	29.4	1.07	.63	1.04	2.95
136.0	4.9	-8.8	29.8	1.06	.63	1.04	2.93
137.0	4.8	-8.7	30.1	1.06	.63	1.03	2.92
138.0	4.8	-8.5	30.5	1.06	.62	1.03	2.90
139.0	4.8	-8.4	30.9	1.06	.62	1.02	2.89
140.0	4.8	-8.2	31.4	1.05	.62	1.02	2.87
141.0	4.8	-8.1	31.8	1.05	.62	1.01	2.85
142.0	4.8	-7.9	32.2	1.05	.61	1.01	2.84
143.0	4.8	-7.8	32.7	1.04	.61	1.01	2.82
144.0	4.8	-7.6	33.2	1.04	.61	1.00	2.80
145.0	4.8	-7.5	33.7	1.03	.61	.99	2.78
146.0	4.8	-7.3	34.3	1.03	.60	.99	2.76
147.0	4.8	-7.2	34.8	1.03	.60	.98	2.74
148.0	4.8	-7.0	35.4	1.02	.60	.98	2.72

Depth (cm)	Salinity (o/oo)	Temp (C)	VB (o/oo)	Sigma T (MPa)	Sigma F (MPa)	Sigma S (MPa)	Eeff (GPa)
149.0	4.8	-6.9	36.0	1.02	.59	.97	2.69
150.0	4.8	-6.7	36.7	1.01	.59	.97	2.67
151.0	4.8	-6.6	37.4	1.01	.59	.96	2.64
152.0	4.8	-6.4	38.1	1.00	.58	.95	2.62
153.0	4.8	-6.3	38.8	1.00	.58	.94	2.59
154.0	4.8	-6.1	39.7	.99	.58	.94	2.56
155.0	4.8	-6.0	40.4	.99	.57	.93	2.54
156.0	4.8	-5.8	41.3	.98	.57	.92	2.51
157.0	4.8	-5.7	42.3	.97	.56	.91	2.47
158.0	4.8	-5.5	43.3	.97	.56	.90	2.44
159.0	4.8	-5.4	44.4	.96	.55	.89	2.41
160.0	4.8	-5.2	45.5	.95	.55	.88	2.37
161.0	4.8	-5.1	46.7	.94	.54	.87	2.33
162.0	4.8	-4.9	48.0	.94	.54	.86	2.29
163.0	4.8	-4.8	49.4	.93	.53	.85	2.25
164.0	4.8	-4.6	50.8	.92	.53	.84	2.20
165.0	4.8	-4.5	52.5	.91	.52	.83	2.15
166.0	4.8	-4.3	54.3	.90	.51	.81	2.10
167.0	4.8	-4.2	56.4	.88	.50	.79	2.03
168.0	4.8	-4.0	58.8	.87	.49	.78	1.97
169.0	4.9	-3.9	61.4	.86	.48	.76	1.89
170.0	4.9	-3.7	64.4	.84	.47	.73	1.81
171.0	5.0	-3.6	67.9	.82	.46	.71	1.72
172.0	5.1	-3.4	71.9	.80	.44	.68	1.61
173.0	5.2	-3.3	76.5	.78	.43	.65	1.50
174.0	5.3	-3.1	82.0	.75	.41	.61	1.36
175.0	5.5	-3.0	88.4	.72	.39	.57	1.21
176.0	5.6	-2.8	96.0	.69	.36	.52	1.04
177.0	5.8	-2.7	105.1	.65	.34	.47	.84
178.0	6.1	-2.5	116.1	.60	.30	.41	.61
179.0	6.4	-2.4	129.6	.55	.27	.34	.35
180.0	6.7	-2.2	146.4	.48	.22	.25	.03
181.0	7.2	-2.1	167.6	.41	.17	.15	0.00
182.0	7.7	-1.9	194.9	.32	.11	.03	0.00
183.0	8.2	-1.8	225.8	.23	.05	0.00	0.00
MEAN	5.5	-15.5	29.5	1.10	.65	1.09	3.13
SDEV	.9	8.0	30.5	.18	.12	.24	.83
MIN	4.8	-29.1	8.1	.23	.05	0.00	0.00
MAX	9.7	-1.8	225.8	1.29	.79	1.34	4.07

NEUTRAL AXIS (CM)	79.7
FLEXURAL RIGIDITY (N-M)	1.58E+09
CHARACTERISTIC LENGTH (M)	19.92
AVERAGE ICE SALINITY (o/oo)	5.48
AVERAGE ICE TEMPERATURE (C)	-15.5
BULK BRINE VOLUME (o/oo)	22.1
BULK TENSILE STRENGTH (MPA)	1.13
BULK FLEXURAL STRENGTH (MPA)	.67
BULK SHEAR STRENGTH (MPA)	1.12
BULK EFFECTIVE MODULUS (GPA)	3.26
BULK FLEXURAL RIGIDITY (N-M)	1.87E+09
BULK CHARACTERISTIC LENGTH (M)	20.79

PROFILE: SG5E-31   DEPTH: 213 CM (7 FT)

Depth (cm)	Salinity (o/oo)	Temp (C)	VB (o/oo)	Sigma T (MPa)	Sigma F (MPa)	Sigma S (MPa)	Eeff (GPa)
.3	9.7	-30.7	8.3	1.29	.78	1.34	4.05
1.0	9.4	-30.6	8.1	1.29	.79	1.34	4.07
2.0	8.9	-30.5	7.8	1.30	.79	1.35	4.09
3.0	8.6	-30.4	7.5	1.30	.79	1.36	4.11
4.0	8.2	-30.2	7.3	1.30	.79	1.36	4.13
5.0	8.0	-30.1	7.2	1.31	.80	1.36	4.14
6.0	7.8	-29.9	7.0	1.31	.80	1.37	4.15
7.0	7.6	-29.8	7.0	1.31	.80	1.37	4.16
8.0	7.4	-29.7	6.9	1.31	.80	1.37	4.17
9.0	7.2	-29.5	6.8	1.31	.80	1.37	4.17
10.0	7.1	-29.4	6.8	1.31	.80	1.37	4.18
11.0	7.0	-29.3	6.7	1.31	.80	1.37	4.18
12.0	6.9	-29.1	6.7	1.31	.80	1.37	4.18

13.0	6.8	-29.0	6.7	1.31	.80	1.37	4.18
14.0	6.7	-28.9	6.7	1.31	.80	1.38	4.18
15.0	6.6	-28.7	6.7	1.31	.80	1.37	4.18
16.0	6.5	-28.6	6.7	1.31	.80	1.37	4.18
17.0	6.4	-28.5	6.7	1.31	.80	1.37	4.18
18.0	6.4	-28.3	6.7	1.31	.80	1.37	4.18
19.0	6.3	-28.2	6.8	1.31	.80	1.37	4.17
20.0	6.2	-28.0	6.8	1.31	.80	1.37	4.17
21.0	6.2	-27.9	6.9	1.31	.80	1.37	4.17
22.0	6.1	-27.8	6.9	1.31	.80	1.37	4.16
23.0	6.1	-27.6	7.0	1.31	.80	1.37	4.16
24.0	6.1	-27.5	7.0	1.31	.80	1.37	4.15
25.0	6.0	-27.4	7.1	1.31	.80	1.37	4.15
26.0	5.9	-27.2	7.2	1.31	.80	1.36	4.14
27.0	5.9	-27.1	7.2	1.31	.80	1.36	4.14
28.0	5.9	-27.0	7.3	1.30	.79	1.36	4.13
29.0	5.8	-26.8	7.4	1.30	.79	1.36	4.12
30.0	5.8	-26.7	7.5	1.30	.79	1.36	4.11
31.0	5.8	-26.5	7.6	1.30	.79	1.35	4.11
32.0	5.7	-26.4	7.7	1.30	.79	1.35	4.10
33.0	5.7	-26.3	7.9	1.30	.79	1.35	4.09
34.0	5.7	-26.1	8.0	1.29	.79	1.35	4.08
35.0	5.7	-26.0	8.1	1.29	.79	1.34	4.07
36.0	5.6	-25.9	8.3	1.29	.78	1.34	4.05
37.0	5.6	-25.7	8.5	1.29	.78	1.34	4.04
38.0	5.6	-25.6	8.6	1.28	.78	1.33	4.03
39.0	5.6	-25.5	8.8	1.28	.78	1.33	4.02
40.0	5.6	-25.3	9.0	1.28	.78	1.33	4.00
41.0	5.5	-25.2	9.2	1.28	.77	1.32	3.99
42.0	5.5	-25.1	9.4	1.27	.77	1.32	3.97
43.0	5.5	-24.9	9.7	1.27	.77	1.31	3.95
44.0	5.5	-24.8	9.9	1.27	.77	1.31	3.94
45.0	5.5	-24.6	10.2	1.26	.77	1.30	3.92
46.0	5.4	-24.5	10.5	1.26	.76	1.30	3.90
47.0	5.4	-24.4	10.8	1.25	.76	1.29	3.88
48.0	5.4	-24.2	11.1	1.25	.76	1.29	3.85
49.0	5.4	-24.1	11.5	1.24	.75	1.28	3.83
50.0	5.4	-24.0	11.9	1.24	.75	1.27	3.81
51.0	5.4	-23.8	12.3	1.23	.75	1.27	3.78
52.0	5.4	-23.7	12.8	1.23	.74	1.26	3.75
53.0	5.3	-23.6	13.3	1.22	.74	1.25	3.72
54.0	5.3	-23.4	13.9	1.22	.73	1.24	3.69
55.0	5.3	-23.3	14.5	1.21	.73	1.23	3.65
56.0	5.3	-23.1	15.2	1.20	.72	1.22	3.61
57.0	5.3	-23.0	15.9	1.19	.72	1.21	3.57
58.0	5.3	-22.9	16.2	1.19	.71	1.21	3.56
59.0	5.3	-22.7	16.2	1.19	.71	1.21	3.56
60.0	5.3	-22.6	16.2	1.19	.71	1.20	3.55
61.0	5.3	-22.5	16.3	1.19	.71	1.20	3.55
62.0	5.3	-22.3	16.4	1.19	.71	1.20	3.55
63.0	5.2	-22.2	16.4	1.19	.71	1.20	3.54
64.0	5.2	-22.1	16.4	1.19	.71	1.20	3.54
65.0	5.2	-21.9	16.5	1.19	.71	1.20	3.54
66.0	5.2	-21.8	16.6	1.19	.71	1.20	3.54
67.0	5.2	-21.7	16.6	1.18	.71	1.20	3.53
68.0	5.2	-21.5	16.7	1.18	.71	1.20	3.53
69.0	5.2	-21.4	16.7	1.18	.71	1.20	3.53
70.0	5.2	-21.2	16.8	1.18	.71	1.20	3.52
71.0	5.2	-21.1	16.9	1.18	.71	1.20	3.52
72.0	5.2	-21.0	16.9	1.18	.71	1.19	3.52
73.0	5.2	-20.8	16.9	1.18	.71	1.19	3.52
74.0	5.2	-20.7	17.0	1.18	.71	1.19	3.51
75.0	5.2	-20.6	17.1	1.18	.71	1.19	3.51
76.0	5.2	-20.4	17.1	1.18	.71	1.19	3.51
77.0	5.2	-20.3	17.2	1.18	.71	1.19	3.50
78.0	5.1	-20.2	17.3	1.18	.71	1.19	3.50
79.0	5.1	-20.0	17.3	1.18	.71	1.19	3.49
80.0	5.1	-19.9	17.4	1.18	.71	1.19	3.49
81.0	5.1	-19.7	17.4	1.18	.71	1.19	3.49
82.0	5.1	-19.6	17.5	1.17	.70	1.19	3.48
83.0	5.1	-19.5	17.6	1.17	.70	1.19	3.48
84.0	5.1	-19.3	17.7	1.17	.70	1.18	3.48
85.0	5.1	-19.2	17.7	1.17	.70	1.18	3.47
86.0	5.1	-19.1	17.8	1.17	.70	1.18	3.47
87.0	5.1	-18.9	17.9	1.17	.70	1.18	3.47
88.0	5.1	-18.8	17.9	1.17	.70	1.18	3.46
89.0	5.1	-18.7	18.0	1.17	.70	1.18	3.46

90.0	5.1	-18.5	18.1	1.17	.70	1.18	3.46
91.0	5.1	-18.4	18.1	1.17	.70	1.18	3.45
92.0	5.1	-18.3	18.2	1.17	.70	1.18	3.45
93.0	5.1	-18.1	18.3	1.17	.70	1.18	3.45
94.0	5.0	-18.0	18.3	1.17	.70	1.17	3.44
95.0	5.0	-17.8	18.4	1.17	.70	1.17	3.44
96.0	5.0	-17.7	18.5	1.17	.70	1.17	3.44
97.0	5.0	-17.6	18.6	1.16	.70	1.17	3.43
98.0	5.0	-17.4	18.7	1.16	.70	1.17	3.43
99.0	5.0	-17.3	18.7	1.16	.70	1.17	3.42
100.0	5.0	-17.2	18.8	1.16	.70	1.17	3.42
101.0	5.0	-17.0	18.9	1.16	.69	1.17	3.42
102.0	5.0	-16.9	19.0	1.16	.69	1.17	3.41
103.0	5.0	-16.8	19.0	1.16	.69	1.17	3.41
104.0	5.0	-16.6	19.1	1.16	.69	1.16	3.40
105.0	5.0	-16.5	19.2	1.16	.69	1.16	3.40
106.0	5.0	-16.3	19.3	1.16	.69	1.16	3.40
107.0	5.0	-16.2	19.4	1.16	.69	1.16	3.39
108.0	5.0	-16.1	19.5	1.16	.69	1.16	3.39
109.0	4.9	-15.9	19.5	1.15	.69	1.16	3.38
110.0	4.9	-15.8	19.6	1.15	.69	1.16	3.38
111.0	4.9	-15.7	19.7	1.15	.69	1.16	3.37
112.0	4.9	-15.5	19.8	1.15	.69	1.15	3.37
113.0	4.9	-15.4	19.9	1.15	.69	1.15	3.37
114.0	4.9	-15.3	20.0	1.15	.69	1.15	3.36
115.0	4.9	-15.1	20.1	1.15	.69	1.15	3.35
116.0	4.9	-15.0	20.2	1.15	.69	1.15	3.35
117.0	4.9	-14.9	20.3	1.15	.69	1.15	3.35
118.0	4.9	-14.7	20.4	1.15	.68	1.15	3.34
119.0	4.9	-14.6	20.5	1.15	.68	1.15	3.34
120.0	4.9	-14.4	20.6	1.14	.68	1.14	3.33
121.0	4.9	-14.3	20.7	1.14	.68	1.14	3.32
122.0	4.9	-14.2	20.8	1.14	.68	1.14	3.32
123.0	4.8	-14.0	20.9	1.14	.68	1.14	3.31
124.0	4.8	-13.9	21.0	1.14	.68	1.14	3.31
125.0	4.8	-13.8	21.2	1.14	.68	1.14	3.30
126.0	4.8	-13.6	21.3	1.14	.68	1.14	3.30
127.0	4.8	-13.5	21.4	1.14	.68	1.13	3.29
128.0	4.8	-13.4	21.5	1.14	.68	1.13	3.29
129.0	4.8	-13.2	21.7	1.13	.68	1.13	3.28
130.0	4.8	-13.1	21.8	1.13	.68	1.13	3.27
131.0	4.8	-12.9	21.9	1.13	.67	1.13	3.27
132.0	4.8	-12.8	22.0	1.13	.67	1.13	3.26
133.0	4.8	-12.7	22.2	1.13	.67	1.12	3.26
134.0	4.8	-12.5	22.3	1.13	.67	1.12	3.25
135.0	4.8	-12.4	22.5	1.13	.67	1.12	3.24
136.0	4.7	-12.3	22.6	1.13	.67	1.12	3.24
137.0	4.7	-12.1	22.7	1.12	.67	1.12	3.23
138.0	4.7	-12.0	22.9	1.12	.67	1.12	3.22
139.0	4.7	-11.9	23.1	1.12	.67	1.11	3.22
140.0	4.7	-11.7	23.2	1.12	.67	1.11	3.21
141.0	4.7	-11.6	23.4	1.12	.67	1.11	3.20
142.0	4.7	-11.5	23.5	1.12	.66	1.11	3.20
143.0	4.7	-11.3	23.7	1.12	.66	1.11	3.19
144.0	4.7	-11.2	23.9	1.11	.66	1.10	3.18
145.0	4.7	-11.0	24.1	1.11	.66	1.10	3.17
146.0	4.7	-10.9	24.2	1.11	.66	1.10	3.16
147.0	4.7	-10.8	24.5	1.11	.66	1.10	3.15
148.0	4.7	-10.6	24.7	1.11	.66	1.09	3.14
149.0	4.6	-10.5	24.8	1.11	.66	1.09	3.14
150.0	4.6	-10.4	25.0	1.10	.65	1.09	3.13
151.0	4.6	-10.2	25.3	1.10	.65	1.09	3.12
152.0	4.6	-10.1	25.5	1.10	.65	1.08	3.11
153.0	4.6	-10.0	25.7	1.10	.65	1.08	3.10
154.0	4.6	-9.8	25.9	1.10	.65	1.08	3.09
155.0	4.6	-9.7	26.2	1.09	.65	1.08	3.08
156.0	4.6	-9.6	26.5	1.09	.65	1.07	3.07
157.0	4.6	-9.4	26.7	1.09	.64	1.07	3.06
158.0	4.6	-9.3	27.0	1.09	.64	1.07	3.04
159.0	4.6	-9.1	27.3	1.08	.64	1.06	3.03
160.0	4.6	-9.0	27.6	1.08	.64	1.06	3.02
161.0	4.6	-8.9	27.9	1.08	.64	1.06	3.01
162.0	4.6	-8.7	28.1	1.08	.64	1.05	3.00
163.0	4.6	-8.6	28.5	1.07	.63	1.05	2.98
164.0	4.5	-8.5	28.8	1.07	.63	1.05	2.97
165.0	4.5	-8.3	29.2	1.07	.63	1.04	2.95

166.0	4.5	-8.2	29.6	1.07	.63	1.04	2.94
167.0	4.5	-8.1	29.9	1.06	.63	1.03	2.93
168.0	4.5	-7.9	30.3	1.06	.62	1.03	2.91
169.0	4.5	-7.8	30.7	1.06	.62	1.03	2.89
170.0	4.5	-7.6	31.2	1.05	.62	1.02	2.88
171.0	4.5	-7.5	31.6	1.05	.62	1.02	2.86
172.0	4.5	-7.4	32.1	1.05	.61	1.01	2.84
173.0	4.5	-7.2	32.5	1.04	.61	1.01	2.82
174.0	4.5	-7.1	33.1	1.04	.61	1.00	2.80
175.0	4.5	-7.0	33.6	1.03	.61	1.00	2.78
176.0	4.5	-6.8	34.2	1.03	.60	.99	2.76
177.0	4.5	-6.7	34.8	1.03	.60	.98	2.74
178.0	4.5	-6.6	35.4	1.02	.60	.98	2.72
179.0	4.5	-6.4	36.0	1.02	.59	.97	2.69
180.0	4.5	-6.3	36.7	1.01	.59	.97	2.67
181.0	4.5	-6.2	37.4	1.01	.59	.96	2.64
182.0	4.5	-6.0	38.1	1.00	.58	.95	2.62
183.0	4.5	-5.9	38.9	1.00	.58	.94	2.59
184.0	4.5	-5.7	39.8	.99	.58	.94	2.56
185.0	4.5	-5.6	40.7	.98	.57	.93	2.53
186.0	4.5	-5.5	41.6	.98	.57	.92	2.50
187.0	4.5	-5.3	42.5	.97	.56	.91	2.47
188.0	4.5	-5.2	43.6	.96	.56	.90	2.43
189.0	4.5	-5.1	44.7	.96	.55	.89	2.40
190.0	4.5	-4.9	45.9	.95	.55	.88	2.36
191.0	4.5	-4.8	47.1	.94	.54	.87	2.32
192.0	4.6	-4.7	48.4	.93	.54	.86	2.28
193.0	4.6	-4.5	49.8	.92	.53	.85	2.23
194.0	4.6	-4.4	51.3	.92	.52	.83	2.19
195.0	4.6	-4.2	53.0	.91	.52	.82	2.14
196.0	4.6	-4.1	54.8	.89	.51	.81	2.08
197.0	4.6	-4.0	57.0	.88	.50	.79	2.02
198.0	4.7	-3.8	59.4	.87	.49	.77	1.95
199.0	4.7	-3.7	62.1	.85	.48	.75	1.87
200.0	4.8	-3.6	65.2	.84	.47	.73	1.79
201.0	4.8	-3.4	68.7	.82	.45	.70	1.70
202.0	4.9	-3.3	72.8	.80	.44	.67	1.59
203.0	5.0	-3.2	77.6	.77	.42	.64	1.47
204.0	5.2	-3.0	83.0	.75	.41	.61	1.34
205.0	5.3	-2.9	89.4	.72	.38	.56	1.19
206.0	5.5	-2.8	97.0	.68	.36	.52	1.02
207.0	5.7	-2.6	106.0	.64	.33	.47	.82
208.0	6.0	-2.5	116.8	.60	.30	.40	.60
209.0	6.3	-2.3	130.0	.55	.27	.33	.34
210.0	6.6	-2.2	146.3	.49	.22	.25	.04
211.0	7.1	-2.1	166.8	.41	.17	.16	0.00
212.0	7.6	-1.9	192.8	.33	.11	.04	0.00
213.0	8.1	-1.8	221.4	.24	.05	0.00	0.00
MEAN	5.3	-16.3	26.9	1.12	.67	1.12	3.24
SDEV	.9	8.4	29.0	.18	.12	.24	.83
MIN	4.5	-30.7	6.7	.24	.05	0.00	0.00
MAX	9.7	-1.8	221.4	1.31	.80	1.38	4.18

NEUTRAL AXIS (CM)	93.0
FLEXURAL RIGIDITY (N-M)	2.60E+09
CHARACTERISTIC LENGTH (M)	22.58
AVERAGE ICE SALINITY (o/oo)	5.29
AVERAGE ICE TEMPERATURE (C)	-16.3
BULK BRINE VOLUME (o/oo)	20.6
BULK TENSILE STRENGTH (MPA)	1.14
BULK FLEXURAL STRENGTH (MPA)	.68
BULK SHEAR STRENGTH (MPA)	1.14
BULK EFFECTIVE MODULUS (GPA)	3.33
BULK FLEXURAL RIGIDITY (N-M)	3.02E+09
BULK CHARACTERISTIC LENGTH (M)	23.43

APPENDIX C: CALCULATED PROFILE AND BULK PROPERTIES OF 30- AND 91-CM-THICK ICE SHEETS

The ice sheets formed on 1 November and 1 February. Day 1 is taken as 1 September, so 1 November is day 62 and 1 February is day 154. The corresponding information for 1 October is in Appendix B.

PROFILE: SG5E-62   DEPTH: 30 CM (1 FT)

Depth (cm)	Salinity (o/oo)	Temp (C)	VB (o/oo)	Sigma T (MPa)	Sigma F (MPa)	Sigma S (MPa)	Eeff (GPa)
.3	14.4	-20.4	48.0	.94	.54	.86	2.29
1.0	13.8	-20.0	46.6	.94	.54	.87	2.33
2.0	12.9	-19.3	44.7	.96	.55	.89	2.39
3.0	12.3	-18.7	43.5	.97	.56	.90	2.44
4.0	11.7	-18.1	42.5	.97	.56	.91	2.47
5.0	11.3	-17.5	41.9	.98	.57	.92	2.49
6.0	10.9	-16.8	41.5	.98	.57	.92	2.50
7.0	10.5	-16.2	41.2	.98	.57	.92	2.51
8.0	10.2	-15.6	41.1	.98	.57	.92	2.51
9.0	10.0	-14.9	41.2	.98	.57	.92	2.51
10.0	9.7	-14.3	41.5	.98	.57	.92	2.50
11.0	9.5	-13.7	41.9	.98	.57	.92	2.49
12.0	9.3	-13.1	42.5	.97	.56	.91	2.47
13.0	9.2	-12.4	43.2	.97	.56	.90	2.44
14.0	9.0	-11.8	44.2	.96	.55	.90	2.41
15.0	8.9	-11.2	45.3	.95	.55	.89	2.37
16.0	8.8	-10.6	46.7	.94	.54	.87	2.33
17.0	8.7	-9.9	48.3	.93	.54	.86	2.28
18.0	8.6	-9.3	50.3	.92	.53	.84	2.22
19.0	8.5	-8.7	52.7	.91	.52	.82	2.15
20.0	8.4	-8.1	55.6	.89	.51	.80	2.06
21.0	8.4	-7.4	59.2	.87	.49	.77	1.96
22.0	8.4	-6.8	63.7	.84	.47	.74	1.83
23.0	8.4	-6.2	69.4	.81	.45	.70	1.68
24.0	8.5	-5.6	76.9	.78	.43	.65	1.49
25.0	8.6	-4.9	87.0	.73	.39	.58	1.24
26.0	8.8	-4.3	100.7	.66	.35	.50	.93
27.0	9.1	-3.7	120.7	.58	.29	.38	.52
28.0	9.5	-3.1	151.6	.47	.21	.23	0.00
29.0	10.2	-2.4	204.4	.29	.09	0.00	0.00
30.0	10.9	-1.8	300.1	.03	0.00	0.00	0.00
MEAN	9.9	-11.2	70.3	.84	.48	.75	1.93
SDEV	1.7	5.7	56.3	.22	.15	.26	.81
MIN	8.4	-20.4	41.1	.03	0.00	0.00	0.00
MAX	14.4	-1.8	300.1	.98	.57	.92	2.51

```
NEUTRAL AXIS (CM)                   12.2
FLEXURAL RIGIDITY (N-M)             3.48E+06
CHARACTERISTIC LENGTH (M)           4.32

AVERAGE ICE SALINITY (o/oo)         9.91
AVERAGE ICE TEMPERATURE (C)        -11.2
BULK BRINE VOLUME (o/oo)            50.6
BULK TENSILE STRENGTH (MPA)          .92
BULK FLEXURAL STRENGTH (MPA)         .53
BULK SHEAR STRENGTH (MPA)            .84
BULK EFFECTIVE MODULUS (GPA)        2.21
BULK FLEXURAL RIGIDITY (N-M)        5.59E+06
BULK CHARACTERISTIC LENGTH (M)       4.86
```

Depth (cm)	Salinity (o/oo)	Temp (C)	VB (o/oo)	Sigma T (MPa)	Sigma F (MPa)	Sigma S (MPa)	Eeff (GPa)
.3	14.2	-26.8	18.1	1.17	.70	1.18	3.46
1.0	13.6	-26.6	17.8	1.17	.70	1.18	3.47
2.0	12.7	-26.4	17.3	1.18	.71	1.19	3.50
3.0	12.0	-26.1	17.1	1.18	.71	1.19	3.51
4.0	11.5	-25.8	17.1	1.18	.71	1.19	3.51
5.0	11.0	-25.5	17.2	1.18	.71	1.19	3.50
6.0	10.6	-25.2	17.4	1.18	.71	1.19	3.49
7.0	10.2	-25.0	17.8	1.17	.70	1.18	3.47
8.0	9.9	-24.7	18.3	1.17	.70	1.18	3.44
9.0	9.6	-24.4	19.0	1.16	.69	1.17	3.41
10.0	9.4	-24.1	19.8	1.15	.69	1.16	3.37
11.0	9.2	-23.9	20.8	1.14	.68	1.14	3.32
12.0	9.0	-23.6	22.1	1.13	.67	1.13	3.26
13.0	8.8	-23.3	23.6	1.12	.66	1.11	3.19
14.0	8.6	-23.0	25.6	1.10	.65	1.08	3.10
15.0	8.5	-22.8	25.9	1.10	.65	1.08	3.09
16.0	8.3	-22.5	25.8	1.10	.65	1.08	3.10
17.0	8.2	-22.2	25.6	1.10	.65	1.08	3.10
18.0	8.1	-21.9	25.5	1.10	.65	1.08	3.11
19.0	8.0	-21.7	25.4	1.10	.65	1.09	3.11
20.0	7.9	-21.4	25.3	1.10	.65	1.09	3.12
21.0	7.8	-21.1	25.2	1.10	.65	1.09	3.12
22.0	7.7	-20.8	25.1	1.10	.65	1.09	3.12
23.0	7.6	-20.6	25.1	1.10	.65	1.09	3.12
24.0	7.5	-20.3	25.1	1.10	.65	1.09	3.13
25.0	7.4	-20.0	25.1	1.10	.65	1.09	3.13
26.0	7.4	-19.7	25.1	1.10	.65	1.09	3.12
27.0	7.3	-19.5	25.1	1.10	.65	1.09	3.12
28.0	7.2	-19.2	25.1	1.10	.65	1.09	3.12
29.0	7.2	-18.9	25.2	1.10	.65	1.09	3.12
30.0	7.1	-18.6	25.2	1.10	.65	1.09	3.12
31.0	7.1	-18.4	25.3	1.10	.65	1.09	3.12
32.0	7.0	-18.1	25.4	1.10	.65	1.09	3.11
33.0	7.0	-17.8	25.5	1.10	.65	1.08	3.11
34.0	6.9	-17.5	25.6	1.10	.65	1.08	3.10
35.0	6.9	-17.2	25.7	1.10	.65	1.08	3.10
36.0	6.8	-17.0	25.8	1.10	.65	1.08	3.09
37.0	6.8	-16.7	26.0	1.10	.65	1.08	3.09
38.0	6.7	-16.4	26.1	1.09	.65	1.08	3.08
39.0	6.7	-16.1	26.3	1.09	.65	1.08	3.08
40.0	6.7	-15.9	26.4	1.09	.65	1.07	3.07
41.0	6.6	-15.6	26.6	1.09	.65	1.07	3.06
42.0	6.6	-15.3	26.8	1.09	.64	1.07	3.05
43.0	6.6	-15.0	27.0	1.09	.64	1.07	3.04
44.0	6.5	-14.8	27.3	1.08	.64	1.06	3.03
45.0	6.5	-14.5	27.5	1.08	.64	1.06	3.02
46.0	6.5	-14.2	27.7	1.08	.64	1.06	3.01
47.0	6.5	-13.9	28.0	1.08	.64	1.06	3.00
48.0	6.4	-13.7	28.3	1.08	.64	1.05	2.99
49.0	6.4	-13.4	28.6	1.07	.63	1.05	2.98
50.0	6.4	-13.1	29.0	1.07	.63	1.04	2.96
51.0	6.4	-12.8	29.3	1.07	.63	1.04	2.95
52.0	6.3	-12.6	29.7	1.07	.63	1.04	2.94
53.0	6.3	-12.3	30.0	1.06	.63	1.03	2.92
54.0	6.3	-12.0	30.4	1.06	.62	1.03	2.91
55.0	6.3	-11.7	30.8	1.06	.62	1.03	2.89
56.0	6.2	-11.5	31.2	1.05	.62	1.02	2.87
57.0	6.2	-11.2	31.7	1.05	.62	1.02	2.85
58.0	6.2	-10.9	32.2	1.05	.61	1.01	2.84
59.0	6.2	-10.6	32.8	1.04	.61	1.00	2.81
60.0	6.2	-10.4	33.4	1.04	.61	1.00	2.79
61.0	6.2	-10.1	34.0	1.03	.60	.99	2.77
62.0	6.1	-9.8	34.6	1.03	.60	.99	2.74
63.0	6.1	-9.5	35.3	1.02	.60	.98	2.72
64.0	6.1	-9.2	36.1	1.02	.59	.97	2.69
65.0	6.1	-9.0	36.9	1.01	.59	.96	2.66
66.0	6.1	-8.7	37.8	1.00	.59	.95	2.63
67.0	6.1	-8.4	38.7	1.00	.58	.95	2.60
68.0	6.1	-8.1	39.7	.99	.58	.94	2.56
69.0	6.1	-7.9	40.8	.98	.57	.93	2.53
70.0	6.1	-7.6	41.9	.98	.57	.92	2.49
71.0	6.1	-7.3	43.3	.97	.56	.90	2.44

Depth	Salinity	Temp	VB	Sigma T	Sigma F	Sigma S	Eeff
72.0	6.0	-7.0	44.6	.96	.55	.89	2.40
73.0	6.0	-6.8	46.1	.95	.55	.88	2.35
74.0	6.0	-6.5	47.7	.94	.54	.86	2.30
75.0	6.0	-6.2	49.6	.93	.53	.85	2.24
76.0	6.0	-5.9	51.7	.91	.52	.83	2.18
77.0	6.1	-5.7	54.0	.90	.51	.81	2.11
78.0	6.1	-5.4	56.6	.88	.50	.79	2.03
79.0	6.1	-5.1	59.6	.87	.49	.77	1.94
80.0	6.2	-4.8	63.2	.85	.48	.74	1.84
81.0	6.2	-4.6	67.5	.82	.46	.71	1.73
82.0	6.3	-4.3	72.6	.80	.44	.67	1.60
83.0	6.4	-4.0	78.7	.77	.42	.63	1.44
84.0	6.6	-3.7	86.1	.73	.39	.59	1.27
85.0	6.8	-3.5	95.2	.69	.37	.53	1.06
86.0	7.0	-3.2	106.8	.64	.33	.46	.80
87.0	7.3	-2.9	121.7	.58	.29	.38	.50
88.0	7.6	-2.6	141.2	.50	.24	.28	.13
89.0	8.1	-2.4	167.9	.41	.17	.15	0.00
90.0	8.7	-2.1	205.7	.29	.09	0.00	0.00
91.0	9.3	-1.8	255.5	.15	0.00	0.00	0.00
MEAN	7.4	-14.4	41.6	1.01	.59	.96	2.69
SDEV	1.8	7.4	38.7	.19	.13	.25	.82
MIN	6.0	-26.8	17.1	.15	0.00	0.00	0.00
MAX	14.2	-1.8	255.5	1.18	.71	1.19	3.51

NEUTRAL AXIS (CM)	39.1
FLEXURAL RIGIDITY (N-M)	1.57E+08
CHARACTERISTIC LENGTH (M)	11.20
AVERAGE ICE SALINITY (o/oo)	7.40
AVERAGE ICE TEMPERATURE (C)	-14.4
BULK BRINE VOLUME (o/oo)	31.5
BULK TENSILE STRENGTH (MPA)	1.05
BULK FLEXURAL STRENGTH (MPA)	.62
BULK SHEAR STRENGTH (MPA)	1.02
BULK EFFECTIVE MODULUS (GPA)	2.86
BULK FLEXURAL RIGIDITY (N-M)	2.02E+08
BULK CHARACTERISTIC LENGTH (M)	11.92

PROFILE: SG5E-154   DEPTH: 30 CM (1 FT)

Depth (cm)	Salinity (o/oo)	Temp (C)	VB (o/oo)	Sigma T (MPa)	Sigma F (MPa)	Sigma S (MPa)	Eeff (GPa)
.3	16.6	-24.5	31.7	1.05	.62	1.02	2.85
1.0	15.8	-24.0	34.9	1.02	.60	.98	2.73
2.0	14.8	-23.2	41.4	.98	.57	.92	2.51
3.0	14.0	-22.4	43.4	.97	.56	.90	2.44
4.0	13.3	-21.7	42.5	.97	.56	.91	2.47
5.0	12.8	-20.9	41.9	.98	.57	.92	2.49
6.0	12.3	-20.1	41.4	.98	.57	.92	2.50
7.0	11.9	-19.4	41.1	.98	.57	.92	2.51
8.0	11.6	-18.6	41.0	.98	.57	.92	2.52
9.0	11.2	-17.9	41.1	.98	.57	.92	2.52
10.0	11.0	-17.1	41.3	.98	.57	.92	2.51
11.0	10.7	-16.3	41.6	.98	.57	.92	2.50
12.0	10.5	-15.6	42.1	.97	.56	.91	2.48
13.0	10.3	-14.8	42.7	.97	.56	.91	2.46
14.0	10.1	-14.0	43.5	.96	.56	.90	2.43
15.0	9.9	-13.3	44.5	.96	.55	.89	2.40
16.0	9.7	-12.5	45.8	.95	.55	.88	2.36
17.0	9.6	-11.7	47.3	.94	.54	.87	2.31
18.0	9.5	-11.0	49.1	.93	.53	.85	2.26
19.0	9.4	-10.2	51.2	.92	.52	.84	2.19
20.0	9.3	-9.4	54.0	.90	.51	.81	2.11
21.0	9.2	-8.7	57.3	.88	.50	.79	2.01
22.0	9.2	-7.9	61.6	.86	.48	.75	1.89
23.0	9.2	-7.2	67.1	.83	.46	.71	1.74
24.0	9.3	-6.4	74.3	.79	.43	.66	1.55
25.0	9.4	-5.6	84.0	.74	.40	.60	1.31
26.0	9.5	-4.9	97.6	.68	.36	.51	1.00
27.0	9.8	-4.1	117.6	.59	.30	.40	.58

55

Depth	Salinity	Temp	VB	Sigma T	Sigma F	Sigma S	Eeff
28.0	10.2	-3.3	149.3	.47	.22	.24	0.00
29.0	10.9	-2.6	206.4	.29	.09	0.00	0.00
30.0	11.7	-1.8	320.4	0.00	0.00	0.00	0.00
MEAN	11.0	-13.3	69.0	.85	.48	.77	1.99
SDEV	2.0	6.9	59.7	.23	.15	.27	.83
MIN	9.2	-24.5	31.7	0.00	0.00	0.00	0.00
MAX	16.6	-1.8	320.4	1.05	.62	1.02	2.85

NEUTRAL AXIS (CM)   12.2
FLEXURAL RIGIDITY (N-M)   3.68E+06
CHARACTERISTIC LENGTH (M)   4.38

AVERAGE ICE SALINITY (o/oo)   11.04
AVERAGE ICE TEMPERATURE (C)   -13.3
BULK BRINE VOLUME (o/oo)   49.8
BULK TENSILE STRENGTH (MPA)   .92
BULK FLEXURAL STRENGTH (MPA)   .53
BULK SHEAR STRENGTH (MPA)   .85
BULK EFFECTIVE MODULUS (GPA)   2.23
BULK FLEXURAL RIGIDITY (N-M)   5.65E+06
BULK CHARACTERISTIC LENGTH (M)   4.88

PROFILE: S65E-154   DEPTH: 91 CM (3 FT)

Depth (cm)	Salinity (o/oo)	Temp (C)	VB (o/oo)	Sigma T (MPa)	Sigma F (MPa)	Sigma S (MPa)	Eeff (GPa)
.3	16.5	-30.4	14.5	1.21	.73	1.23	3.65
1.0	15.8	-30.1	14.1	1.21	.73	1.24	3.67
2.0	14.7	-29.8	13.5	1.22	.74	1.25	3.71
3.0	13.9	-29.5	13.1	1.22	.74	1.25	3.73
4.0	13.2	-29.2	12.9	1.23	.74	1.26	3.75
5.0	12.7	-28.9	12.7	1.23	.74	1.26	3.76
6.0	12.2	-28.6	12.6	1.23	.74	1.26	3.76
7.0	11.7	-28.2	12.5	1.23	.74	1.26	3.77
8.0	11.3	-27.9	12.5	1.23	.74	1.26	3.77
9.0	11.0	-27.6	12.6	1.23	.74	1.26	3.76
10.0	10.7	-27.3	12.7	1.23	.74	1.26	3.75
11.0	10.4	-27.0	12.9	1.23	.74	1.26	3.74
12.0	10.1	-26.7	13.2	1.22	.74	1.25	3.73
13.0	9.9	-26.4	13.5	1.22	.74	1.25	3.71
14.0	9.7	-26.0	13.9	1.22	.73	1.24	3.69
15.0	9.5	-25.7	14.3	1.21	.73	1.23	3.66
16.0	9.3	-25.4	14.9	1.20	.72	1.23	3.63
17.0	9.1	-25.1	15.5	1.20	.72	1.22	3.59
18.0	9.0	-24.8	16.3	1.19	.71	1.20	3.55
19.0	8.8	-24.5	17.2	1.18	.71	1.19	3.50
20.0	8.7	-24.1	18.3	1.17	.70	1.17	3.44
21.0	8.6	-23.8	19.7	1.15	.69	1.16	3.38
22.0	8.5	-23.5	21.3	1.14	.68	1.13	3.30
23.0	8.4	-23.2	23.4	1.12	.66	1.11	3.20
24.0	8.3	-22.9	25.3	1.10	.65	1.09	3.12
25.0	8.2	-22.6	25.2	1.10	.65	1.09	3.12
26.0	8.1	-22.3	25.3	1.10	.65	1.09	3.12
27.0	8.0	-21.9	25.3	1.10	.65	1.09	3.12
28.0	7.9	-21.6	25.3	1.10	.65	1.09	3.12
29.0	7.9	-21.3	25.4	1.10	.65	1.09	3.12
30.0	7.8	-21.0	25.4	1.10	.65	1.09	3.11
31.0	7.7	-20.7	25.5	1.10	.65	1.09	3.11
32.0	7.7	-20.4	25.6	1.10	.65	1.08	3.11
33.0	7.6	-20.1	25.6	1.10	.65	1.08	3.11
34.0	7.6	-19.7	25.7	1.10	.65	1.08	3.10
35.0	7.5	-19.4	25.8	1.10	.65	1.08	3.10
36.0	7.4	-19.1	25.9	1.10	.65	1.08	3.09
37.0	7.4	-18.8	26.1	1.09	.65	1.08	3.09
38.0	7.3	-18.5	26.2	1.09	.65	1.08	3.08
39.0	7.3	-18.2	26.3	1.09	.65	1.08	3.08
40.0	7.2	-17.9	26.5	1.09	.65	1.07	3.07
41.0	7.2	-17.5	26.6	1.09	.65	1.07	3.07
42.0	7.2	-17.2	26.8	1.09	.64	1.07	3.06
43.0	7.1	-16.9	27.0	1.09	.64	1.07	3.05
44.0	7.1	-16.6	27.2	1.08	.64	1.06	3.03

45.0	7.0	-16.3	27.4	1.08	.64	1.06	3.03
46.0	7.0	-16.0	27.7	1.08	.64	1.06	3.02
47.0	7.0	-15.7	27.9	1.08	.64	1.06	3.01
48.0	6.9	-15.3	28.2	1.08	.64	1.05	3.00
49.0	6.9	-15.0	28.5	1.07	.63	1.05	2.98
50.0	6.9	-14.7	28.8	1.07	.63	1.05	2.97
51.0	6.8	-14.4	29.0	1.07	.63	1.04	2.96
52.0	6.8	-14.1	29.4	1.07	.63	1.04	2.95
53.0	6.8	-13.8	29.7	1.06	.63	1.04	2.93
54.0	6.8	-13.4	30.1	1.06	.63	1.03	2.92
55.0	6.7	-13.1	30.5	1.06	.62	1.03	2.90
56.0	6.7	-12.8	30.9	1.05	.62	1.02	2.88
57.0	6.7	-12.5	31.4	1.05	.62	1.02	2.87
58.0	6.7	-12.2	31.9	1.05	.62	1.01	2.85
59.0	6.6	-11.9	32.4	1.04	.61	1.01	2.83
60.0	6.6	-11.6	32.9	1.04	.61	1.00	2.81
61.0	6.6	-11.2	33.5	1.04	.61	1.00	2.79
62.0	6.6	-10.9	34.1	1.03	.60	.99	2.76
63.0	6.6	-10.6	34.8	1.03	.60	.98	2.74
64.0	6.5	-10.3	35.5	1.02	.60	.98	2.71
65.0	6.5	-10.0	36.3	1.01	.59	.97	2.68
66.0	6.5	-9.7	37.1	1.01	.59	.96	2.65
67.0	6.5	-9.4	38.0	1.00	.58	.95	2.62
68.0	6.5	-9.0	38.9	1.00	.58	.94	2.59
69.0	6.5	-8.7	39.9	.99	.57	.93	2.55
70.0	6.4	-8.4	41.0	.98	.57	.92	2.52
71.0	6.4	-8.1	42.2	.97	.56	.91	2.48
72.0	6.4	-7.8	43.6	.96	.56	.90	2.43
73.0	6.4	-7.5	45.0	.96	.55	.89	2.39
74.0	6.4	-7.2	46.7	.94	.54	.87	2.33
75.0	6.4	-6.8	48.4	.93	.54	.86	2.28
76.0	6.4	-6.5	50.4	.92	.53	.84	2.22
77.0	6.4	-6.2	52.6	.91	.52	.82	2.15
78.0	6.4	-5.9	55.2	.89	.51	.80	2.07
79.0	6.4	-5.6	58.2	.87	.50	.78	1.98
80.0	6.5	-5.3	61.7	.86	.48	.75	1.89
81.0	6.5	-4.9	65.8	.83	.47	.72	1.77
82.0	6.6	-4.6	70.8	.81	.45	.69	1.64
83.0	6.7	-4.3	76.8	.78	.43	.65	1.49
84.0	6.9	-4.0	84.0	.74	.40	.60	1.31
85.0	7.0	-3.7	93.1	.70	.37	.54	1.10
86.0	7.3	-3.4	104.7	.65	.34	.47	.85
87.0	7.5	-3.1	119.7	.59	.29	.39	.54
88.0	7.9	-2.7	139.6	.51	.24	.29	.16
89.0	8.4	-2.4	167.4	.41	.17	.15	0.00
90.0	9.0	-2.1	207.5	.28	.08	0.00	0.00
91.0	9.6	-1.8	262.9	.13	0.00	0.00	0.00
MEAN	8.1	-16.1	39.6	1.03	.60	.99	2.79
SDEV	2.2	8.4	39.9	.20	.14	.26	.89
MIN	6.4	-30.4	12.5	.13	0.00	0.00	0.00
MAX	16.5	-1.8	262.9	1.23	.74	1.26	3.77

NEUTRAL AXIS (CM)	38.4
FLEXURAL RIGIDITY (N-M)	1.66E+08
CHARACTERISTIC LENGTH (M)	11.34
AVERAGE ICE SALINITY (o/oo)	8.09
AVERAGE ICE TEMPERATURE (C)	-16.1
BULK BRINE VOLUME (o/oo)	31.8
BULK TENSILE STRENGTH (MPA)	1.05
BULK FLEXURAL STRENGTH (MPA)	.62
BULK SHEAR STRENGTH (MPA)	1.01
BULK EFFECTIVE MODULUS (GPA)	2.85
BULK FLEXURAL RIGIDITY (N-M)	2.01E+08
BULK CHARACTERISTIC LENGTH (M)	11.91

57

A facsimile catalog card in Library of Congress MARC format is repro-
duced below.